สารออกฤทธิ์ทางชีวภาพจากเปลือกลำต้นหยีทะเล *Derris indica* (Lamk.) Bennet

นางสาวพรภัทร อนุศิริ

วิทยานิพนธ์นี้เป็นส่วนหนึ่งของการศึกษาตามหลักสูตรปริญญาวิทยาศาสตรมหาบัณฑิต
สาขาวิชาเทคโนโลยีชีวภาพ
คณะวิทยาศาสตร์ จุฬาลงกรณ์มหาวิทยาลัย
ปีการศึกษา 2556
ลิขสิทธิ์ของจุฬาลงกรณ์มหาวิทยาลัย

BIOACTIVE COMPOUNDS FROM STEM BARK OF *Derris indica* (Lamk.) Bennet

Miss Pornpat Anusiri

A Thesis Submitted in Partial Fulfillment of the Requirements
for the Degree of Master of Science Program in Biotechnology
Faculty of Science
Chulalongkorn University
Academic Year 2013

Thesis Title	BIOACTIVE COMPOUNDS FROM STEM BARK OF *Derris indica* (Lamk.) Bennet
By	Miss Pornpat Anusiri
Field of Study	Biotechnology
Thesis Advisor	Assistant Professor Khanitha Pudhom, Ph.D.
Thesis Co-Advisor	Associate Professor Nattaya Ngamrojanavanich, Ph.D.

Accepted by the Faculty of Science, Chulalongkorn University in Partial Fulfillment of the Requirements for the Master's Degree

.....Dean of the Faculty of Science

(Professor Supot Hannongbua, Dr.rer.nat.)

THESIS COMMITTEE

.....Chairman

(Associate Professor Vudhichai Parasuk, Ph.D.)

.....Thesis Advisor

(Assistant Professor Khanitha Pudhom, Ph.D.)

.....Thesis Co-Advisor

(Associate Professor Nattaya Ngamrojanavanich, Ph.D.)

.....Examiner

(Associate Professor Chanpen Chanchao, Ph.D.)

.....External Examiner

(Damrong Sommit, Ph.D.)

พรภัทร อนุศิริ : สารออกฤทธิ์ทางชีวภาพจากเปลือกลำต้นหยีทะเล *Derris indica* (Lamk.) Bennet. (BIOACTIVE COMPOUNDS FROM STEM BARK OF *Derris indica* (Lamk.) Bennet) อ.ที่ปรึกษาวิทยานิพนธ์หลัก: ผศ. ดร.ขนิษฐา พุดหอม, อ.ที่ปรึกษาวิทยานิพนธ์ร่วม: รศ. ดร.นาตยา งามโรจนวณิชย์, 141 หน้า.

งานวิจัยนี้ศึกษาการแยกและพิสูจน์ทราบโครงสร้างสารออกฤทธิ์ทางชีวภาพจากเปลือกต้นหยีทะเล *Derris indica* (Lamk.) Bennet. โดยนำสารสกัดหยาบเอธิลอะซีเตทของเปลือกต้นหยีทะเลมาทำการแยกให้ได้สารบริสุทธิ์โดยใช้เทคนิคโครมาโทกราฟี จากการตรวจหาองค์ประกอบทางเคมีของหยีทะเลนี้ ทำให้สามารถแยกและพิสูจน์ทราบโครงสร้างของสารกลุ่มฟลาโวนอยด์ใหม่ 2 ชนิด คือ derrisins A (5) และ B (9) รวมทั้งสารที่มีการรายงานมาก่อนหน้านี้แล้วอีก 11 ชนิด ซึ่งได้แก่ desmethoxy kanugin (1), pongaglabrone (2), pongachromene (3), pongapin (4), karanjin (6), 3,7,4'–trimethoxyflavone (7), fisetin tetramethyl ether (8), pinnatin (10), lacneolatin B (11), pongaflavone (12) และ 5-methoxy-3',4'-methylenedioxy(8,7-4'',5'')flavone (13) สารบริสุทธิ์ที่แยกได้ทั้งหมดทำการพิสูจน์ทราบโครงสร้างโดยอาศัยเทคนิคทางสเปกโทรสโกปี ร่วมกับการเปรียบเทียบกับข้อมูลทางสเปกโทรสโกปีของสารที่มีการรายงานมาก่อน เมื่อนำมาทดสอบฤทธิ์ต้านการอักเสบและฤทธิ์ต้านการเกิดไกลเคชั่นพบว่าสาร pongaflavone (12) และ desmethoxy kanugin (1) แสดงฤทธิ์ต้านการอักเสบโดยยับยั้งการผลิตไนตริกออกไซด์ด้วยค่า IC_{50} เท่ากับ 14.59 μM และ 22.83 μM ตามลำดับ ในขณะที่ derrisin B (9) แสดงฤทธิ์ในการยับยั้งการสร้างผลิตภัณฑ์แอดวานซ์ ไกลเคชั่น เอ็น โปรดักส์ โดยดักจับหมู่เมทิลไกลโอซอลซึ่งมีค่า IC_{50} เท่ากับ 18.00 μM

สาขาวิชา เทคโนโลยีชีวภาพ ลายมือชื่อนิสิต .....

ปีการศึกษา 2556 ลายมือชื่อ อ.ที่ปรึกษาวิทยานิพนธ์หลัก .....

ลายมือชื่อ อ.ที่ปรึกษาวิทยานิพนธ์ร่วม .....

5472257623 : MAJOR BIOTECHNOLOGY
KEYWORDS: DERRIS INDICS / FLAVONOIDS / ANTI-INFLAMMATORY ACTIVITY / AGES

PORNPAT ANUSIRI: BIOACTIVE COMPOUNDS FROM STEM BARK OF *Derris indica* (Lamk.) Bennet. ADVISOR: ASST. PROF. KHANITHA PUDHOM, Ph.D., CO-ADVISOR: ASSOC. PROF. NATTAYA NGAMROJANAVANICH, Ph.D., 141 pp.

The present study focuses on isolation and characterization of bioactive compounds from stem bark of *Derris indica* (Lamk.) Bennet. The ethyl acetate crude extract was purified by chromatographic techniques. Chemical examination of *D. indica* resulted in isolation and characterization of two new flavonoids, derrisins A (5) and B (9), together with 11 known compounds including desmethoxy kanugin (1), pongaglabrone (2), pongachromene (3), pongapin (4), karanjin (6), 3,7,4'–trimethoxyflavone (7), fisetin tetramethyl ether (8), pinnatin (10), lacneolatin B (11), pongaflavone (12), and 5-methoxy-3',4'-methylenedioxy(8,7-4'',5'')flavone (13). Their chemical structures were determined on the basis of spectroscopic data analysis and by comparison with those in the literature. All compounds were tested for anti-inflammatory and antiglycation activities. Pongaflavone (12) and desmethoxy kanugin (1) displayed anti-inflammatory activity by suppressing nitric oxide production with the IC_{50} values of 14.59 and 22.83 μM, respectively, while derrisin B (9) exhibited the most potent inhibitory activity against the formation of advanced glycation end products (AGEs) by trapping reactive methylglyoxal with the IC_{50} value of 18.00 μM.

Field of Study: Biotechnology Student's Signature .....

Academic Year: 2013 Advisor's Signature .....

Co-Advisor's Signature .....

ACKNOWLEDGEMENTS

Firstly, I would like to express my sincere gratitude to my thesis advisor, Assistant Professor Dr. Khanitha Pudhom, and co-advisor, Associate Professor Dr. Nattaya Ngamrojnavanich, Department of Chemistry, Faculty of Science, Chulalongkorn University, for great guidance, kind support and supervision throughout this work.

Furthermore, I am grateful to the Chairperson: Associate Professor Dr. Vudhichai Parasuk, Department of Chemistry, Faculty of Science, Chulalongkorn University; the thesis examiners: Associate Professor Dr. Chanpen Chanchao, Department of Biology, Faculty of Science, Chulalongkorn University and Dr. Damrong Sommit, Mahanakorn University of Technology, for their invaluable discussion and suggestion.

I would like to sincere thank Assistant Professor Dr. Sirichai Adisakwattana, Department of Nutrition and Dietetics, Faculty of Allied Health Sciences, Chulalongkorn University for antiglycation assay and kind guidance. The author also thanks Dr. Thapong Teerawatananond, Department of Chemistey, Faculty of Science, Chulalongkorn University who kindly performed the X-ray crystallographic analysis.

Moreover, I would like to thank Miss Siwattra Choodej for assistance about structure elucidation of all compounds isolated. Special thanks to member in the Laboratory (MHMK 1532), Department of Chemistry, Faculty of Science, Chulalongkorn University for their generousness, help and good friendship.

I wish to thank The 90th Anniversary of Chulalongkorn University Fund (Ratchadaphiseksomphot Endowment Fund) for granting in partial financial support to conduct this research.

Lastly, the most thanks to my family for their love and encouragement throughout my M.Sc. study and thesis.

CONTENTS

Page

Page

Page

LIST OF TABLES

Page

LIST OF FIGURES

Page

Page

Page

Page

LIST OF SCHEMES

Page

LIST OF ABBREVIATIONS

J	Coupling constant
δ	Chemical shift
δ_H	Chemical shift of proton
δ_C	Chemical shift of carbon
s	Singlet (for NMR spectra)
d	Doublet (for NMR spectra)
dd	Doublet of doublet (for NMR spectra)
m	Multiplet (for NMR spectra)
brs	Broad singlet (for NMR spectra)
calcd.	Calculated
^{1}H NMR	Proton nuclear magnetic resonance
^{13}C NMR	Carbon-13 nuclear magnetic resonance
2D NMR	Two dimensional nuclear magnetic resonance
^{1}H-^{1}H COSY	Homonuclear (proton-proton) correlation spectroscopy
NOESY	Nuclear overhauser effect spectroscopy
HSQC	Heteronuclear single quantum coherence
HMBC	Heteronuclear multiple bond correlation
ORTEP	Oak ridge thermal ellipsoid plot
HPLC	High performance liquid chromatography
HRESIMS	High resolution electrospray ionization mass spectrometry
ESIMS	Electrospray ionization mass spectrometry
CC	Column chromatography
TLC	Thin layer chromatography
MIC	Minimum inhibitory concentration
IC_{50}	Half maximal inhibitory concentration
$CDCl_3$	Deuterated chloroform
MeOH	Methanol
EtOH	Ethanol
$CHCl_3$	Chloroform
CH_2Cl_2	Dichloromethane

EtOAc	Ethyl acetate
DMSO	Dimethylsulfoxide
KBr	Potassium bromide
$(NH_4)_6Mo_7O_{24}$	Ammonium molybdate
H_2SO_4	Sulfuric acid
SiO_2	Silicon dioxide
g	Gram (s)
mg	Milligram (s)
mL	Milliliter (s)
μg	Microgram (s)
μL	Microliter (s)
μM	Micromolar
mM	Millimolar
L	Liter (s)
M	Molar
min	Minute
h	Hour
m	Meter (s)
mm	Millimeter (s)
cm	Centimeter (s)
nm	Nanometer
Hz	Hertz
MHz	Megahertz
cm^{-1}	Reciprocal centimeter (unit of wave number)
ppm	part per million
NMR	Nuclear magnetic resonance
MS	Mass spectrometry
IR	Infared
UV	Ultraviolet
m.p.	Melting point
α	Alpha

β	Beta
Δ	Delta
m/z	Mass to charge ratio
$[M+H]^+$	Protonated molecule
$[M+Na]^+$	Pseudomolecular ion
$[\alpha]_D^{20}$	Specific rotation at 20 $^{\circ}$C and sodium D line (589 nm)
λ_{max}	Wavelength of maximum absorption
c	Concentration
ε	Molar extinction coefficient
Å	Angstrom
°C	Degree celcius
deg.	Degree
sp.	Species
No.	Number
AGEs	Advanced glycation end products
MGO	Methylglyoxal

CHAPTER I
INTRODUCTION

Pharmaceutical drugs have been continually discovered and developed to use in medication, treatment or prevention of diseases. Nature is one of the dominant sources for use in new drug discovery and design. Natural products are organic compounds produced and isolated from living organisms such as microbes, plants and animals. They have been used in traditional medicines for thousand years ago. Natural products have also been incessantly reported to possess various bioactive activities and as new drugs. From 2000 to 2010, approximately 40 new drugs prescribed in the market, were applied from substances of plants, microorganisms, animals and marine organisms [1].

Recently, the World Health Organization (WHO) assessed that about 80% of world's population relies on traditional plant medicines for their health care or treatment [2]. At the present time, the herbal medicine is one of the popular alternatives for therapeutics and disease prevention worldwide such as cancer, diabetes, inflammation, AIDS and other. [1]. Moreover, about 60% of anticancer drugs and 75% of drugs for infectious diseases in the market came from natural products and their derivatives [3].

It is well known that plant is a rich and interested source for new bioactive compounds that can be used as pharmaceutical drugs, because plant-based systems continue to play a crucial role in folk medicine. In global, more than 70,000 species of plants have been searched for their medicinal uses [4]. Tropical forests in Asia countries have a high density of plant species. In addition, they have the most abundant mineral nutrients for plants. Therefore, plants collected from tropical rainforests should be important sources for new bioactive compounds.

1.1 *Derris indica*

1.1.1 Botanical classification of *Derris indica*

Derris indica (Lamk.) Bennet [synonyms, *Pongamia pinnata* (L.), *Pongamia glabra* (Vent.) *Galedupa indica* (L.)] is a mangrove plant which belongs to family Leguminosae or Fabaceae (subfamily, Papilionaceae). It common name is karanj and the local name in Thailand is yi-talay. Taxonomic classification of *D. indica* is shown in Table 1.1. This plant is a medium sized tree growing up to 15 m or higher which is widely distributed in the tropical regions of India, Southeast Asia and Pacific Islands. Bark is thin gray to grayish brown. Branchlets are hairess with pale stipule scars. Leaves are alternate and odd-pinnate compounds, 2-4 inches long with color pinkish-red when young and glossy green when full-grown. Flowers are pea shaped, short-stalked, 15-18 mm long, lavender and white to pinkish. Fruits are pods, 3-6 cm long, smooth, thick-walled and indehiscent. Pods are yellowish-gray to brown when ripe and 1-2 seeded in pods. Seeds are elliptical or compressed ovoid, wrinkle, 1.7-2.0 cm broad and dark brown [5, 6]. Various parts of *D. indica* are depicted in Figure 1.1.

Table 1.1 Taxonomic classification of *D. indica*.

Kingdom	Plantae
Division	Magnoliophyta
Class	Magnoliopsida
Order	Fabales
Family	Leguminosae or Fabaceae
Genus	*Derris*
Species	*Derris indica* (Lamk.) Bennet

Figure 1.1 Parts of *D. indica* (Lamk.) Bennet

Source of photos: http://marinegiscenter.dmcr.go.th/km/derris-indica/

http://www.qsbg.org/database/botanic_book%20full%20option/search_detail.asp?botanic_id=2374

1.1.2 Uses of *D. indica*

Historically, all parts of *D. indica* have been used as flock medicine, green manure, animal fodder, timber, dyestuff and fuel. Moreover, seeds were used as a source of oil for the biofuel industry [7]. In folk medicines, crude of *D. indica* has been used for treatment of tumors, piles, skin diseases, wounds and ulcers [8]. The phytochemical investigation of this plant indicated the presence of flavonoids furanoflavonoids, terpenoids and alkaloids. Flavonoids obtained from *D. indica* were found to exhibit a wide range of biological activities, for example anticancer, antioxidant and anti-inflammatory. In addition, the crude of *D. indica* has been reported to have biological actives such as anticancer, anti-inflammatory, antioxidant, anti-hyperglycemic, anti-diabetic and antimicrobial [9]. Therefore, the present study is aimed to isolate and charaeterize bioactive compounds from *D. indica* stem bark and assess their biological activities, particularly anti-inflammatory and antiglycation activities. Although crude of this plant has been reported to possess anti-inflammatory activity, the compounds isolated have not been reported for this activity. In addtion, antiglycation activity is one of the prevention of diabetic complications, and a mumber of publications reported the anti-diabetic of *D. indica* crude extract. However, antiglycation activity of this plant has not been investigated yet.

Objectives of this study are as follows

1. To extract, isolate and study on chemical constituents of *Derris indica* stem bark.
2. To determine the chemical structures of isolated compounds by spectroscopic methods.
3. To assess biological activities of isolated compounds, particularly anti-inflammatory and antiglycation activities.

CHAPTER II
LITERATURE REVIEWS

2.1 Traditional medicine of *D. indica*.

A long time ago, *D. indica* has been used in herbal medicine in India and neighboring regions.

The barks are used to cure bleeding piles, tumors, wounds, skin diseases, itch, ulcers and beriberi. Moreover, Ayurvedic medicine system of India has reported use of the bark as anthelmintic, and in eye diseases and enlargement of abdomen [5]. The stem bark is used for treating diabetes and as antimicrobial agent [10, 11].

The seed oil of *D. indica* is massaged as embrocation on skin diseases, ulcers, abscess and rheumatic arthritis [12]. Powdered seeds are applied for expectorant in bronchitis and whopping cough, and they are also used as febrifuge and tonic. In addition, the seeds are carminatives, useful in inflammations and cure earache [5].

Juice from flowers is used for anti-diabetic action, dyspepsia in diabetes and for bleeding piles [13, 14].

Juice from leaves is used for treatment of cold, cough, dyspepsia, diarrhea, flatulence, gonorrhea and leprosy [8, 15, 16]. Moreover, their juice is used on herpes and itches. A hot infusion of leaves is used for relieve rheumatism [6]. The leaves are anthelmintic, laxative and digestive and used for inflammations, piles and wounds [5].

The roots are used for cleaning gums, teeth and ulcers [15]. Juice from roots is used for cleaning foul ulcers and closing fistulous sores [17]. In addition, their juice with coconut milk and lime water is used for treatment of gonorrhea [8, 18]. Young shoots have been reported to apply for treatment of rheumatism [19].

2.2 Phytochemicals of *D. indica*

D. indica is also rich in flavonoids. The phytochemical studies of this plant reported the presence of furanoflaovones, furanoflavonols, chromenoflavones, flavones, furanodiketones and flavonoid glycosides [20-22]. Furthermore, other classes of compounds were detected in this plant such as alkaloid, sesquiterpene, diterpenes, triterpenes, steroids, esters, fatty acids, amino acid derivatives and disaccharides [9].

2.2.1 Flavonoids

Flavonoids are common polyphenolic compounds of plant secondary metabolites containing 15 carbon atoms and two benzene rings are joined together with a linear three carbon chain. Flavonoids consist of six major subgroups such as chalcone, flavone, flavonol, flavanone, anthocyanins and isoflavonoids. These compounds have been distributed in plant materials, dietary fruits, vegetables, nuts and plant derived beverages like tea, wine, coffee, beer, and fruit drinks. Flavonoids have been reported to possess a wide range of biological activities in the prevention of diseases, treatment of health problems, coronary heart diseases, neurodegenerative diseases and gastrointestinal disorders. Moreover, they have been reported to apply for anti-cancer, anti-allergic, antioxidant, anti-inflammatory, anti-viral, anti-platelet and other [23, 24].

The chemical structures of flavonoids are based on a benzene ring (A) condensed with a six-member ring (C) in which the 2-position carries a phenyl ring (B) as a substituent (Fig 2.1). Flavonoids are classified according to substitutions. Both the oxidation state of the heterocyclic ring and the position of ring B are important in the classification (Fig 2.2) [25]. Flavonoids isolated from *D. indica* differ in the arrangements of hydroxyl, methoxy, and glycosidic side groups, as well as conjugation between the A and B rings. These are shown in Table 2.1.

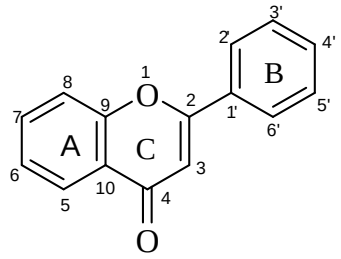

Figure 2.1 General chemical structure of flavonoid

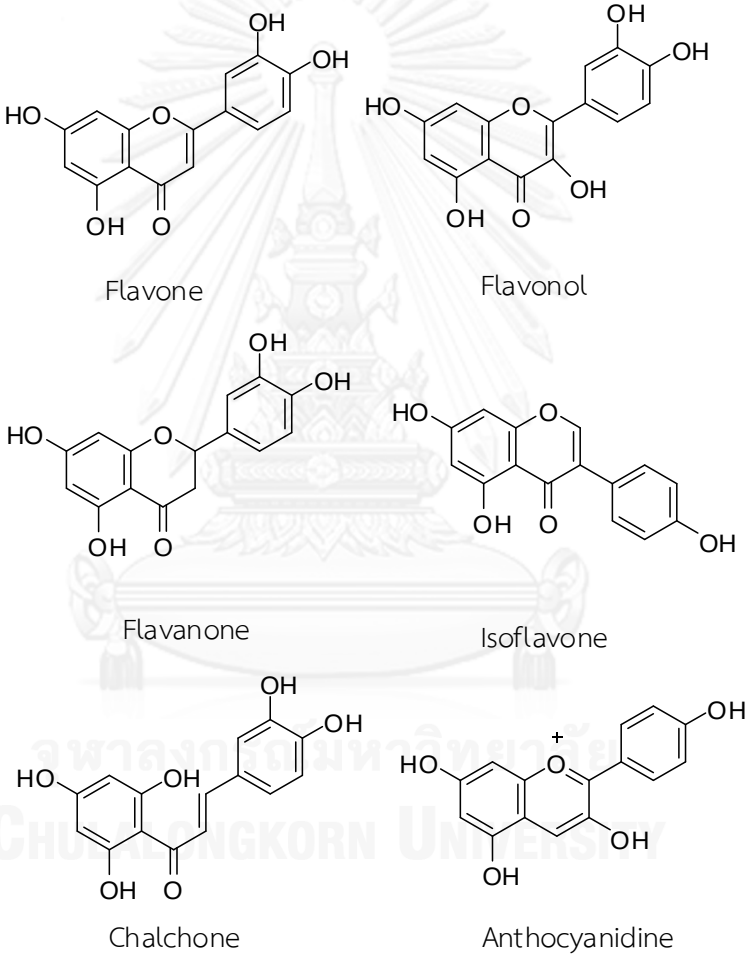

Figure 2.2 Chemical structures of the main classes of flavonoids

Table 2.1 Flavonoids isolated from *D. indica*.

Compound name and structure	Type	Plant part	Reference
Fisetin tetramethyl ether 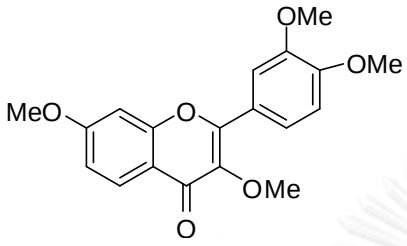	Flavone	Flower, stem bark	[26, 27]
3,7-dimethoxyflavone 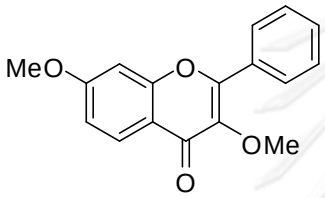	Flavone	Root bark	[11, 27]
Luteolin 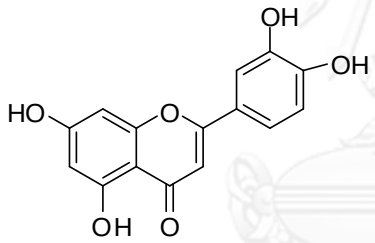	Flavone	Stem	[28]
7-O-methyl chrysin 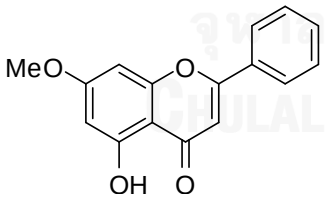	Flavone	Root	[29]
7,4′-dimethoxy-5 -hydroxyflavone 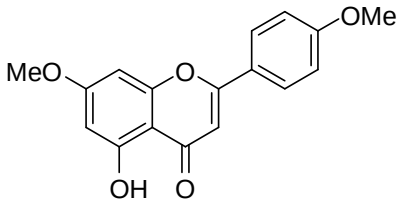	Flavone	Root	[29]

Table 2.1 Flavonoids isolated from *D. indica*. (continued)

Compound name and structure	Type	Plant part	Reference
Kaempferol 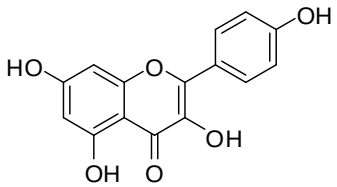	Flavonol	Leaves	[30]
Quercetin 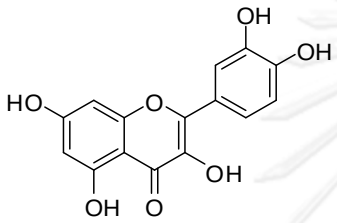	Flavonol	Leaves	[30]
Demethoxykanugin 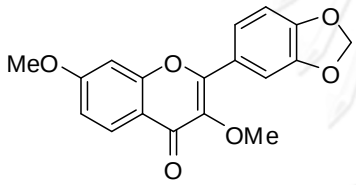	Methylenedioxy flavone	Root bark, flower, stem bark	[26, 27, 31]
3-methoxy-7-hydroxy-3 ,4-methylenedioxyflavone 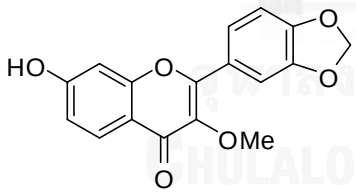	Methylenedioxy flavone	Root	[29]
Kanugin 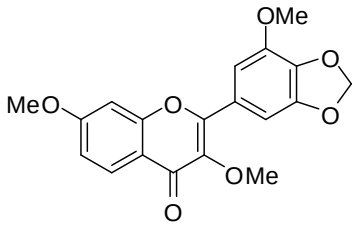	Methylenedioxy flavone	Root, flower, stem bark	[26, 32]

Table 2.1 Flavonoids isolated from *D. indica*. (continued)

Compound name and structure	Type	Plant part	Reference
3,4-methylenedioxy-10-methoxy-7-oxo[2]benzopyrano [4,3-b]benzopyran 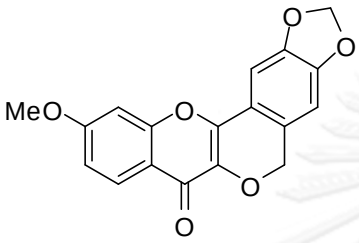	Methylenedioxy flavone	Root,stem	[11]
Lanceolatin B 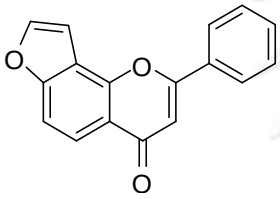	Furanoflavone	Flower, bark, root bark	[26, 27, 33]
Karanjin 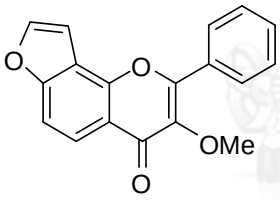	Furanoflavone	Seed, flower, root, stem bark	[26, 27]
3′-methoxyfuro[8,7:4″,5″] flavone 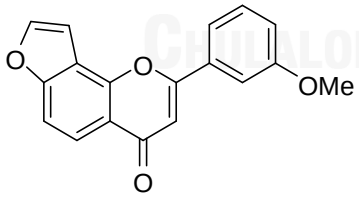	Furanoflavone	Fruit	[22]

Table 2.1 Flavonoids isolated from *D. indica*. (continued)

Compound name and structure	Type	Plant part	Reference
Pongaglabol methyl ether 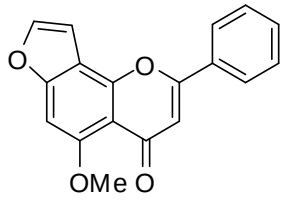	Furanoflavone	Flower	[32]
Pachycarin D 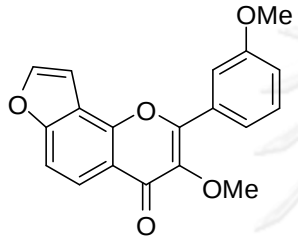	Furanoflavone	Root,stem	[11]
Pongol 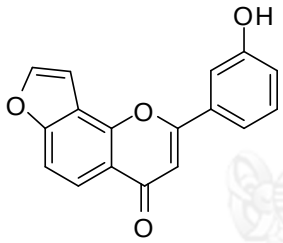	Furanoflavone	Fruit	[22]
Pongaglabol 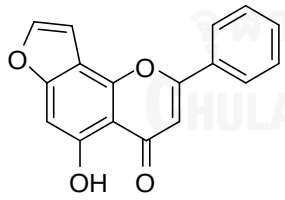	Furanoflavone	Flower	[21]
Isopongaglabol 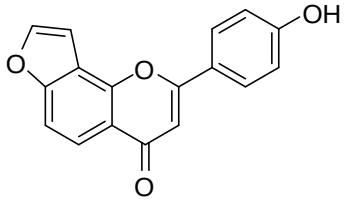	Furanoflavone	Flower	[32]

Table 2.1 Flavonoids isolated from *D. indica*. (continued)

Compound name and structure	Type	Plant part	Reference
Kanjone 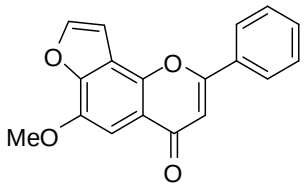	Furanoflavone	Flower, seed	[21, 34]
6-methoxyisopongaglabol 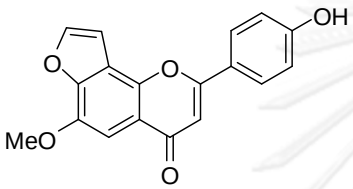	Furanoflavone	Flower	[32]
6-methoxyisopongaglabol methyl ether 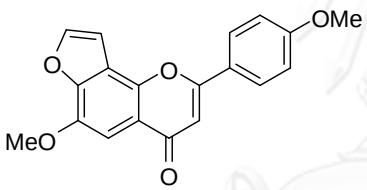	Furanoflavone	Flower	[32]
Pongapinnol C 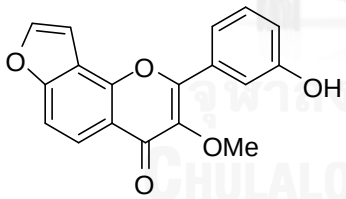	Furanoflavone	Fruit	[22]
Pongapinnol D 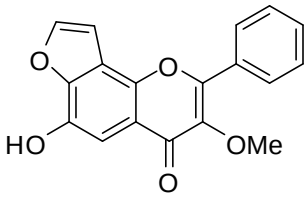	Furanoflavone	Fruit	[22]

Table 2.1 Flavonoids isolated from *D. indica*. (continued)

Compound name and structure	Type	Plant part	Reference
2′,5′-dimethoxyfuro[8,7:4″,5″] flavone 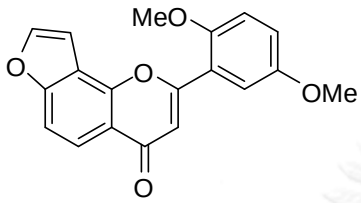	Furanoflavone	Fruit	[22]
Millettocalyxin C 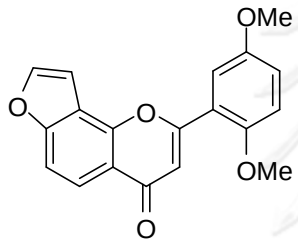	Furanoflavone	Stem bark	[31]
Pongapinnol B 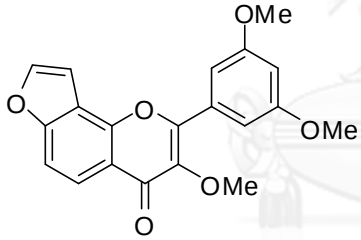	Furanoflavone	Fruit	[22]
Pongapinnol A 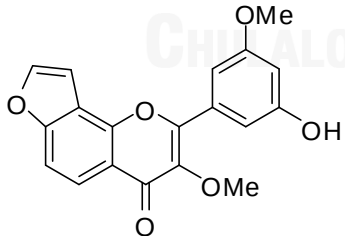	Furanoflavone	Fruit	[22]

Table 2.1 Flavonoids isolated from *D. indica*. (continued)

Compound name and structure	Type	Plant part	Reference
3',4'-dihydroxy-4H-furo[2,3-h] chromen-4-one 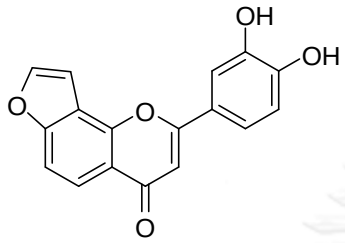	Furanoflavone	Root	[29]
3,3' ,4'-trihydroxy-4H-furo[2,3-h] chromen-4-one 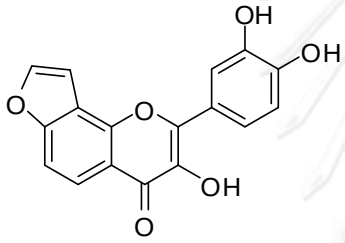	Furanoflavone	Root	[29]
Pongaglabrone 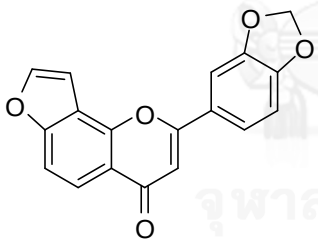	Furanoflavone	Seed, root bark	[27, 34]
Pongapin 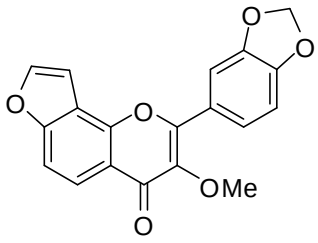	Furanoflavone	Seed, root bark, stem bark	[26, 27, 33]

Table 2.1 Flavonoids isolated from *D. indica*. (continued)

Compound name and structure	Type	Plant part	Reference
5-methoxy-3′, 4′-methylenedioxyfurano (8,7-4″,5″) flavone 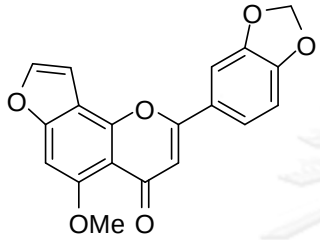	Furanoflavone	Flower	[32]
2′-methoxy-4′, 5′-methylenedioxyfurano [7,8:4″,5″]-flavone 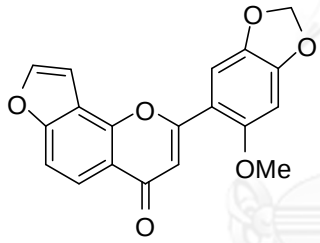	Furanoflavone	Root, stem	[11]
3′-methoxypongapin 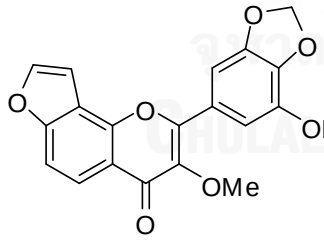	Furanoflavone	Stem bark	[28, 35]

Table 2.1 Flavonoids isolated from *D. indica*. (continued)

Compound name and structure	Type	Plant part	Reference
Pinnatin 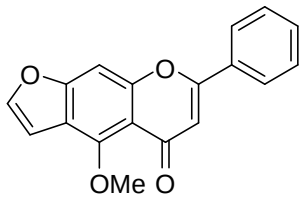	Furanoflavone	Flower	[21]
Glabone 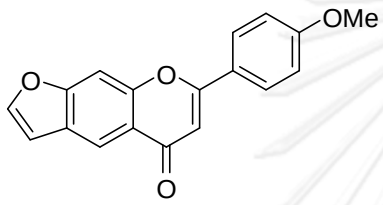	Furanoflavone	Flower	[36]
Ponganone XI 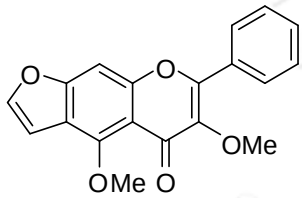	Furanoflavone	Root bark	[27]
Pongamone D 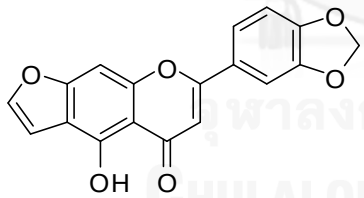	Furanoflavone	Stem	[28]
Pongaflavone/ karanjachromene 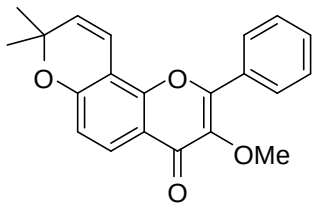	Chromenoflavone	Seed Stem Root	[11, 37]

Table 2.1 Flavonoids isolated from *D. indica*. (continued)

Compound name and structure	Type	Plant part	Reference
Isopongaflavone/candidin 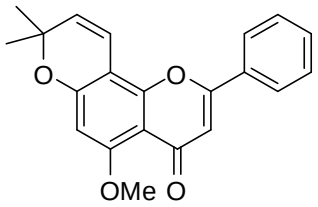	Chromenoflavone	Stem bark Root bark	[27, 33, 35]
5-methoxy-(3″,4″-dihydro-3″,4″-diacetoxy)-2″,2″-dimethylpyrano-(7,8:5″,6″)-flavone 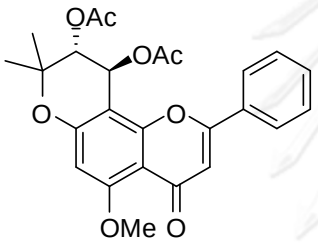	Chromenoflavone	Stem bark	[33, 35]
3-methoxy-(3″,4″-dihydro-3″,4″-diacetoxy)-2″,2″ dimethylpyrano-(7,8:5″,6″)-flavone 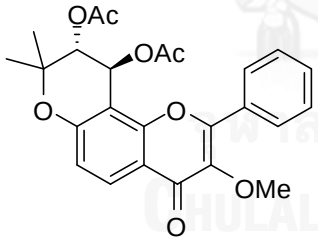	Chromenoflavone	Root, stem	[11]

Table 2.1 Flavonoids isolated from *D. indica*. (continued)

Compound name and structure	Type	Plant part	Reference
3-methoxy-(3″,4″-dihydro-3″-hydroxy-4″- acetoxy)-2″,2″-dimethylpyrano-(7,8:5″,6″)- flavone 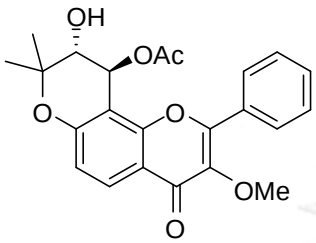	Chromenoflavone	Stem bark	[38]
3-methoxy-(3″,4″-dihydro-4″-hydroxy-3″- acetoxy)-2″,2″-dimethylpyrano-(7,8:5″,6″)- flavone 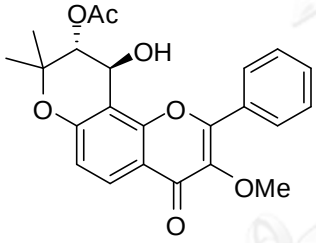	Chromenoflavone	Stem bark	[38]
Isopongachromene 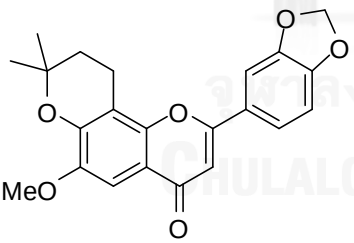	Chromenoflavone	Seed	[34]

Table 2.1 Flavonoids isolated from *D. indica*. (continued)

Compound name and structure	Type	Plant part	Reference
5-methoxy-3′,4′-methylenedioxy-2″,2″- dimethylpyrano(7,8-6″,5″) flavone 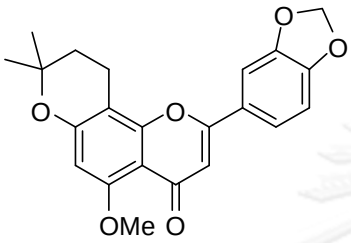	Chromenoflavone	Stem bark	[26]
Pongachromene 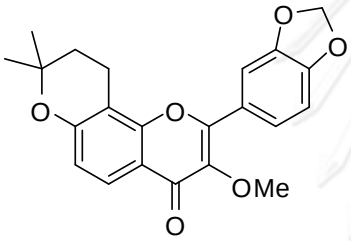	Chromenoflavone	Root, stem	[11, 26]
Pongamoside A 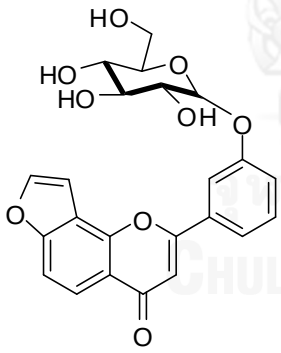	Flavonoid glycoside	Fruit	[20]

Table 2.1 Flavonoids isolated from *D. indica*. (continued)

Compound name and structure	Type	Plant part	Reference
Pongamoside B 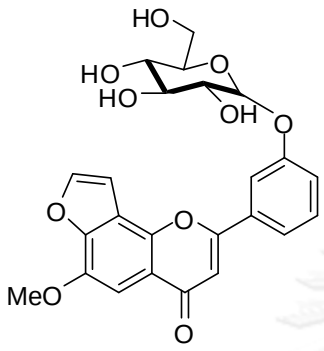	Flavonoid glycoside	Fruit	[20]
Pongamoside C 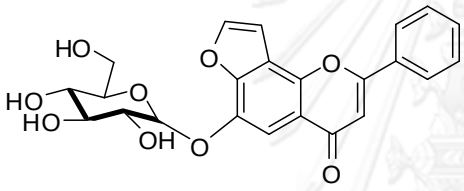	Flavonoid glycoside	Fruit	[20]
Pongamoside D 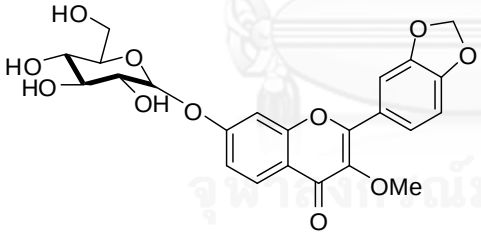	Flavonoid glycoside	Fruit	[20]
Vitexin 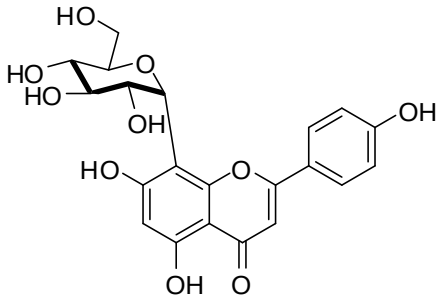	Flavonoid glycoside	Leaves	[30]

Table 2.1 Flavonoids isolated from *D. indica*. (continued)

Compound name and structure	Type	Plant part	Reference
Isoquercitrin 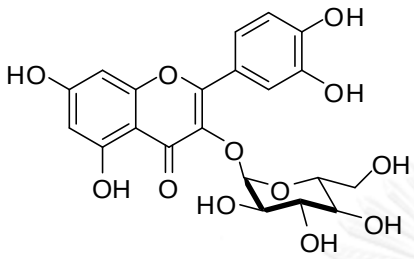	Flavonoid glycoside	Leaves	[30]
Kaempferol 3-O-β-D-glucopyranoside 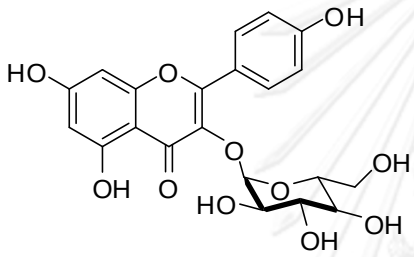	Flavonoid glycoside	Leaves	[30]
Kaempferol 3-O-β-D-rutinoside 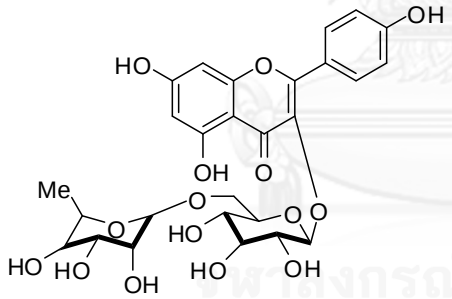	Flavonoid glycoside	Leaves	[30]
Rutin 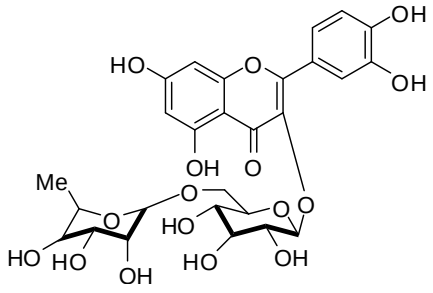	Flavonoid glycoside	Leaves	[30]

Table 2.1 Flavonoids isolated from *D. indica*. (continued)

Compound name and structure	Type	Plant part	Reference
Vicenin-2 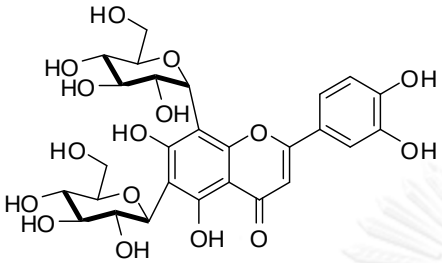	Flavonoid glycoside	Leaves	[30]
4′-O-methyl-genistein7-O-β-D-rutinoside 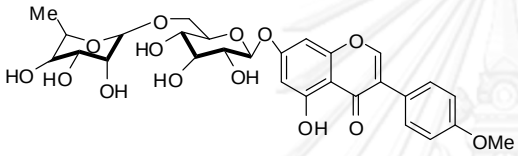	Flavonoid glycoside	Leaves	[30]
2′,5′-dimethoxy-genistein7-O-β-D-apiofuranosyl-(1″-6″)-O-β-D-glucopyranoside 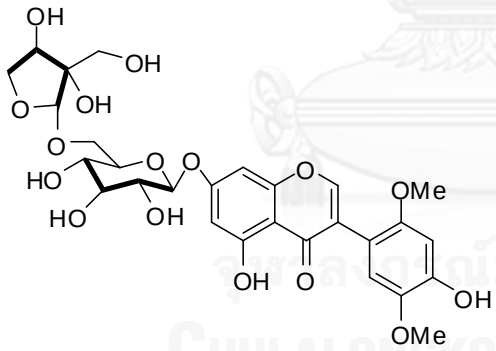	Flavonoid glycoside	Leaves	[30]
Ovalifolin 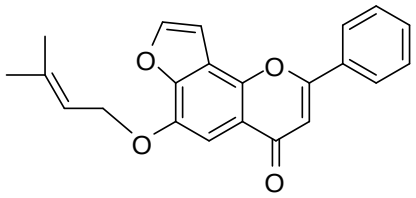	Furanoflavone	Root bark	[27]

Table 2.1 Flavonoids isolated from *D. indica*. (continued)

Compound name and structure	Type	Plant part	Reference
Pongamone A 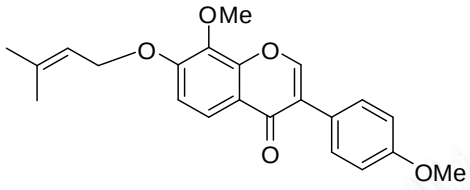	Isoflavone	Root, stem	[11, 28]
5-hydroxy-4′-methoxy-7-[(3-methyl-2-butenyl)oxy]-isoflavone 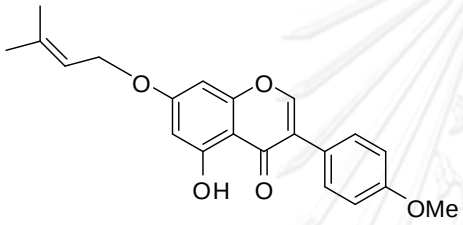	Isoflavone	Stem	[28]
Pongacoumestan 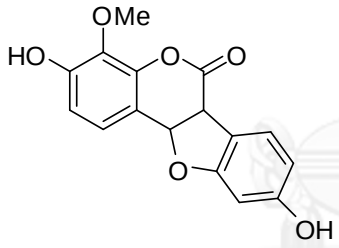	Coumestan	Fruit	[22]
Maackiain 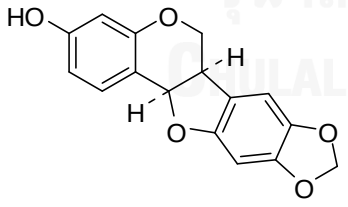	Pterocarpan	Root, stem	[11]
Medicarpin 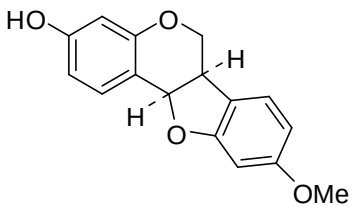	Pterocarpan	Root, stem	[11]

Table 2.1 Flavonoids isolated from *D. indica*. (continued)

Compound name and structure	Type	Plant part	Reference
11,12a-dihidroxy-munduserone 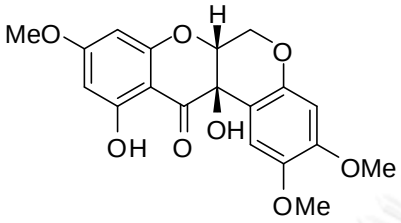	Rotenoid	Leaves	[30]
12a-hydroxy-**α**-toxicarol 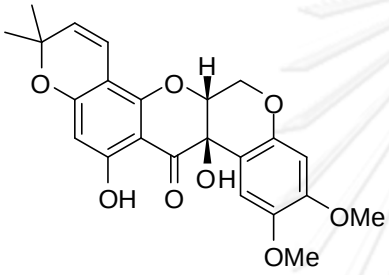	Rotenoid	Leaves	[30]
Pongamiaflavonylflavonol 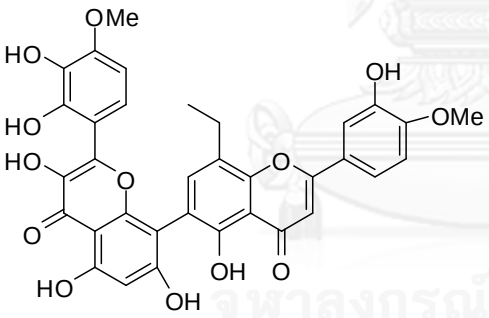	Diflavone	Pod	[39]
(2S)-5,7-dimethoxy-8-formylflavanone 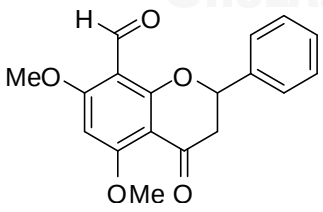	Flavanone	Stem bark	[35]

Table 2.1 Flavonoids isolated from *D. indica*. (continued)

Compound name and structure	Type	Plant part	Reference
Pongamone E 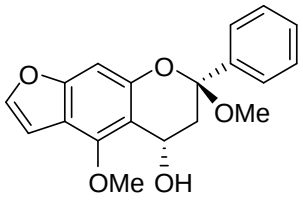	Furanoflavan-4-ol	Stem	[28]
(2S)-(2″,3″:7,8)-furanoflavanone 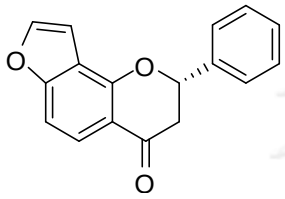	Furanoflavanone	Fruit	[33]
3′,4′-methylenedioxy-(4″,5″:7,8)-furanoflavanone 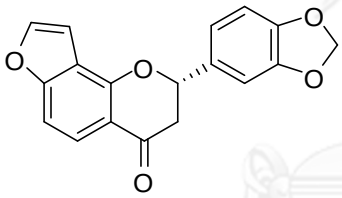	Furanoflavanone	Stem	[28]
Isolonchocarpin 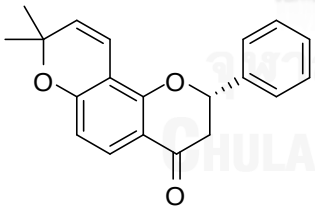	Chromenoflavanone	Flower, Stem bark	[33, 40]
Pongachin 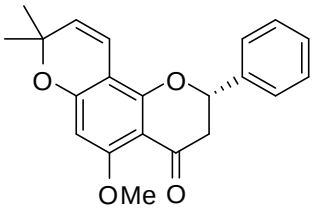	Chromenoflavanone	Stem	[28]

Table 2.1 Flavonoids isolated from *D. indica*. (continued)

Compound name and structure	Type	Plant part	Reference
Ponganone III 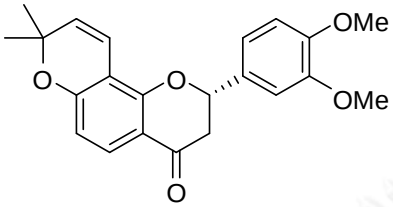	Chromenoflavanone	Root bark	[27]
Ponganone IV 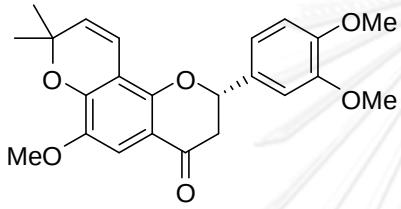	Chromenoflavanone	Root bark	[27]
Ovalichromene B 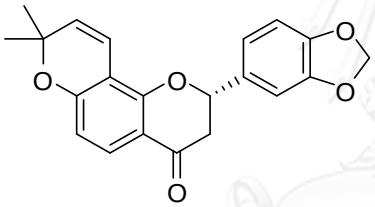	Chromenoflavanone	Flower	[28]
5-Methoxy-3' ,4'-methylenedioxy-6" ,6" –dimethylpyrano-[2" ,3":7,8] flavone 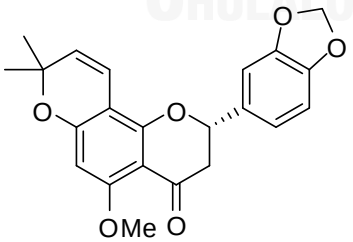	Chromenoflavanone	Root bark	[26, 27]

Table 2.1 Flavonoids isolated from *D. indica*. (continued)

Compound name and structure	Type	Plant part	Reference
Pongamone B 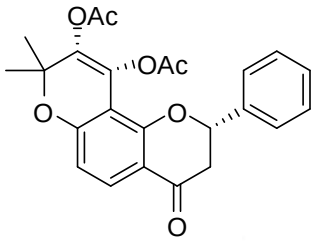	Chromenoflavanone	Stem	[28]
Pongaflavanol 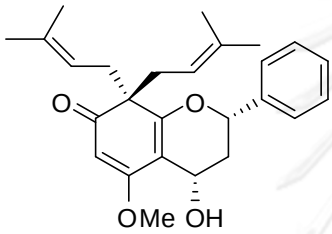	Flavan-4-ol	Stem bark	[38]
Ovaliflavanone A 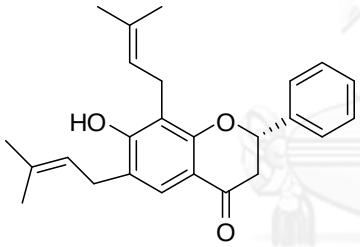	Flavanone	Stem bark	[40]
Candidone 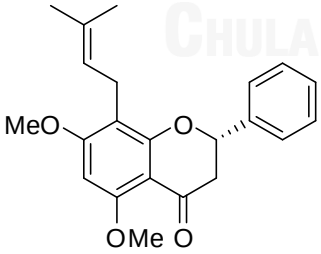	Flavanone	Stem bark	[35]
Ponganone V 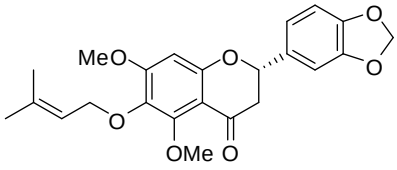	Flavanone	Root bark	[27]

Table 2.1 Flavonoids isolated from *D. indica*. (continued)

Compound name and structure	Type	Plant part	Reference
(2S)-5,7-dimethoxy-8-(2R-hydroxy- 3-methyl-3-butenyl)flavanone 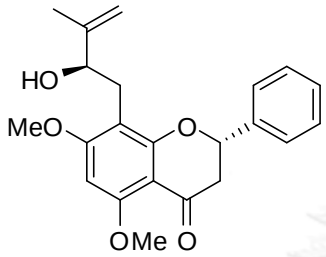	Flavanone	Stem bark	[35]
(2S)-5,7-dimethoxy-8-(2S-hydroxy- 3-methyl-3-butenyl)flavanone 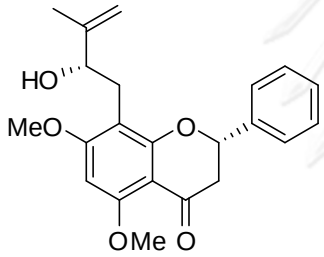	Flavanone	Stem bark	[35]
(2S)-5,7-dimethoxy-8-(2S-hydroxy- 3-methyl-3-butenyl)-3′,4′-methylenedioxyflavanone 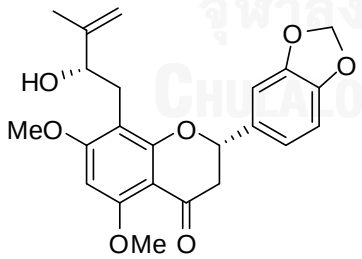	Flavanone	Stem bark	[35]

Table 2.1 Flavonoids isolated from *D. indica*. (continued)

Compound name and structure	Type	Plant part	Reference
Pongapinone B 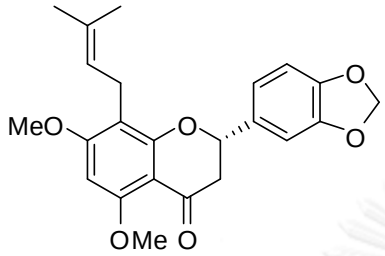	Flavanone	Stem bark	[35]
Pongamone C 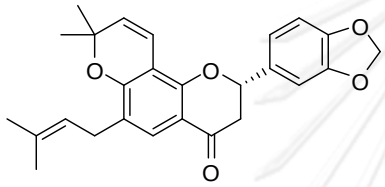	Chromenoflavanone	Stem	[28]
6,7,2″,2″-dimethylchromono-8-dimethylallylflavanone 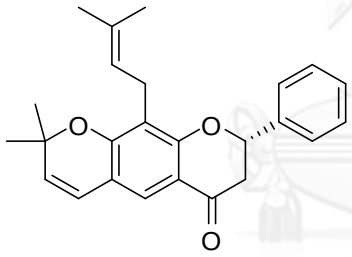	Chromenoflavanone	Stem bark	[38]
2′-hydroxy-3,4,4′, 6′-tetramethoxychalcone 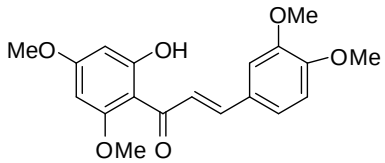	Chalcone	Root bark	[27]

Table 2.1 Flavonoids isolated from *D. indica*. (continued)

Compound name and structure	Type	Plant part	Reference
Ponganone X 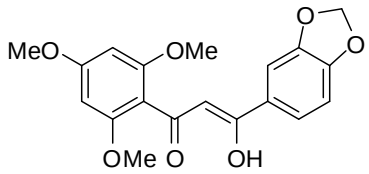	Furanochalcone	Root bark	[27]
Milletenone 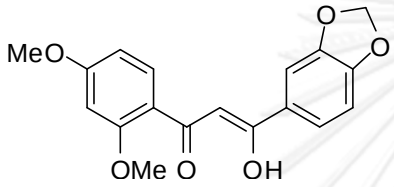	Furanochalcone	Root bark	[27]
Ponganone VII 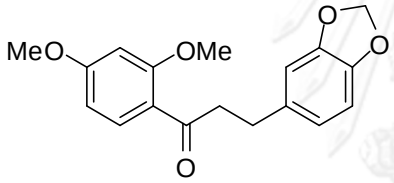	Furanochalcone	Root bark	[27]
Dihydromilletenone methyl ether 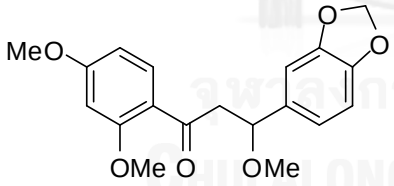	Furanochalcone	Root bark	[27]
Pongamol 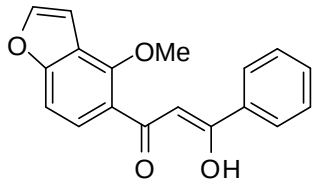	Furanochalcone	Seed, flower, root	[27, 33]

Table 2.1 Flavonoids isolated from *D. indica*. (continued)

Compound name and structure	Type	Plant part	Reference
Ovalitenone 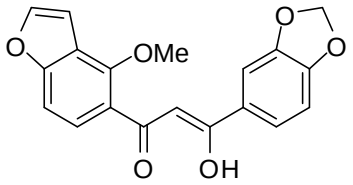	Furanochalcone	Flower, stem bark, root	[26, 27]
Ovalitenin B 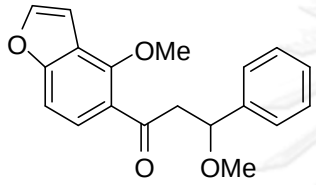	Furanochalcone	Root bark	[27]
Ponganone IX 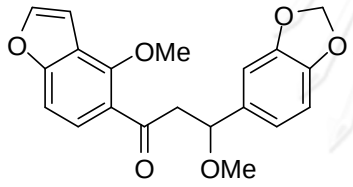	Furanochalcone	Root bark	[27]
Obovatachalcone 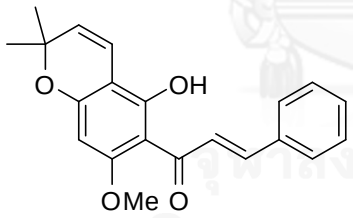	Chromenochalcone	Seed, stem bark	[34, 38]
Ponganone VI 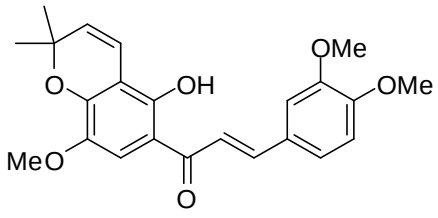	Chromenochalcone	Root bark	[27]

Table 2.1 Flavonoids isolated from *D. indica*. (continued)

Compound name and structure	Type	Plant part	Reference
Glabrachalcone 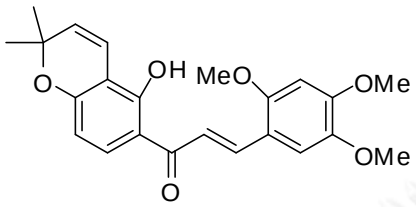	Chromenochalcone	Seed	[34]
Glabrachromene 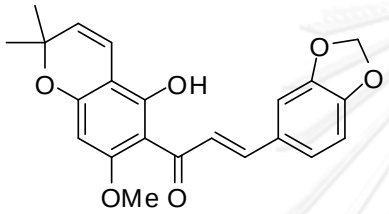	Chromenochalcone	Stem bark	[26]
Ponganone I 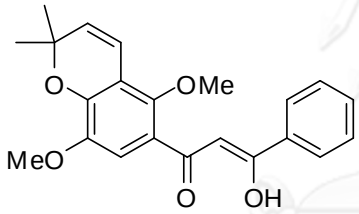	Chromenochalcone	Root bark	[27]
Praecansone B 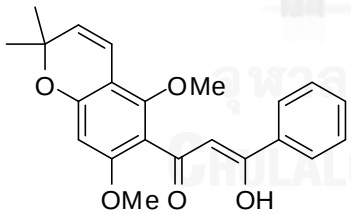	Chromenochalcone	Stem bark	[35]
Ponganone II 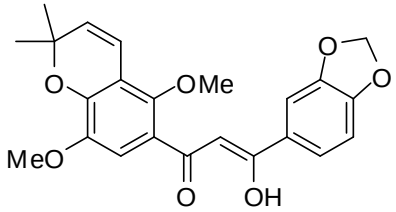	Chromenochalcone	Root bark	[27]

Table 2.1 Flavonoids isolated from *D. indica*. (continued)

Compound name and structure	Type	Plant part	Reference
Pongapinone A 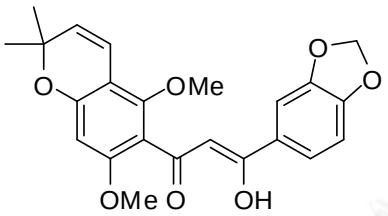	Chromenochalcone	Stem bark	[35, 41]
Glabrachromene II 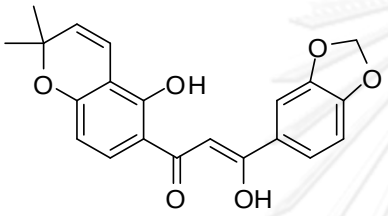	Chromenochalcone	Seed	[28]
7-methoxypraecansone B 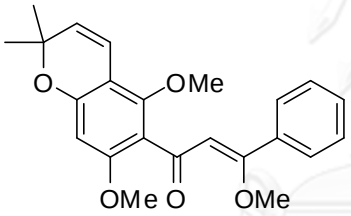	Chromenochalcone	Stem bark	[35]
Ponganone VIII 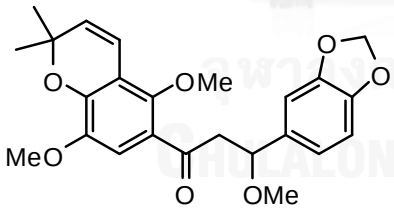	Chromenochalcone	Root bark	[27]

Table 2.1 Flavonoids isolated from *D. indica*. (continued)

Compound name and structure	Type	Plant part	Reference
Pongagallone A 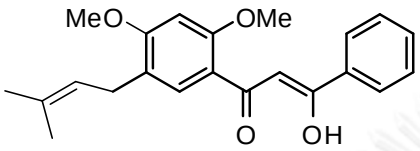	Chalcone	Leaves	[42]
Pongagallone B 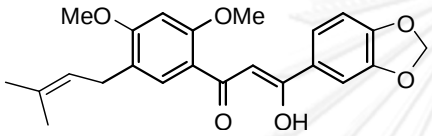	Chalcone	Leaves	[42]
Tunicatachalcone 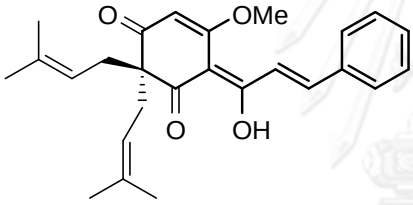	Enolchalcone	Stem bark	[40]

2.3 Pharmacological activities

Extensive traditional medicines of *D. indica* led to many pharmacological studies of this plant.

2.3.1 Anti- inflammatory activity

In 2001, Srinivasan and coworkers reported the ethanolic extract of *D. indica* (*Pongamia pinnata*) leaves exhibited significant anti-inflammatory activity in acute (carrageenin, histamine, 5-hydroxytryptamine, and prostaglandin E2-induced paw edema), subacute (kaolin-carrageenin and formaldehyde-induced paw edema), chronic (cotton pellet-induced granuloma) inflammation in rat model at doses of 300, 1000 mg/kg. Moreover, this extract did not show any sign of toxicity and mortality up to a dose level of 10.125 g/kg, per oral (p.o.) in rats [43].

In 2008, Ganesh and coworkers evaluated anti-inflammatory activity of *D. indica* (*P. glabra)* crude extract. The leaf gall extract with ethanol at doses of 200 and 400 mg/kg, p.o. showed inhibition on carrageenan, histamine and serotonin-induced paw edema (acute inflammation), as well as cotton pellet-induced granuloma (chronic inflammation), in rat. In analgesic activity, the extract significantly reduced the writhing responses induced by an intraperitoneal injection of acetic acid in rats [44].

In 2010, Sager and coworkers studied anti-inflammatory activity of stem bark of *D. indica* (*P. pinnata*). The methanolic extract (200, 500 and 1000 mg/kg) exhibited significant anti-inflammatory activity in acute (carrageenan-induced paw edema) and chronic (cotton pellet-induced granuloma) in rat. In addition, it did not show any sign of toxicity and mortality up to a dose level of 10.125 g/kg, p.o. in mice. [45].

In 2012, Badole and coworkers have reported the alcoholic extract of *D. indica* (*P. pinnata*) bark. The crude extract showed significant analgesic and anti-inflammatory activity in acute and chronic models in rats. This extract displayed a significant inhibition in carrageenin-induced rat hind paw edema at doses of 300 and 1000 mg/kg. In cotton pellet granuloma, It significantly decreased the granuloma weight at doses of 100, 300 and 1000 mg/kg [46].

2.3.2 Antimicrobial activity

In 2006, Koysomboon and coworkers discovered four new flavonoids, namely 3-methoxy-(3",4"-dihydro-3",4"-diacetoxy)-2",2"-dimethylpyrano-(7,8:5",6")-flavone, 2'–methoxy-4',5'-methylenedioxyfurano [7,8:4",5"]-flavone, 8,4'-dimethoxy-7-O-c,c-dimethylally-lisoflavone, and 3,4-methylenedioxy-10-methoxy-7-oxo[2]benzo

pyrano[4,3-b]benzopyran, from the stems and roots of *D. indica*. Moreover, ten known flavonoids, including desmethoxy kanugin, karanjin, lacheolatin B, pongachromene, 3,7-dimethoxyflavone, pachycarin D, maackiain, medicarpin, karanjachromene, and pinnatin were obtained. These flavonoids exhibited antimycobacterial activity against *Mycobacterium tuberculosis H37Ra*, with MIC

between 6.25 and 200 µg/mL, while 2'–methoxy-4',5'-methylenedioxyfurano [7,8:4",5"]-flavone and karanjin did not show any significant activity [11].

In 2010, Kesari and coworkers discovered antimicrobial activity of *D. indica* (*P. pinnata*). The oil displayed antibacterial activity against *Yersinia enterococcai*, *Listeria monocytogens*, *Escherichia coli* and *Salmonella paratyphi*. The 90% oil concentration with DMSO gave more inhibition rather 100% oil. Besides, it showed maximum antifungal activity against *Aspergillus niger, Candida albicans* and *Aspergillus terreus* at 100% oil concentration [47].

In 2013, Rani and coworkers studied antibacterial activity of *D. indica* (*P. pinnata*) seeds. The methanol and ethanol extract of *P. pinnata* seeds at concentration of 100 µg/mL exhibited significant antibacterial activity. Both extracts gave the maximum inhibition against *Pseudomonas aeruginosa*, with inhibition zone of 20 mm and 18.5 mm, respectively [48].

2.3.3 Anticancer activity

In 2012, Chinnasamy and coworkers presented anti-cancer activity of *D. indica* (*P. glabra*) seed oil. It exhibited inhibitory effect on human cancer cell lines, MCF-7 and HeLa, with the same IC_{50} value of 6 mg/ml [49].

2.3.4 Anti-diabetic activity

In 2006, Punitha and coworkers evaluated antihyperglycemic activity of *D. indica* (*P. pinnata*) flowers in alloxan induced diabetic rats. Its ethanolic extract at a dose of 300 mg/kg demonstrated significant antihyperglycemic activity, which considerably reduced the blood glucose levels in comparison with glibenclamide at a dose of 600 mg/kg in alloxan induced diabetic rats [50].

In 2008, Tamrakar and coworkers identified pongamol and karanjin as lead compounds with antihyperglycemic activity from fruits of *D. indica* (*P. pinnata*). In streptozotocin-induced diabetic rats, pongamol and karanjin showed significant antihyperglycemic activity of 12.8% and 11.7% at dose of 50 mg/kg, and 22.0% and 20.7% at dose of 100 mg/kg respectively. Besides, both compounds significantly lowered blood glucose level of 35.7% and 30.6% at dose of 100 mg/kg, respectively, in diabetes and dyslipidemia mice (db/db mice) [51].

In 2009, Ranga Rao and coworkers reported the isolation and characterization of two new furanoflavanoids, named 3',4'-dihydroxy-4H-furo[2,3-h] chromen-4-one and 3,3',4'-trihydroxy-4H-furo[2,3-h] chromen-4-one from roots of *D. indica*. These furanoflavanoids demonstrated moderate intestinal α-glucosidase inhibitory by 25.6% and 37.9% at 25 μg/mL concentration, respectively. Furthermore, they also showed DPPH scavenging activity by 55.1% and 64.9% at 50 μg/mL concentration, respectively [29].

CHAPTER III

EXPERIMENTS

3.1 Plant material

The stem bark of *Derris indica* (Lamk.) Benet was collected from mangrove forest in Satun province, Thailand, in November 2012. The plant was identified and authenticated by Mrs. Pranom Chumriang, Forestry Technical Officer, Senior Professional Level of Mangrove Extension, Learing and Development Center 5 (Satun), Thailand.

3.2 Chemicals for preparation and isolation

3.2.1 Solvents

The commercial grade solvents used for extraction, Thin-layer chromatography (TLC) and column chromatography were hexane, chloroform ($CHCl_3$) dichlormethane (CH_2Cl_2), ethyl acetate (EtOAc), acetone and methanol (MeOH). All solvent were purified by distillation prior to use.

Chloroform-D ($CDCl_3$), a deuterated solvent was used for NMR experiments.

3.2.2 Other materials

TLC analysis was carried out on Merck's TLC silica gel 60 F_{254} aluminum sheets, 20x20 cm. Detection was visualized under ultraviolet light at a wavelength of 254 nm and dipped with $(NH_4)_6Mo_7O_{24}$ solution in 5% H_2SO_4/EtOH.

Column chromatography was performed by using Merck's silica gel 60 code No. 7734 and No. 9385, and Pharmacia's Sephadex LH-20 code No. 17-0090-01 as open column packing materials.

3.3 General experimental procedures

3.3.1 Nuclear magnetic resonance spectrometer (NMR)

The NMR (^{1}H- and ^{13}C-NMR) spectra were recorded on a Bruker AV-400 spectrometer operating at 400 MHz for ^{1}H and at 100 MHz for ^{13}C nuclei, respectively. Chemical shifts were reported in ppm relative to TMS (tetramethylsilane) as an internal standard.

3.3.2 Mass spectrometer (MS)

HRESIMS spectra were recorded on a Bruker micrOTOF-Q II.

3.3.3 Optical rotation

Optical rotations of the compounds were measured on a Perkin-Elmer 341 polarimeter using a sodium lamp at 589 nm.

3.3.4 Ultraviolet-visible spectrophotometer (UV-vis)

UV-vis data were examined by a CARY 50 Probe UV-visible spectrophotometer. Compounds were prepared in solution of MeOH.

3.3.5 X-ray crystallography

The crystal structures were elucidated by Single-crystal X-Ray Diffraction analysis and direct methods. Crystallographic data, excluding structure factors, have been deposited at the Cambridge Crystallographic Data Centre.

3.3.6 Melting point

Melting points of isolated compounds were measured on a Fisher-Johns melting point apparatus.

3.4 Extraction and isolation

The air-dried and powered stem bark of *D. indica* (2 kg) was extracted three times with MeOH at room temperature each for 2 day. The solution of *D. indica* extract was filtered and evaporated under vacuum. The combined MeOH crude extract was suspended in H_2O, then partitioned with EtOAc (250 mL) to yield the dark brown EtOAc crude extract (27 g).

The EtOAc crude extract was subjected to quick column chromatography over silica gel eluted with gradient mixtures of EtOAc-hexane (10%-100%) and MeOH-CH_2Cl_2 (5%-20%) to give 11 major fractions. All fractions were analyzed by TLC and ^{1}H NMR spectroscopy. Fraction 7 was chromatographed on silica gel column eluted with EtOAc-hexane (10%-50%) to give 12 subfractions and to afford compound **1** (3.7 mg). Subfraction 7.2 was further applied to Sephadex LH-20 column using MeOH to yield compound **2** (7.1 mg). Subfraction 7.7 was purified by silica gel column chromatography using mixture of acetone-hexane (15%-40%) to obtain compound **3** (21.1 mg). Subfraction 7.10 was chromatographed on silica gel column eluting with acetone-hexane (15%-40%) to afford compound **4** (9.6 mg). Furthermore, subfraction 7.5 was separated by silica gel column chromatography eluted with EtOAc-hexane (20%-50%) to yield compound **5** (4 mg), compound **6** (4.2 mg), while purification of subfraction 7.6 by the same condition led to the isolation of compound **7** (3.9 mg).

Fraction 8 was separated by silica gel column chromatography eluted with acetone-hexane (10%-50%) to afford compound **8** (47.4 mg) and to give 20 subfractions. Subfraction 8.17 was further subjected to silica gel column chromatography eluting with acetone-hexane (10%-50%) to give compound **9** (25.5 mg), and subfraction 8.14 afforded compound **10** (171.8 mg) by using the same condition and method. Fraction 6 was subjected to silica gel column chromatography with gradient mixtures of acetone-hexane (15%-60%) to furnish compound **11**. Fraction 3 was separated by silica gel column chromatography using EtOAc-hexane (15%-50%) and then recrystallized with $CHCl_3$ to afford compound **12** (50.6 mg). Fraction 10 was chromatographed on silica gel column eluting with acetone-CH_2Cl_2 (15%-40%) and then with mixtures of MeOH-CH_2Cl_2 (5%-10%) to obtain compound **13** (7.4 mg).

The schemes 3.1 and 3.2 summarize the extraction and isolation of the EtOAc extract of *D. indica* stem bark.

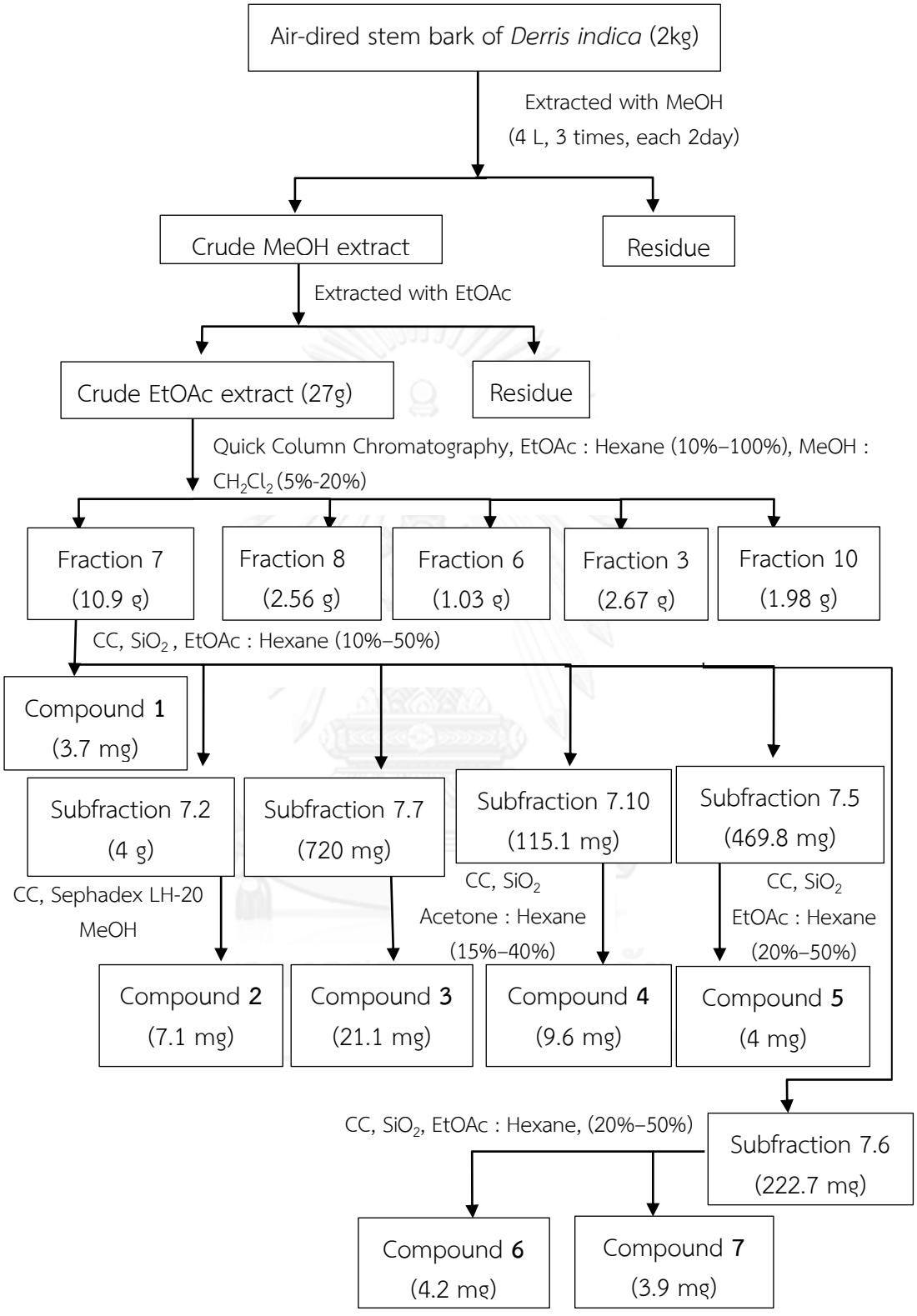

Scheme 3.1 The extraction and isolation procedure of *D. indica* stem bark

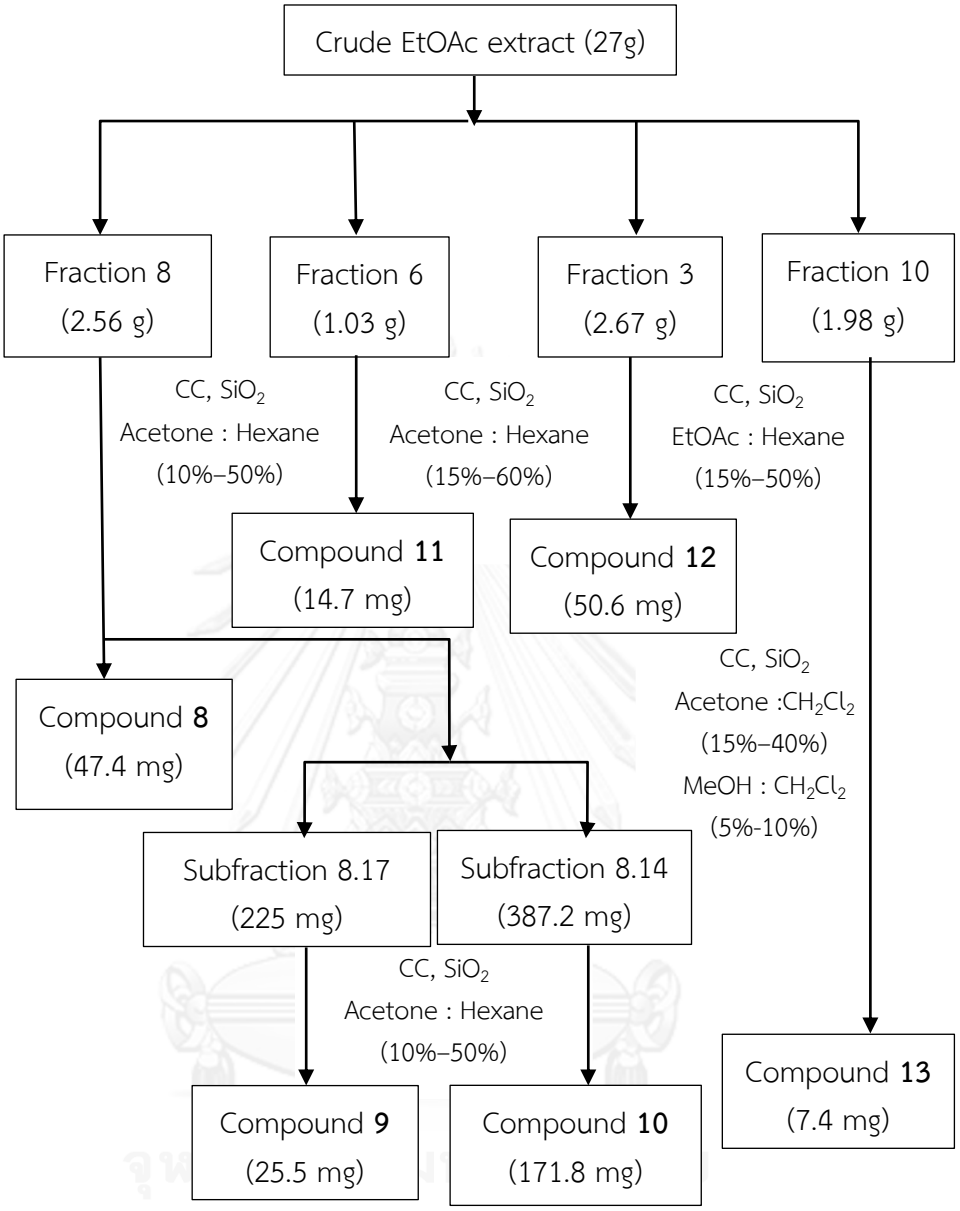

Scheme 3.2 The extraction and isolation procedure of *D. indica* stem bark

(continued)

3.4 Anti-inflammatory assay

3.4.1 Cell line

Murine macrophage J774.A1 cell lines were continuously cultured in Dulbeco's modified Eagle's medium (DMEM) supplemented with 10% fetal bovine serum (FBS), 11.0 mg/mL sodium pyruvate, 238.3 mg/mL HEPES, 100 units/mL penicillin and 100 µg/mL streptomycin. The cultured cell lines were maintained at 37 °C in humidity atmosphere of 5% CO_2.

3.4.2 Preparation of stock solution of compounds

Each compound was dissolved in dimethyl sulfoxide (DMSO) for cell culture grade at concentrations of 50, 25, 12.5, 6.25, 3.125 mM as stock solutions.

3.4.3 Nitric Oxide inhibitory assay

Nitric oxide (NO) production was determined by measuring the amount of nitrite in lipopolysaccharide (LPS)-activated J774.A1 cells with Griess reagent (a mixture of 1% sulfanilamide and 0.1% naphthylethylenediamine dihydrochloride in 5% phosphoric acid). Macrophage J774.A1 cell lines were seeded in 96-well plate with $5x10^4$ cells/well and allowed to adhere for 1 h in 5% CO_2 incubator at 37 °C. The cells were pretreated with various concentrations of test compounds and vehicle (DMSO) for 2 h, and then activated with 1 µg/mL of LPS for additional 18 h. The cell culture supernatant (50 µL) of each well was then collected for NO measurement. Subsequently, 1% sulfanilamide (50 µL) was added into each well of culture supernatant, followed by incubation for 10 min under dark condition at room temperature. After that, 0.1% naphthylethylenediamine dihydrochloride in 5% phosphoric acid (50µL) was added to each well and incubated further for 10 min under the same condition. The absorbance was measured at 540 nm by using a microplate reader.

The results were presented as the percentage of inhibition and the half maximal inhibitory concentration (IC_{50}).

Calculation of the percentage of inhibition

$$\% \text{ inhibition} = 100 - \left(\frac{A_N}{A_C} \times 100 \right)$$

A_N = Absorbance of test – Absorbance of blank

A_C = Absorbance of control – Absorbance of blank

The IC_{50} values were calculated from line graph between the percentage of inhibition (Y axis) and the concentration of compound (X axis).

3.4.4 Cytotoxic assay (MTT assay)

Cell viability was assessed by the mitochondrial-respiration-dependent 3-(4,5-dimethylthiazol-2-yl)-2,5-diphenyl-tetrazolium bromide (MTT) colorimetric method. The succinate dehydrogenase in living cells can reduce the yellow tetrazolium salt MTT to a purple formazan crystals. The cell lines were seeded in 96-well plate with $5x10^4$ cells/well and allowed to adhere for 1 h at 37 ℃ in 5% CO_2. The cells were treated with various concentrations of test compounds and DMSO (blank and control) for 18 h. After incubation, MTT solution (10 µL, 5 mg/mL in phosphate buffer saline) was added into each well of cell culture and incubated for 3 h at 37 ℃ in 5% CO_2 incubator. Supernatants were removed and 100 µL of DMSO was added into each well to dissolve formazan crystals. The absorbance was measured at 540 nm by using a microplate reader.

The results were calculated as the percentage of cell viability as compared with control groups.

Calculation of the percentage of cell viability

$$\% \text{ cell viability} = \frac{\text{Absorbance of tested cells}}{\text{Absorbance of control cells}} \times 100$$

3.5. Antiglycation assay in BSA-methylglyoxal model

In vitro glycation of bovine serum albumin (BSA) was modeled by incubating BSA with methylglyoxal (MGO). The test compounds were dissolved in DMSO as concentrations of 0.1, 0.05, 0.025, 0.0125 and 0.00625 mM. The solution of 10 mg/mL BSA in 0.1 M PBS (125 µL, pH 7.4) was mixed with 1 mM of MGO (115 µL) in eppendorf tubes. Blank BSA-MGO reactions were used by 0.1 M PBS of BSA. Then, the various concentrations of test compounds were added in BSA-MGO reaction and blank BSA-MGO reaction, and were incubated at 37 °C for 1 week. For comparison, aminoguanidine (AG) was used as a positive control and DMSO was used as a negative control. After incubation, BSA-MGO reaction (100 µL) and blank BSA-MGO (100 µL) reaction were added into each well of 96 well plate. The fluorescence intensity was measured at the excitation wavelength of 355 nm and an emission wavelength of 460 nm by using the EnSpire Multilabel Plate Reader.

The results were calculated as the percentage of AGEs inhibition and the half maximal inhibitory concentration (IC_{50}).

Calculation of the percentage of inhibition

$$\% \text{ inhibition} = \frac{F_N - F_T}{F_N} \times 100$$

F_N = Negative control – Negative blank control

F_T = Sample reaction - Sample blank reaction

The IC_{50} values were calculated from line graph between the percentage of inhibition (Y axis) and the concentration of compound (X axis).

CHAPTER IV
RESULTS AND DISCUSSION

4.1 Isolated compounds from stem bark of *Derris indica* (Lamk.) Bennet.

The ethyl acetate crude extract of stem bark of *D. indica* was purified by column chromatography over silica gel and Sephadex LH-20 to afford two new flavonoids, derrisins A (**5**) and B (**9**), together with 11 known flavones. These included demethoxy kanugin (**1**), pongaglabrone (**2**), pongachromene (**3**), pongapin (**4**), karajin (**6**), 3,7,4'–trimethoxyflavone (**7**), fisetin tetramethyl ether (**8**) pongaglabol methyl ether (**10**), lanceolatin B (**11**), pongaflavone (**12**) and 5-methoxy-3',4'-methylenedioxy(8,7-4",5")flavone (**13**). The structures of isolated compounds are shown in Figure 4.1.

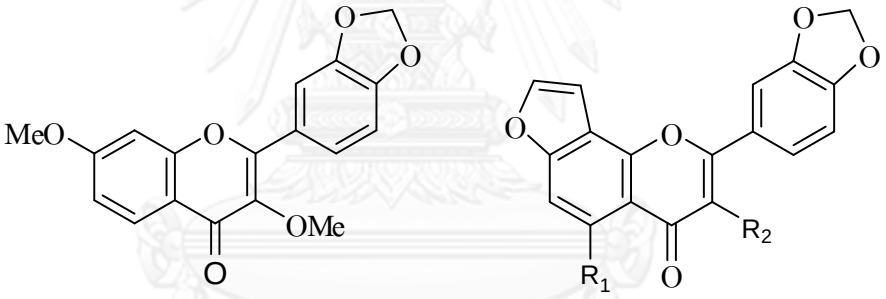

1

2: $R_1 = R_2$=H
4: R_1 =H R_2=OMe
13: R_1 = OMe R_2=H

Figure 4.1 Chemical structures of isolated compounds from *D. indica*

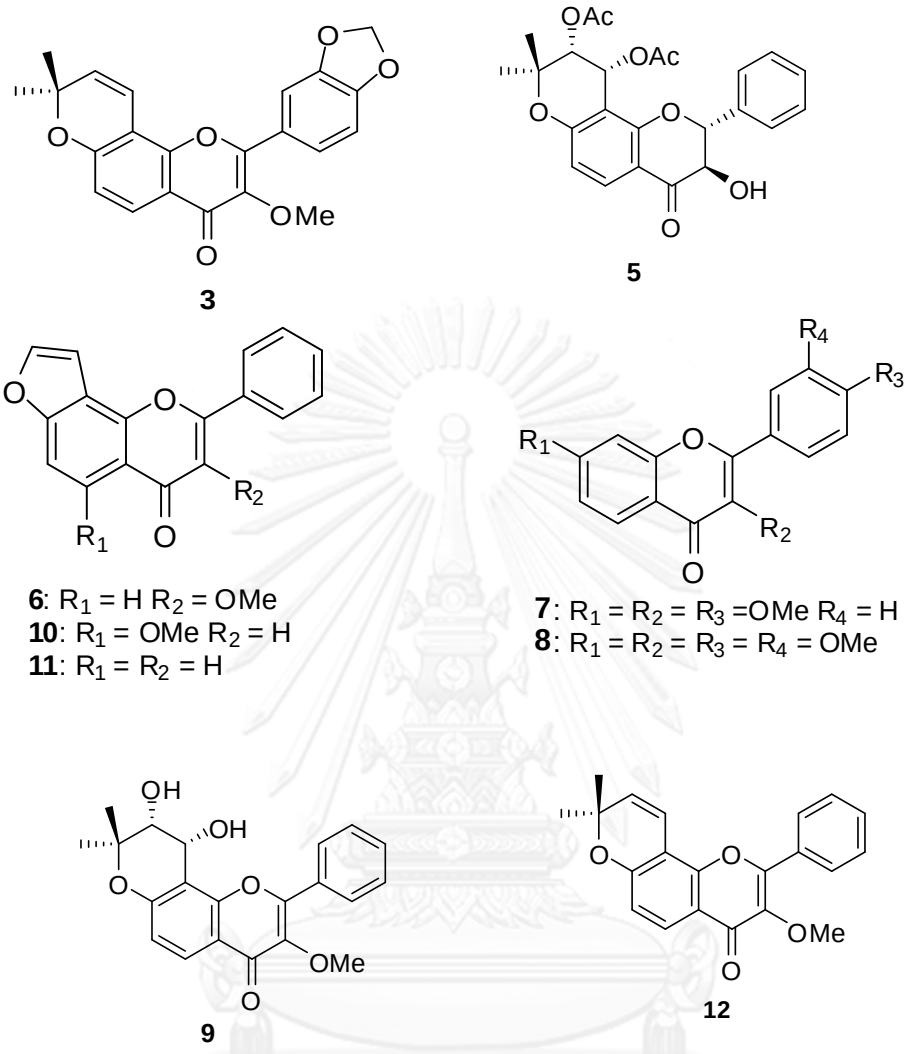

Figure 4.1 Chemical structures of isolated compounds from *D. indica* (continued)

4.1.1 Structure elucidation of compound 1

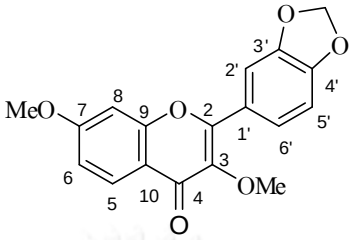

Figure 4.2 Compound **1**

Molecular formula	$C_{18}H_{14}O_6$
Appearance	White amorphous solid
m.p.	140-142 °C
UV (MeOH) λ_{max}	208, 240, 255, 312 and 340 nm
ESIMS *m/z*	326 [M^+] calcd. 326.30
^{1}H and ^{13}C NMR ($CDCl_3$)	See Table 4.1

Compounds **1** was isolated as white amorphous solid with a m.p. 140-142 °C, and its molecular formula was determined as $C_{18}H_{14}O_6$ on basis of ESIMS (*m/z* 326 [M^+] calcd. 326.30) and NMR data analysis. The ^{1}H NMR spectral data (Table 4.1) presented signals for an aromatic ring at δ_H 6.89 (d, *J*= 2.0 Hz), 6.97 (dd, *J*= 2.0, 7.2 Hz), 8.14 (d, *J*= 8.8 Hz), as well as a trisubstituted phenyl B ring at δ_H 6.94 (d, *J*= 8.4 Hz), 7.61 (d, *J*= 1.2 Hz) and 7.69 (dd, *J*= 1.2, 8.4 Hz). These characteristics were supported by ^{1}H-^{1}H COSY, HSQC, and HMBC correlations (Figure 4.3). In addition, its ^{1}H and ^{13}C spectra revealed the presence of methylenedioxy moiety [δ_H 6.06 s; δ_C 101.6] and two methoxyl groups [δ_H 3.88 s, 3.91 s; δ_C 55.8, 60.0]. A singlet signal at δ_H 6.06 displaying HMBC correlation with C-3', indicated the location of methylenedioxy group on phenyl B ring. Furthermore, two methoxyl groups were placed at C-3 and C-7 from HMBC correlations between methoxyl protons at δ_H 3.88 and C-3, and between the other methoxyl protons at δ_H 3.91 and C-9. Consequently, Compound **1** was identified as desmethoxy kanugin [52]. The structure of **1** was finally confirmed

by comparing its NMR data with those previously reported as shown in Table 4.1. It has ever been found in *D. indica* roots by Mittal and Seshadri (1956) [53] , and in *Gelonium multiflorum* [52].

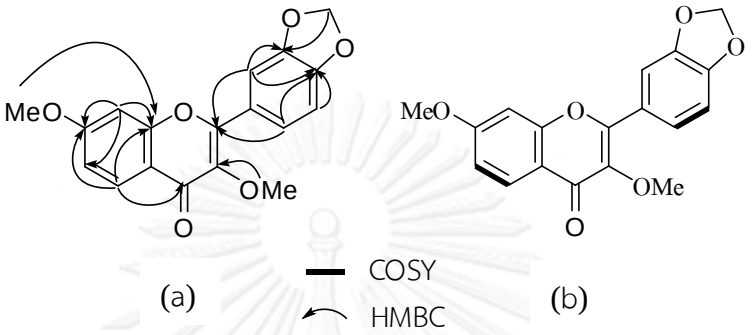

Figure 4.3 Key HMBC (a) and ^{1}H-^{1}H COSY (b) correlations of compound **1**

Table 4.1 NMR spectroscopic data ($CDCl_3$) of compound **1** and desmethoxy kanugin

Position	Desmethoxy kanugin[a]		Compound **1**[b]	
	δ_H (mult, *J* in Hz)	δ_C	δ_H (mult, *J* in Hz)	δ_C
2		154.7		154.6
3		140.8		140.8
4		174.4		174.4
5	8.14 (d, *J*= 8.8 Hz)	127.1	8.14 (d, *J*= 8.8 Hz)	127.1
6	6.96 (dd, *J*= 2.4, 8.8 Hz)	114.3	6.97 (dd, *J*= 2.0, 8.8 Hz)	114.2
7		156.8		156.8
8	6.89 (d, *J*= 2.4 Hz)	99.9	6.89 (d, *J*= 2.0 Hz)	99.9
9		164.0		164.0
10		118.0		118.0
1'		124.8		124.8
2'	7.61 (d, *J*= 1.8 Hz)	108.6	7.61 (d, *J*= 1.2 Hz)	108.6
3'		147.9		147.8
4'		149.5		149.4
5'	6.94 (d, *J*= 8.2 Hz)	108.4	6.94 (d, *J*= 8.4 Hz)	108.4
6'	7.69 (dd, *J*= 1.8, 8.2 Hz)	123.4	7.69 (dd, *J*= 1.2, 8.4 Hz)	123.4
-OCH_2O-	6.06 (s)	101.6	6.06 (s)	101.6
3-OMe	3.88 (s)	60.0	3.88 (s)	60.0
7-OMe	3.91 (s)	55.8	3.91 (s)	55.8

[a] recorded on 500 MHz NMR spectrometer.

[b] recorded on 400 MHz NMR spectrometer.

4.1.2 Structure elucidation of compound 2

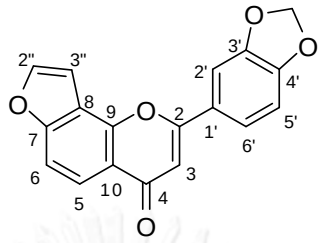

Figure 4.4 Compound **2**

Molecular formula	$C_{18}H_{10}O_5$
Appearance	White amorphous solid
m.p.	228-230 °C
UV (EtOH) λ_{max} (log ε)	223 (4.47), 249 (4.52) and 329 (4.32) nm
ESIMS *m/z*	306 [M^+], calcd. 306.27
^{1}H and ^{13}C NMR ($CDCl_3$)	See Table 4.2

Compound **2** was obtained as white amorphous solid, m.p. 228-230 °C and the molecular formula was established as $C_{18}H_{10}O_5$ by ESIMS (*m/z* 306 [M^+], calcd. 306.27) and NMR data analysis. The UV maxima absorption at 223, 249 and 329 nm were indicative of a furanoflavone skeleton [11, 54]. Its ^{1}H and ^{13}C NMR spectra (Table 4.2) displayed the presence of characteristic signals for furan ring [δ_H 7.19, 7.80 (each d, *J*= 2.4 Hz); δ_C 104.2, 145.8] and methylenedioxy group [δ_H 6.10 s and δ_C 101.9]. Two doublets of aromatic protons at δ_H 7.58 and 8.15 (*J*= 8.8 Hz), displaying ^{1}H-^{1}H cosy correlation each other, were assigned as H-6 and H-5 in A ring due to their HMBC cross-peaks as shown in Figure 4.5. Olefinic proton at δ_H 6.77 (s), showing HMBC correlations to C-2, C-10 and the ketone carbonyl (C-4), was identified as H-3. Furthermore, two doublet protons at δ_H 6.96 (*J*= 8.0 Hz), 7.40 (*J*= 1.6 Hz) and a double doublet proton at δ_H 7.54 (*J*= 8.8, 1.6 Hz) indicated the existence of the other

aromatic ring, phenyl B ring. The furan ring was attached to C-7 and C-8, as deduced by HMBC correlations of H-2'' with C-7, C-8 and C-6, and H-3'' with C-7, C-8 and C-2'', as well as the ^{1}H-^{1}H COSY correlation between H-2'' and 3'' (Figure 4.5). The location of the methylenedioxy group at C-3' and C-4' on the B ring was confirmed by HMBC correlations of methylenedioxy protons to C-3' and C-4'. Based on the above evidences, compound **2** was determined as pongaglabrone (Figure 4.4). Its structure was confirmed by comparing its NMR data with those reported in the literature (Table 4.2).

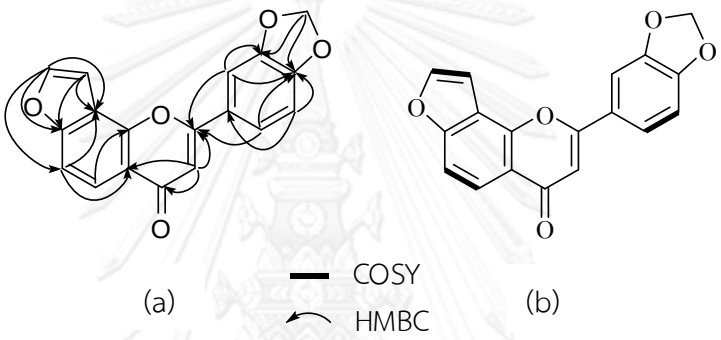

Figure 4.5 Key HMBC (a) and ^{1}H-^{1}H COSY (b) correlations of compound **2**

Table 4.2 NMR spectroscopic data ($CDCl_3$) of compound **2** and pongaglabrone

Position	Pongaglabrone[a]	Compound **2**[b]	
	δ_H (mult, *J* in Hz)	δ_H (mult, *J* in Hz)	δ_C
2			162.4
3	6.80 (s)	6.77 (s)	107.0
4			178.1
5	8.22 (d, *J*= 8.0 Hz)	8.15 (d, *J*= 8.8 Hz)	121.8
6	7.59 (d, *J*= 8.0 Hz)	7.58 (d, *J*= 8.8 Hz)	110.1
7			158.4
8			117.1
9			150.7
10			119.3
1'			125.8
2'	7.40 (d, *J*= 2.0 Hz)	7.40 (d, *J*= 1.6 Hz)	106.2
3'			148.6
4'			150.6
5'	7.00 (d, *J*= 8.0 Hz)	6.96 (d, *J*= 8.0 Hz)	108.9
6'	7.59 (dd, *J*= 8.0, 2.0 Hz)	7.54 (dd, *J*= 8.0, 1.6 Hz)	121.4
2''	7.82 (d, *J*= 2.0 Hz)	7.80 (d, *J*= 2.4 Hz)	145.8
3''	7.20 (d, *J*= 2.0 Hz)	7.19 (d, *J*= 2.4 Hz)	104.2
$-OCH_2O-$	6.14 (s)	6.10 (s)	101.9

[a] recorded on 100 MHz NMR spectrometer.

[b] recorded on 400 MHz NMR spectrometer.

4.1.3 Structure elucidation of compound 3

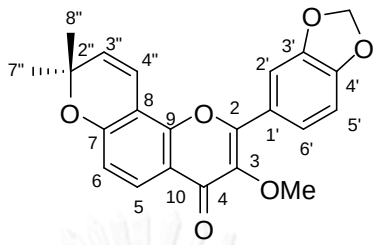

Figure 4.6 Compound **3**

Molecular formula	$C_{22}H_{18}O_6$
Appearance	Pale yellow crystals
m.p.	198-200 °C
ESIMS *m/z*	378 [M^+], calcd. 378.37
^{1}H and ^{13}C NMR ($CDCl_3$)	See Table 4.3

Compound **3** was isolated as pale yellow crystals, m.p. 198-200 °C and assigned molecular formula $C_{22}H_{18}O_6$ based on ESIMS (*m/z* 378 [M^+], calcd. 378.37) and NMR spectral data. The ^{1}H NMR data of **3** (Table 4.3) also exhibited typical signals associated with methylenedioxyflavone, particulary a methylenedioxyl singlet at δ_H 6.07 (CH_2). Based on the ^{1}H, ^{13}C and 2D informations (^{1}H-^{1}H COSY, HSQC, and HMBC), two doublets at δ_H 6.85 and 8.00 (*J* = 8.8 Hz) were assigned as H-6 and H-5 for an aromatic A ring, whereas the other set of aromatic signals at δ_H 6.94 (dd, *J*= 1.6, 8.4 Hz), 7.60 (d, *J*= 1.6 Hz), and 7.67 (d, *J* = 1.6 Hz) was assigned to the aromatic protons in the B ring at the positions 5', 2' and 6' respectively. Indeed, the NMR data of **3** were closely related to those of **1**, except for thepresence of an additional isoprene unit and the disappearance of one methoxyl group in **1**. The existence of the isoprene unit was confirmed by COSY correlation of H-3"/H-4" as well as by HMBC correlations of Me-7"/C-2", Me-8"/C-2", H-3"/C-7", H-4"/C-8", and H-4"/C-2" (Figure 4.7). This unit was further connected to the aromatic A ring at C-7 and C-8

due to the observed HMBC cross-peaks between H-4'' and C-7, between H-3'' and C-8'', and between H-6 and C-2''. Moreover, observed HMBC correlations of methylendioxy protons (δ_H 6.07 s) with C-3' and C-4' clarified it position on C-3' and C-4' in B ring, while the correlation of methoxyl protons (δ_H 3.87 s) with C-3 revealed its location at C-3 position. According to the above correlations, the structure of **3** was determined to be a chromenoflavone and it was identified as pongachromene, the first chromenoflavone isolated from *D. indica* in 1969 [54]. Thus, this is the first report for the complete assignment of NMR data for pongachromene.

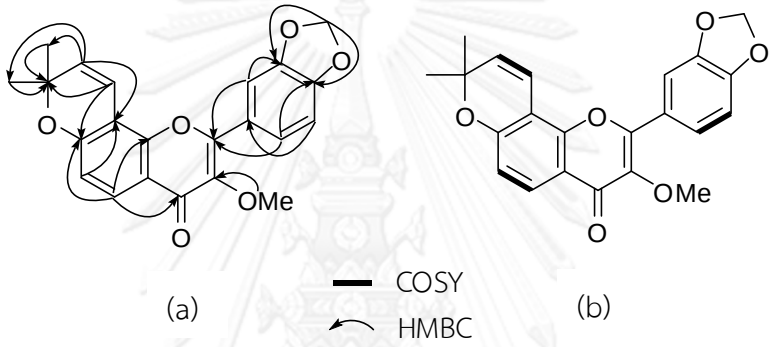

Figure 4.7 Key HMBC (a) and ^{1}H-^{1}H COSY (b) correlations of compound **3**

Table 4.3 NMR spectroscopic data of compound **3** (400 MHz, $CDCl_3$)

Position	Compound **3**	
	δ_H (mult, *J* in Hz)	δ_C
2		154.2
3		140.7
4		175.0
5	8.00 (d, *J*= 8.8 Hz)	126.1
6	6.85 (d, *J*= 8.8 Hz)	114.9
7		157.3
8		109.1
9		151.2
10		118.0
1'		125.0
2'	7.60 (d, *J*= 1.6 Hz)	108.5
3'		147.9
4'		149.4
5'	6.94 (d, *J*= 8.4 Hz)	108.4
6'	7.67 (dd, *J*= 1.6, 8.4 Hz)	123.3
2''		77.7
3''	5.71 (d, *J*= 10.0 Hz)	130.3
4''	6.87 (d, *J*= 10.0 Hz)	115.1
7''-Me	1.50 (s)	28.1
8''-Me	1.50 (s)	28.1
$-OCH_2O-$	6.07 (s)	101.6
3-OMe	3.87 (s)	60.0

4.1.4 Structure elucidation of compound 4

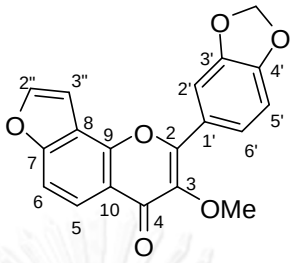

Figure 4.8 Compound **4**

Molecular formula	$C_{19}H_{12}O_6$
Appearance	Pale yellow needles
m.p.	190-191 °C
^{1}H and ^{13}C NMR ($CDCl_3$)	See Table 4.4

Compound **4** was obtained as pale yellow needles with m.p 190-191 °C. The molecular formula was established as $C_{19}H_{12}O_6$ based on the analysis of NMR data. The NMR data (Table 4.4) showed characteristic of a methlenedioxy-furanoflavone skeleton with a furan ring [$\boldsymbol{\delta}_H$ 7.17, 7.77 (each d, *J*= 1.6 Hz); $\boldsymbol{\delta}_C$ 104.2, 145.7], and methylenedioxy moiety [$\boldsymbol{\delta}_H$ 6.10 s; $\boldsymbol{\delta}_C$ 101.9] The location of furan ring on an aromatic ring A was established from the HMBC correlation of H-2" with C-7, C-9 and H-3" with C-7, C8, in addition to the ^{1}H-^{1}H COSY correlation between H-2" and 3" (Figure 4.9). Observed HMBC correlations of methylenedioxy protons at $\boldsymbol{\delta}_H$ 6.10 (s) and C-3' led to the attachment of this functional group onto the aromatic B ring at C-3' and C-4' as in compounds **1**-**3**. Actually, the NMR data of **4** were virtually identical to those of pongaglabrone (**2**). The only difference was the appearance of a three-proton singlet due to a mehtoxyl group at $\boldsymbol{\delta}_H$ 3.92, while the signal of the olefinic proton at $\boldsymbol{\delta}_H$ 6.77 (s) in **2** had disappeared. This indicated that olefinic proton had been replaced by a methoxyl group. Moreover, it was confirmed by HMBC cross-peak between mehtoxyl proton and C-3. Based on the literature search, compound **4**

was identified as pongapin [29, 55]. Comparsion of ^{13}C NMR data with those of pongapin was also performed as shown in Table 4.4.

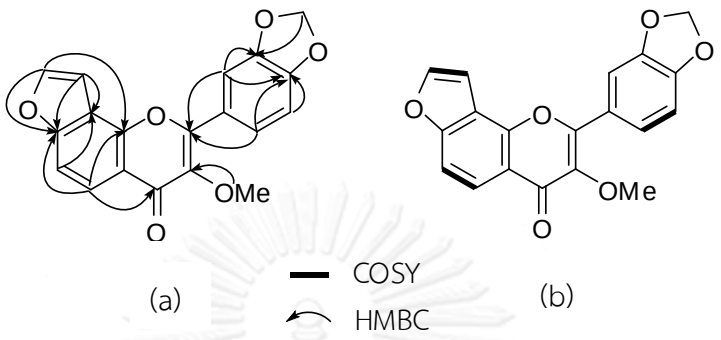

Figure 4.9 Key HMBC (a) and ^{1}H-^{1}H COSY (b) correlations of compound **4**

Table 4.4 NMR spectroscopic data of compound **4** and pongapin

Position	Pongapin[a]	Compound **4**[b]	
	δ_C	δ_H (mult, *J* in Hz)	δ_C
2	153.7		154.4
3	140.5		141.2
4	173.4		174.8
5	120.9	8.19 (d, *J*= 8.8 Hz)	123.4
6	109.7	7.55 (d, *J*= 8.8 Hz)	109.9
7	157.4		158.1
8	116.7		116.9
9	149.1		149.6
10	119.1		119.6
1'	124.1		121.8
2'	107.9	7.67 (d, *J*= 2.0 Hz)	108.6
3'	147.6		147.9
4'	149.3		149.7
5'	108.2	6.98 (d, *J*= 8.4 Hz)	108.5
6'	123.2	7.76 (m)	124.7
2''	146.9	7.77 (m)	145.7
3''	104.2	7.17 (d, *J*= 1.6 Hz)	104.2
-OCH_2O-	101.6	6.10 (s)	101.7
3-OMe	59.3	3.92 (s)	60.0

[a] recorded in DMSO-d_6 on 25.15 MHz NMR spectrometer.

[b] recorded in $CDCl_3$ on 400 MHz NMR spectrometer.

4.1.5 Structure elucidation of compound 5

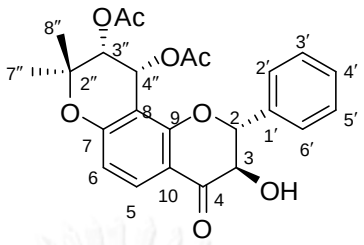

Figure 4.10 Compound **5**

Molecular formula	$C_{24}H_{24}O_8$
Appearance	Colourless crystals
m.p.	195-198 °C
UV (EtOH) λ_{max}	254 and 316 nm
$[\alpha]_D^{20}$	-13 (*c* 0.1, MeOH)
HRESIMS *m/z*	441.1598 $[M+H]^+$ calcd. 441.1544
^1H and ^{13}C NMR ($CDCl_3$)	See Table 4.5

Compound **5** was isolated as colourless crystals, m.p. 195-198 °C and its molecular formula was determined as $C_{24}H_{24}O_8$ by HRESIMS (*m/z* 441.1598 $[M+H]^+$ calcd. 441.1544), implying 13 degrees of unsaturation. The ^1H NMR data, taken in conjunction with the UV absorption maxima at 254 and 316 nm, were indicative of a flavanone skeleton. The ^1H NMR spectrum (Table 4.6) of **5** displayed characteristic signals for two tertiary methyls (δ_H 1.41 s, 1.45 s), two acetyl methyls (δ_H 1.94 s, 2.05 s), and one unsubstituted phenyl ring (δ_H 7.39 m, 2H; 7.40 m, 1H; 7.46 m, 2H). In addition, signals for *ortho*-coupled aromatic protons at δ_H 6.63 and 7.85 (each d, *J*= 8.8 Hz) were observed, attributable for an additional aromatic ring. Analysis of ^{13}C NMR and HSQC data further revealed the presence of two tertiary methyls, two acetyl methyls, four oxygenated methines, one oxygenated quaternary carbon, 12 aromatic carbons (two oxygenated), and three carbonyls (two esters and one

ketone). On the basis of the above NMR data, compound **5** had a tetracyclic skeleton due to nine units of the 12 unsaturations coming from three carbonyl groups and six carbon–carbon double bonds of two aromatic rings. The existence of a 2,2-dimethyl-3,4-diacetyl-3,4-dihydro-2*H*-pyran moiety was corroborated by strong COSY correlations between H-3" and H-4", and HMBC correlations from both tertiary methyls (2"-Me × 2) to oxygenated C-2" and C-3" (Figure 4.11). The location of two acetyl groups at C-3" and C-4" was confirmed by HMBC correlations from H-3" and H-4" to their carbonyl carbons. Indeed, the NMR data of **5** were very similar to those of 3-methoxy-(3",4"-dihydro-3",4"-diacetoxy)-2",2"-dimethylpyrano-(7,8:5",6")-flavone [11], except for the replacement of the $\Delta^{2,3}$ double bond by the –CH(2)–CH(OH)(3)– unit in **5**. Finally, a single-crystal X-ray diffraction study confirmed the gross structure of **5** and allowed the determination of its relative configuration as depicted in Figure 4.12. The crystal data and structure refinement of **5** are shown in table 4.5. Consequebthy, compound **5** was determined to be a new chromenoflavanone, and has been named derrisin A.

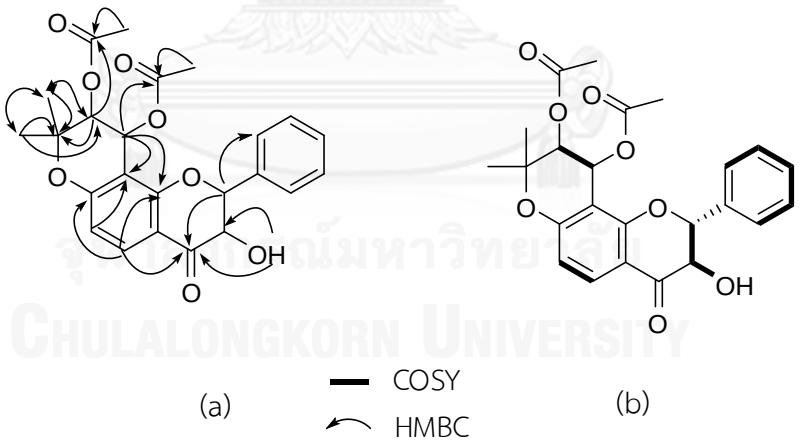

Figure 4.11 Key HMBC (a) and ^{1}H-^{1}H COSY (b) correlations of compound **5**

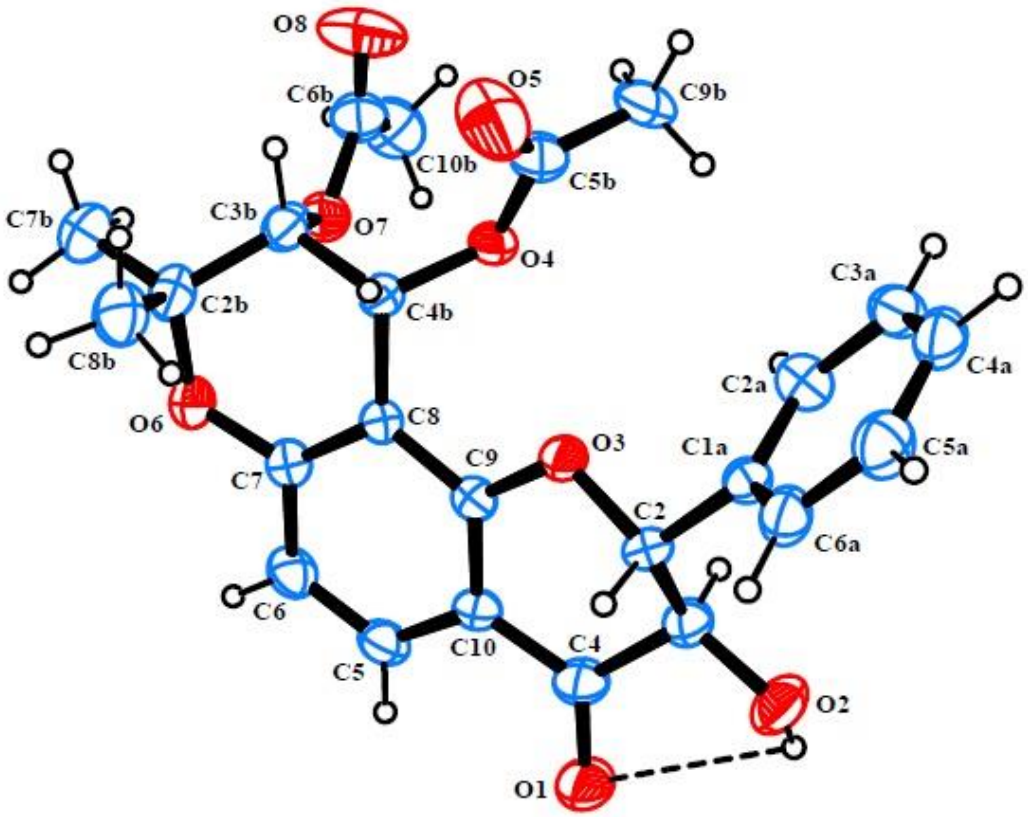

Figure 4. 12 ORTEP diagram of compound **5**

Table 4.5 Crystal data and structure refinement for compound **5**

Identification code	Derrisin A
Empirical formula	C_{24} H_{24} O_8
Formula weight	440.43
Temperature	296(2) K
Wavelength	0.71073 Å
Crystal system, space group	triclinic, P1
Unit cell dimensions	a = 9.2968(7) Å alpha = 76 deg.
	b = 12.0179(12) Å beta = 85 deg.
	c = 20.457(2) Å gamma = 88 deg.
Volume	2220.5(4) $Å^3$
Z, Calculated density	4, 1.317 Mg/m^3
Absorption coefficient	0.099 mm^{-1}
F(000)	928
Crystal size	0.34 x 0.08 x 0.04 mm
Theta range for data collection	1.02 to 25.06 deg.
Limiting indices	-11<=h<=10, -14<=k<=14,-24<=l<=24
Reflections collected / unique	13081 / 6901 [R_{int} = 0.025]
Refinement method	Full-matrix least-squares on F^2
Data / restraints / parameters	6901 / 1195 / 1174
Goodness-of-fit on F^2	0.970
Final R indices [I>2sigma(I)]	R_1 = 0.0562, *wR2* = 0.1021
R indices (all data)	R_1 = 0.1343, *wR2* = 0.1355
Absolute structure parameter	-0.5(9)

Table 4.6 NMR spectroscopic data (400 MHz) of compound **5** ($CDCl_3$)

Position	Compound **5**	
	δ_H (mult, *J* in Hz)	δ_C
2	5.10 (d, *J*= 12.4 Hz)	83.9
3	4.58 (dd, *J*= 2.0, 12.4 Hz)	72.8
4		192.1
5	7.85 (d, *J*= 8.8 Hz)	129.2
6	6.63 (d, *J*= 8.8 Hz)	112.7
7		161.9
8		107.3
9		160.6
10		111.9
1'		136.1
2'	7.46 (m)	127.3
3'	7.39 (m)	129.3
4'	7.40 (m)	128.5
5'	7.39 (m)	129.3
6'	7.46 (m)	127.3
2''		77.5
3''	5.17 (d, *J*= 4.8 Hz)	70.7
4''	6.26 (d, *J*= 4.8 Hz)	61.0
7''-Me	1.41 (s)	25.6
8''-Me	1.45 (s)	21.9
3''-OAc	2.05 (s)	169.8, 20.6
4''-OAc	1.94 (s)	169.5, 20.4
3-OH	3.70 (d, *J*= 1.6 Hz)	

4.1.6 Structure elucidation of compound 6

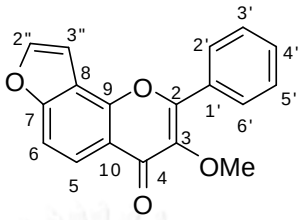

Figure 4.13 Compound **6**

Molecular formula	$C_{18}H_{12}O_4$
Appearance	Colourless crystals
m.p.	161-163°C
UV (Water) λ_{max} (log ε)	259 (4.56) nm
ESIMS *m/z*	293 $[M+H]^+$ calcd. 292
^1H and ^{13}C NMR ($CDCl_3$)	See Table 4.6

Compound **6** was obtained as colourless crystals with m.p. 161-163 °C. Its molecular formula $C_{18}H_{12}O_4$ was determined based on ESIMS (*m/z* 293 $[M+H]^+$ calcd. 292) and NMR data. The ^1H NMR data displayed signals at δ_H 7.55, 8.20 (each d, *J*= 8.8 Hz) for an aromatic ring A and multiplet signals at δ_H 7.53, 7.54, 8.14 and 8.16 for an unsubstituted aromatic B ring. Two doublets at δ_H 7.18 and 7.76 (each *J*= 2.4 Hz), showing COSY correlation each other, indicated the presence of a furan ring. Additionally, comparision of its NMR data with those of compound **4** suggested both compounds had the same furanoflavone skeleton, with the difference being only the lack of a methylenedioxy on a B ring in **4**. This supported the existence of an unsubstituted aromatic B ring signals, which was confirmed by COSY correlations of H-2'/H-3', H-3'/H-4', H-4'/H-5', and H-5'/H-6' (Figure 4.14). The furan ring placed at C-7 and C-8 on aromatic A ring was established from HMBC correlations of H-2"/C-7, H-2"/C-8, H3"/C-7, and H-3"/C-8. In addition, observed HMBC correlation between the singlet signal at δ_H 3.93 and C-3 indicated the location of methoxyl group at C-3

position. Finally, structure of **6** was confirmed by comparing its ^{1}H and ^{13}C NMR data with those previously published (Table 4.7). Compound **6** was these characterized as karanjin [55, 56]. This compound was the first compound isolated from *D. indica* seed oil in 1925 [9]. In this study, karanjin was obtained as a major compound with the yield of 0.92% (248.6 mg).

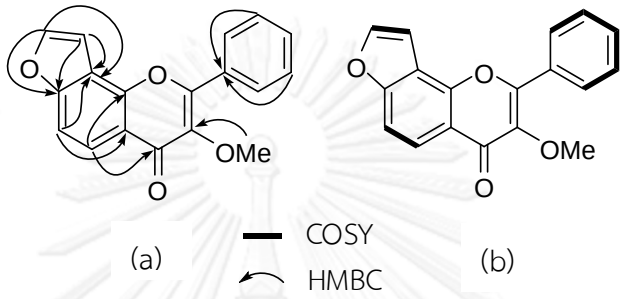

Figure 4.14 Key HMBC (a) and ^{1}H-^{1}H COSY (b) correlations of compound **6**

Table 4.7 NMR spectroscopic data ($CDCl_3$) of compound **6** and karanjin

Position	Karanjin[a]		Compound **6**[b]	
	δ_H (mult, *J* in Hz)	δ_C	δ_H (mult, *J* in Hz)	δ_C
2		154.5		154.8
3		141.5		141.8
4		174.7		175.0
5	8.22 (d, *J*= 8.5 Hz)	121.6	8.20 (d, *J*= 8.8 Hz)	121.9
6	7.57 (d, *J*= 8.5 Hz)	109.7	7.55 (d, *J*= 8.8 Hz)	110.0
7		157.8		158.2
8		116.7		117.0
9		149.6		150.0
10		119.4		119.7
1'		130.7		131.0
2'	8.17 m	128.0	8.16 (m)	128.3
3'	7.60 m	128.3	7.54 (m)	128.6
4'	7.60 m	130.3	7.53 (m)	130.6
5'	7.60 m	128.3	7.54 (m)	128.6
6'	8.17 m	128.0	8.14 (m)	128.3
2''	7.78 (d, *J*= 2.0 Hz)	145.7	7.76 (d, *J*= 2.4 Hz)	145.7
3''	7.20 (d, *J*= 2.0 Hz)	103.9	7.18 (d, *J*= 2.4 Hz)	104.2
3-OMe	3.85 (s)	59.9	3.93 (s)	60.2

[a] recorded on 500 MHz NMR spectrometer.

[b] recorded on 400 MHz NMR spectrometer.

4.1.7 Structure elucidation of compound 7

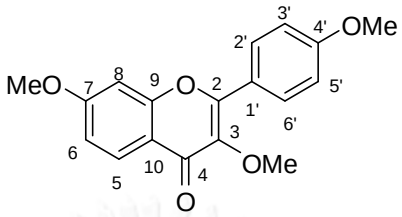

Figure 4.15 Compound **7**

Molecular formula	$C_{18}H_{16}O_5$
Appearance	Pale yellow crystals
m.p.	139-141 °C
IR (KBr)	1636 cm^{-1}
ESIMS *m/z*	312 [M^+], calcd. 312.32
^1H and ^{13}C NMR ($CDCl_3$)	See Table 4.7

Compound **7** was obtained as pale yellow crystals, m.p. 139-141 °C and had the molecular formula $C_{18}H_{16}O_5$ as established by ESIMS (*m/z* 312 [M^+], calcd. 312.32) and NMR data analysis. Similarly, NMR data of compound **7** displayed typical signals associated with a flavone type structure. Analysis of ^1H, ^{13}C and 2D NMR data confirmed the presence of two aromatic rings, bridged by an α,β-unsaturated ketone [δ_C 140.6, 155.1, 174.4] linkage, as in general structure of flavone. For this compounds, three singlet signals for methyl groups appeared at δ_H 3.87, 3.90 and 3.91 and they was located at C-3, C-4' and C-7, respectively, due to their HMBC correlations to those carbons (Figure 4.16) According to those evidences, compound **7** was determined to be 3,7,4'–trimethoxyflavone [57]. Comparison of NMR data of **7** with those reported in the literature also helped to confirm its structure as shown in Table 4.8.

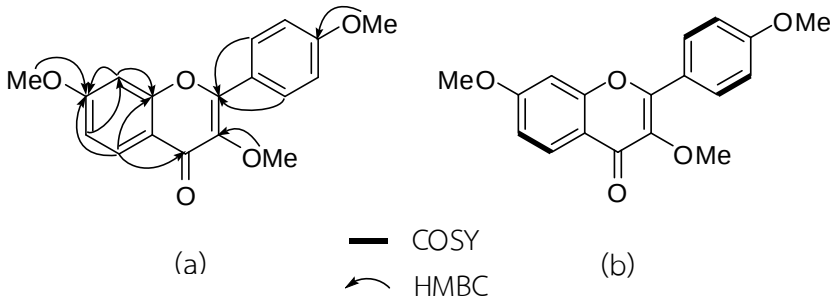

Figure 4.16 Key HMBC (a) and ^{1}H-^{1}H COSY (b) correlations of compound **7**

Table 4.8 NMR spectroscopic data ($CDCl_3$) of compound **7** and 3,7,4'–trimethoxyflavone

Position	3,7,4' –Trimethoxyflavone[a]		Compound **7**[b]	
	δ_H (mult, *J* in Hz)	δ_C	δ_H (mult, *J* in Hz)	δ_C
2		155.5		155.1
3		141.0		140.6
4		174.9		174.4
5	8.15 (d, *J*= 8.9 Hz)	127.5	8.15 (d, *J*= 8.8 Hz)	127.1
6	6.96 (dd, *J*= 8.9, 2.4 Hz)	114.6	6.95 (dd, *J*= 8.8, 2.4 Hz)	114.2
7		164.3		164.0
8	6.90 (d, *J*= 2.3 Hz)	100.3	6.90 (d, *J*= 2.4 Hz)	100.0
9		157.3		157.0
10		118.5		118.2
1'		123.7		123.4
2'	8.09 (d, *J*= 9.1 Hz)	130.4	8.10 (d, *J*= 8.8 Hz)	130.0
3'	7.02 (d, *J*= 9.1 Hz)	114.3	7.02 (d, *J*= 8.8 Hz)	114.0
4'		161.7		161.3
5'	7.02 (d, *J*= 9.1 Hz)	114.3	7.02 (d, *J*= 8.8 Hz)	114.0
6'	8.09 (d, *J*= 9.1 Hz)	130.4	8.09 (d, *J*= 8.8 Hz)	130.0
3-OMe	3.87 (s)	60.3	3.87 (s)	60.0
7-OMe	3.92 (s)	56.2	3.91 (s)	55.8
4'-OMe	3.89 (s)	55.8	3.90 (s)	55.4

[a] recorded on 300 MHz NMR spectrometer.

[b] recorded on 400 MHz NMR spectrometer.

4.1.8 Structure elucidation of compound 8

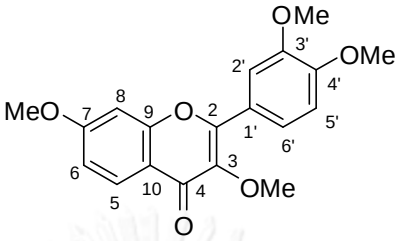

Figure 4.17 Compound **8**

Molecular formula	$C_{19}H_{18}O_6$
Appearance	Pale yellow needles
m.p.	147-148 °C
IR (KBr)	2943, 2839, 1620, 1516, 1448, 1383 and 835 cm^{-1}
^1H and ^{13}C NMR ($CDCl_3$)	See Table 4.8

Compound **8** was isolated as pale yellow needles, m.p. 147-148 °C, and its molecular formula was established as $C_{19}H_{18}O_6$ on the basis of NMR data analysis. The NMR spectrum of compound **8** and its 2D NMR information (^1H-^1H COSY, HSQC, HMBC) showed signals for two aromatic rings [$\boldsymbol{\delta}_H$ 6.91 (d, *J*= 2.0 Hz), 6.96 (dd, *J*= 6.8, 2.4 Hz), 8.15 (d, *J*= 8.8 Hz); $\boldsymbol{\delta}_C$ 100.0, 114.2, 118.2, 127.2, 157.2, 163.9, 174.4] for A ring, $\boldsymbol{\delta}_H$ 6.98 (d, *J*= 2.4 Hz), 7.72 (brs), 7.74 (dd, *J*= 8.8, 2.0 Hz); $\boldsymbol{\delta}_C$ 110.9, 111.5, 121.9, 123.6, 148.7, 151.0, for B ring, and four methoxyl groups [$\boldsymbol{\delta}_H$ 3.87, 3.92, 3.97 (each s); $\boldsymbol{\delta}_C$ 55.8, 55.9, 56.1, 60.0]. These were corroborated from the ^1H-^1H COSY and HMBC correlations (Figure 4.18). The NMR data of **8** were very similar to those of **7**, except for the replacement of one aromatic proton in B ring of **7** by a methoxyl group. This additional methoxy was placed at C-3' owing to its strong HMBC correlation to C-3', while the remaining three methoxyl groups were assigned to attach to C-3, C-7, and C-4' by their HMBC correlations to these carbon atoms as shown in Figure 4.18. Based

on the above NMR data could be concluded that compound **8** was fisetin tetramethyl ether [58]. Besides, comparison of its NMR data with those in literature confirmed its structure as determined (Table 4.9). This compound has been previously found in *D. indica* part flower by Talapatra et al (1982) [32], and in *Vitex rotundifolia*.

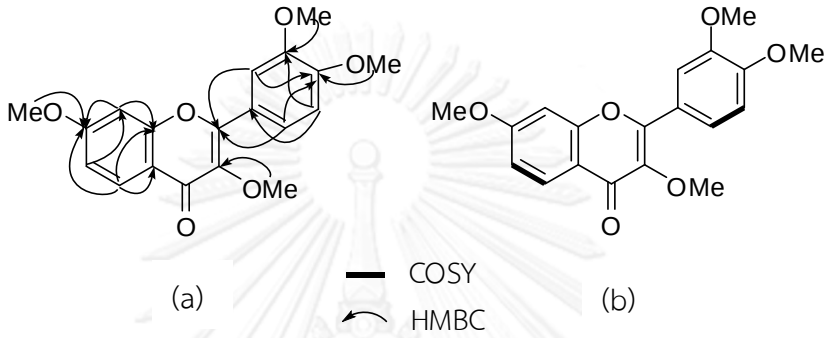

Figure 4.18 Key HMBC (a) and ^{1}H-^{1}H COSY (b) correlations of compound **8**

Table 4.9 NMR spectroscopic data ($CDCl_3$) of compound **8** and fisetin tetramethyl ether

Position	Fisetin tetramethyl ether [a]	Compound **8** [b]	
	δ_H (mult, *J* in Hz)	δ_H (mult, *J* in Hz)	δ_C
2			155.0
3			140.7
4			174.4
5	8.16 (d, *J*= 8.6 Hz)	8.15 (d, *J*= 8.8 Hz)	127.2
6	6.97 (dd, *J*= 8.6, 2.3 Hz)	6.96 (dd, *J*= 8.8, 2.4 Hz)	114.2
7			163.9
8	6.91 (d, *J*= 2.3 Hz)	6.91 (d, *J*= 2.0 Hz)	100.0
9			157.2
10			118.2
1'			123.6
2'	7.72 (brs)	7.72 (brs)	111.5
3'			148.7
4'			151.0
5'	7.00 (d, *J*= 8.6 Hz)	6.98 (d, *J*= 8.8 Hz)	110.9
6'	7.74 (dd, *J*= 8.8, 2.3 Hz)	7.74 (dd, *J*= 8.8, 2.0 Hz)	121.9
3-OMe	3.88 (s)	3.87 (s)	60.0
7-OMe	3.93 (s)	3.92 (s)	55.8
3'-OMe	3.97 (s)	3.97 (s)	55.9
4'-OMe	3.97 (s)	3.97 (s)	56.1

[a] recorded on 500 MHz NMR spectrometer.

[b] recorded on 400 MHz NMR spectrometer.

4.1.9 Structure elucidation of compound 9

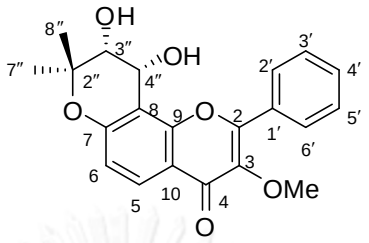

Figure 4.19 Compound **9**

Molecular formula	$C_{21}H_{20}O_6$
Appearance	White solid
m.p.	160-162 °C
UV (EtOH) λ_{max}	239, 258, and 312 nm
$[\alpha]_D^{20}$	+6.5 (*c* 0.1, MeOH)
HRESIMS *m/z*	367.12168 $[M+H]^+$ calcd. 367.11761
^1H and ^{13}C NMR ($CDCl_3$)	See Table 4.9

Compound **9** was obtained as a white solid, m.p. 160-162 °C, and analyzed the molecular formula $C_{21}H_{20}O_6$ from its HRESIMS (*m/z* 367.1217 $[M+H]^+$ calcd. 367.1176). It provided a typical flavone UV spectrum (λ_{max} 239, 258, and 312 nm). The NMR data suggested that the structure of **9** was closely related to that of pongachromene (**3**), except for the appearance of two additional oxygenated methines [δ_H 3.90 (dd, *J* = 5.2, 6.4 Hz), 5.20 (dd, *J* = 5.2, 5.2 Hz); δ_C 62.0, 71.5] as well as the loss of a methylenedioxy group in **3**. Moreover, two exchangeable protons, observed at 3.28 and 3.54 (each d, *J* = 8.0 Hz), were assigned to OH-3" and OH-4", respectively, by the COSY correlations with their vicinal protons (Figure 4.20a). The HMBC correlation between the methoxyl protons and the double bond carbon C-3 confirmed its location at the C-3 position. The relative configuration at C-3" and C-4" was deduced from the NOESY interactions to be the same as that of **5**, due to the

correlations of H-3"/H-4" and OH-3" and OH-4" (Figure 4.20c). Therefore compound **9** was identified as a new chromenoflavone and was named derrisin B.

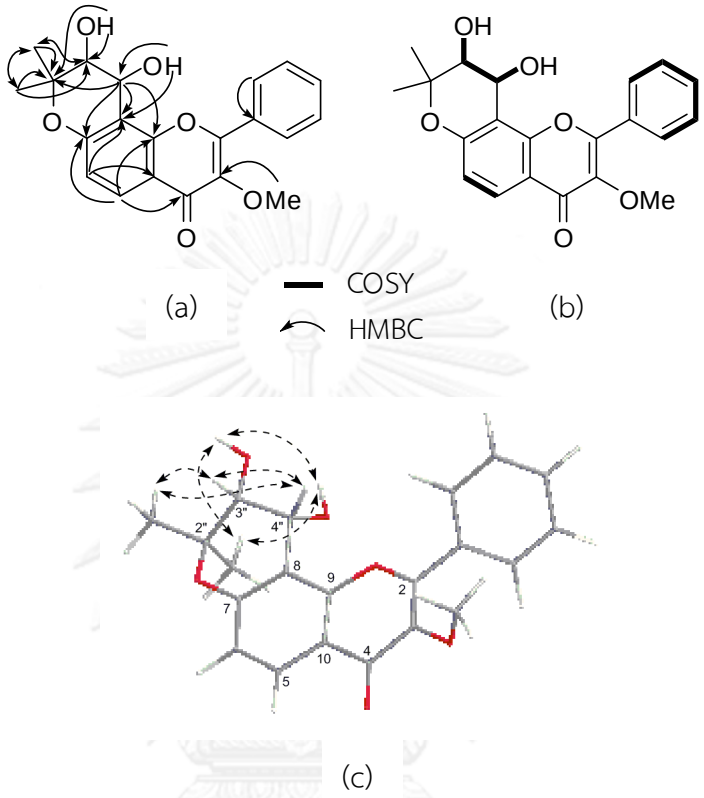

Figure 4.20 Key HMBC (a), ^{1}H-^{1}H COSY (b) NOESY (c) correlations of compound **9**

Table 4.10 NMR spectroscopic data (400 MHz) of compound **9** ($CDCl_3$)

Position	Compound **9**	
	δ_H (mult, *J* in Hz)	δ_C
2		154.8
3		141.3
4		174.5
5	7.93 (d, *J*= 8.8 Hz)	126.9
6	6.83 (d, *J*= 8.8 Hz)	116.2
7		155.6
8		110.0
9		157.5
10		118.1
1'		130.8
2'	8.10 (m)	128.3
3'	7.48 (m)	130.7
4'	7.46 (m)	128.7
5'	7.48 (m)	130.7
6'	8.10 (m)	128.3
2''		79.2
3''	3.90 (dd, *J*= 5.2, 6.4)	71.5
4''	5.20 (dd, *J*= 5.2, 5.2)	62.0
7''-Me	1.44 (s)	25.0
8''-Me	1.55 (s)	22.0
3''-OH	3.28 (d, *J*= 5.6 Hz)	
4''-OH	3.54 (d, *J*= 5.6 Hz)	
3-OMe	3.80 (s)	60.1

4.1.10 Structure elucidation of compound 10

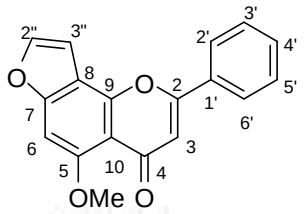

Figure 4. 21 Compound **10**

Molecular formula	$C_{18}H_{12}O_4$
Appearance	Light yellow needles
m.p.	181-182 °C
UV (EtOH) λ_{max} (log ε)	221.5 (4.51), 228 (4.50), 256 (4.37), 274 (4.49) and 321 (3.76)
IR (KBr)	1640, 1400, 1303, 1140, 1108, 1065 and 765 cm^{-1}
^1H and ^{13}C NMR ($CDCl_3$)	See Table 4.10

Compound **10** was obtained as light yellow needles, m.p. 181-182 °C, and had molecular formula of $C_{18}H_{12}O_4$ as established by NMR data analysis, being the same as that of compound **6**. The UV absorptions bands at 221.5, 228, 256, 274 and 321, together with NMR spectroscopic data analysis, were suggestive of the presence of furanoflavonoid nucleus [21]. In addition, analysis of ^1H, ^{13}C and 2D NMR data revealed that compound **10** contained the same functional groups as in **6**, including an unsubstituted aromatic ring, an aromatic ring connected with a furan ring, an α,β-unsatturated ketone, and a methoxyl group. The unsubstituted phenyl B ring was corraborated by ^1H-^1H COSY correlations of H-2'/H-3', H-3'/H-4', H-4'/H-5,' and H-5'/H-6' (Figure 4.22). Furthermore, the HMBC correlations of H-3 with C-1', C-2, C-10, and carbonyl carbon (C-4) were observed. The furan ring located at C-7, C-8 was deduced

from the HMBC correlations of H-2" with C-8, C-6 and C-9, as well as of H-3" with C-8 and C-9. From the above assignment, it was shown that compound **6** and **10** shared the same skeleton, except for the position of the methoxyl group. Strong HMBC correlation of the singlet methoxy protons at δ_H 4.21 with C-5 clatifited its location at C-5. Based on the literature review, compound **10** was pongaglabol methyl ether. This was also confirmed by comparison of its ^{1}H NMR data with those previously reported on presented in Table 4.11.

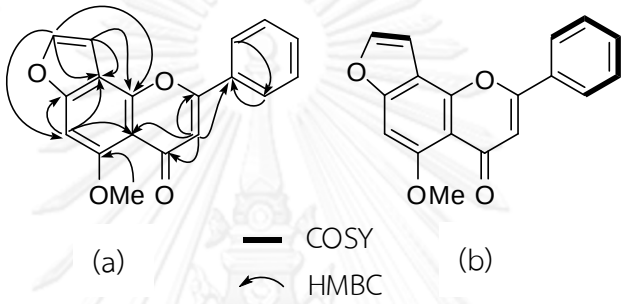

Figure 4.22 Key HMBC (a) and ^{1}H-^{1}H COSY (b) correlations of compound **10**

Table 4.11 NMR spectroscopic data ($CDCl_3$) of compound **10** and pongaglabol methyl ether

Position	Pongaglabol methyl ether[a]	Compound **10**[b]	
	δ_H (mult, *J* in Hz)	δ_H (mult, *J* in Hz)	δ_C
2			161.3
3	6.80 (s)	6.69 (s)	107.9
4			178.4
5			153.7
6	7.01 (d, *J*= 0.9 Hz)	7.38 (d, *J*= 0.8 Hz)	95.4
7			155.7
8			117.3
9			158.0
10			112.9
1'			131.4
2'	7.92 (m)	7.90 (m)	126.1
3'	7.49 (m)	7.51 (m)	131.6
4'	7.52 (m)	7.52 (m)	128.9
5'	7.49 (m)	7.51 (m)	131.6
6'	7.92 (m)	7.90 (m)	126.1
2''	7.64 (d, *J*= 2.3 Hz)	7.61 (d, *J*= 2.4 Hz)	145.2
3''	7.09 (dd, *J*= 2.3, 0.9 Hz)	7.05 (dd, *J*= 2.4, 0.8 Hz)	105.3
5-OMe	4.00 (s)	4.21 (s)	61.8

[a] recorded on 80 MHz NMR spectrometer.

[b] recorded on 400 MHz NMR spectrometer.

4.1.11 Structure elucidation of compound 11

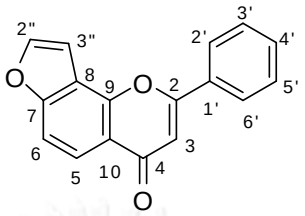

Figure 4.23 Compound **11**

Molecular formula	$C_{17}H_{10}O_3$
Appearance	Pale yellow needles
m.p.	134-137 °C
UV (EtOH) λ_{max} (log ε)	224 (4.30), 264 (4.33) and 297 (4.21) nm
MS *m/z*	262 [M^+], calcd. 262.26
^{1}H and ^{13}C NMR ($CDCl_3$)	See Table 4.11

Compound **11** was isolated as pale yellow needles, m.p. 134-137 °C and possessed molecular formula of $C_{17}H_{10}O_3$ as determined by MS (*m/z* 262 [M^+], calcd. 262.26) and NMR data. The ^{1}H NMR spectrum presented two doublets proton signals for an aromatic ring A at δ_H 7.57 and 8.19 (*J*= 8.8 Hz), two multiplet signals at δ_H 7.56 (3H) and 7.98 (2H) for an unsaturated aromatic B ring, and two doublet signals at δ_H 7.22 and 7.78 (each *J*= 2.0 Hz) for a furan ring, which was supported by the ^{1}H-^{1}H COSY experiment (Figure 4.24). In addition, a singlet signal at δ_H 6.89 was placed to be adjacent to carbonyl carbon (δ_C 178.2) due to its HMBC correlations to C-2, C-3, and C-10. As same as in compounds **6** and **10**, the furan ring was corroborated on C-7 and C-8 because of HMBC correlations of H-2"/C-6, H-2"/C-7, H-2"/C-8, H-3"/C-7, and H-3"/C-8. Therefore, compound **11** had the same structure as in compound **6** and **10**, without any methoxyl group in the structure. Finally, Comparison of its NMR

data with those previously reported revealed that compound **11** was lacheolatin B as presented in Table 4.12 [54].

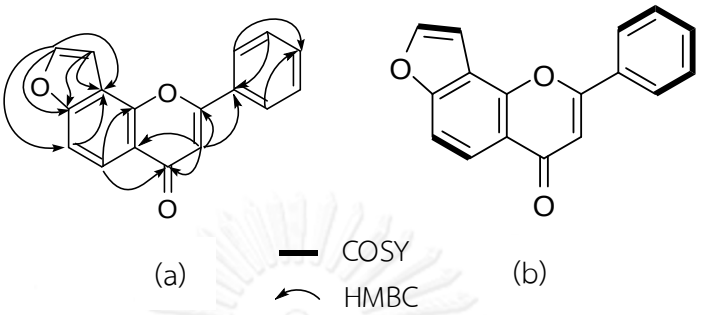

Figure 4.24 Key HMBC (a) and ^{1}H-^{1}H COSY (b) correlations of compound **11**

Table 4.12 NMR spectroscopic data ($CDCl_3$) of compound **11** and lacheolatin B

Position	Lacheolatin B[a]		Compound **11**[b]	
	δ_H (mult, *J* in Hz)	δ_C	δ_H (mult, *J* in Hz)	δ_C
2		162.7		162.7
3	6.88 (s)	108.1	6.89 (s)	108.1
4		178.2		178.2
5	8.22 (d, *J*= 9.0 Hz)	121.8	8.19 (d, *J*= 8.8 Hz)	121.8
6	7.62 (d, *J*= 9.0 Hz)	110.2	7.57 (d, *J*= 8.8 Hz)	110.2
7		158.4		158.4
8		117.2		117.2
9		150.9		150.9
10		119.4		119.4
1'		131.8		131.9
2'	8.02 (m)	126.2	7.98 (m)	126.2
3'	7.62 (m)	129.1	7.56 (m)	129.1
4'	7.62 (m)	131.5	7.56 (m)	131.5
5'	7.62 (m)	129.1	7.56 (m)	129.1
6'	8.02 (m)	126.2	7.98 (m)	126.2
2''	7.80 (d, *J*= 2.0 Hz)	145.8	7.78 (d, *J*= 2.0 Hz)	145.8
3''	7.20 (d, *J*= 2.0 Hz)	104.2	7.22 (d, *J*= 2.0 Hz)	104.2

[a] recorded on 100 MHz NMR spectrometer.

[b] recorded on 400 MHz NMR spectrometer.

4.1.12 Structure elucidation of compound 12

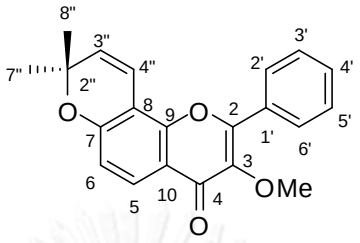

Figure 4.25 Compound **12**

Molecular formula	$C_{21}H_{18}O_4$
Appearance	Colourless needles
m.p.	148-150 °C
^{1}H and ^{13}C NMR ($CDCl_3$)	See Table 4.12

Compound **12** was isolated as colourless needles, m.p. 148-150 °C, and analyzed molecular formula $C_{21}H_{18}O_4$ based on its NMR data analysis. Acombined analysis of ^{1}H, ^{13}C and 2D NMR spectra indicated the presence of unsubsititued aromatic B ring [$\boldsymbol{\delta}_H$ 7.50 m, 7.52 m, 8.07 m; $\boldsymbol{\delta}_C$ 128.3, 128.6, 130.5], an α,β-unsaturated ketone [$\boldsymbol{\delta}_C$ 141.3, 154.6, 174.6], another aromatic A ring [$\boldsymbol{\delta}_H$ 6.85, 8.02 (each d, *J*= 8.8 Hz); $\boldsymbol{\delta}_C$ 109.2, 115.1, 118.1, 126.1, 151.4, 157.4] and a methoxy group [$\boldsymbol{\delta}_H$ 3.88 s; $\boldsymbol{\delta}_C$ 60.1] In addition, the characteristic signals for an isoprene unit, established by ^{1}H-^{1}H correlation of H-3"/H-4" and by HMBC correlations of H-8"/C-7", H-8"/C-2", H-8"/C-4", H-3"/C-2", H-3"/C-8" (Figure 4.26), were observed. The attachment of this unit on C-8 and the closure via the oxygen bridge on C-7 was confirmed by HMBC cross-peak between H-3" and C-8 and the down field shift of C-7 to 151.4 ppm. These data suggested that compound **12** was a chomenoflavone derivative. Indeed, the NMR data of compound **12** was very similar to those of pongachromene (**3**), with the only difference being the loss of signals for a methylenedioxy in **3**. The presence of the unsubstituted B ring was also confirmed by ^{1}H-^{1}H correlations of H-2'/H-3', H-3'/H-4', H-4'/H-5', and H-5'/H-6'. The location of the methoxy group at C-3 was further

determined from HMBC correlation of the singlet methoxyl protons and C-3. According to the literature search, compound **12** was found to be pongaflavone and also known as karanjachromene [11].

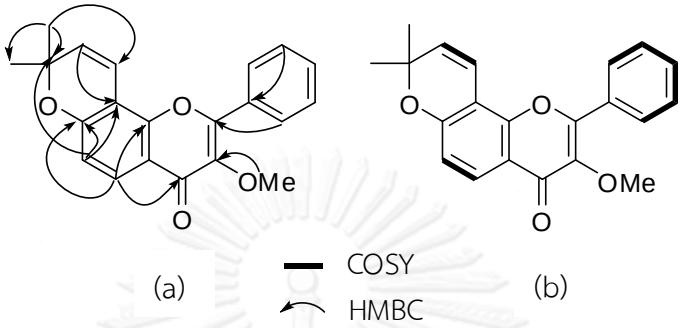

Figure 4.26 Key HMBC (a) and ^{1}H-^{1}H COSY (b) correlations of compound **12**

Table 4.13 NMR spectroscopic data ($CDCl_3$) of compound **12** and pongaflavone

Position	Pongaflavone[a]		Compound **12**[b]	
	δ_H (mult, *J* in Hz)	δ_C	δ_H (mult, *J* in Hz)	δ_C
2		154.6		154.6
3		141.2		141.3
4		174.6		174.6
5	8.09 (d, *J*= 8.5 Hz)	125.9	8.02 (d, *J*= 8.8 Hz)	126.1
6	6.86 (d, *J*= 8.8 Hz)	114.9	6.85 (d, *J*= 8.8 Hz)	115.1
7		157.3		157.4
8		109.1		109.2
9		151.3		151.4
10		117.9		118.1
1'		130.2		131.2
2'	8.08 (m)	128.2	8.07 (m)	128.3
3'	7.63 (m)	131.1	7.50 (m)	130.5
4'	7.63 (m)	-	7.52 (m)	128.6
5'	7.63 (m)	131.1	7.50 (m)	130.5
6'	8.08 (m)	128.2	8.07 (m)	128.3
2''		77.7		77.7
3''	5.74 (d, *J*= 5.0 Hz)	130.5	5.71 (d, *J*= 10.0 Hz)	130.3
4''	6.89 (d, *J*= 5.0 Hz)	115.0	6.88 (d, *J*= 10.0 Hz)	115.0
7''-Me	1.51 (s)	20.8	1.50 (s)	28.1
8''-Me	1.51 (s)	20.8	1.50 (s)	28.1
3-OMe	3.88 (s)	60.1	3.88 (s)	60.1

[a] recorded on 500 MHz NMR spectrometer.

[b] recorded on 400 MHz NMR spectrometer.

4.1.13 Structure elucidation of compound 13

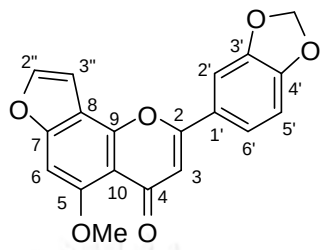

Figure 4.27 Compound **13**

Molecular formula	$C_{21}H_{18}O_4$
Appearance	Colourless needles
m.p.	262-263 °C
UV (EtOH) λ_{max} (log ε)	230 (4.58), 246 (4.46), 274 (4.21) and 330.5 (4.34)
IR (KBr)	1643, 1600, 1452, 1323, 1253, 1155, 1065, 1027, 920 and 835 cm^{-1}
MS m/z	336 [M^+] , calcd. 336.29
^1H and ^{13}C NMR ($CDCl_3$)	See Table 4.13

Compound **13** was isolated as colourless needles with m.p 262-263 °C, and assigned molecular formula $C_{21}H_{18}O_4$ based on MS (m/z 336 [M^+] , calcd. 336.29) and NMR data analysis, as being the same that of compound **4**. Furthermore, analysis of 1D and 2D NMR data revealed that all functional groups found in compound **13** wrer the same as in **4**. These included two aromatic ring, ring A [δ_H 7.36 (d, *J*= 0.8); δ_C 95.4, 112.8, 117.4, 153.6, 155.7, 157.9] and ring B [δ_H 6.93 (dd, *J*= 8.0, 0.8 Hz), 7.35 (d, *J*= 0.8 Hz), 7.48 (dd, *J*= 8.0, 1.6 Hz); δ_C 106.2, 108.7, 121.2, 125.6, 148.4, 150.4], a furan ring [δ_H 7.05 (dd, *J*= 2.4, 1.2 Hz), 7.61 (d, *J*= 2.4 Hz); δ_C 105.4, 145.2], an α,β-unsaturated ketone [δ_H 6.57 (s); δ_C 106.9, 161.0, 178.3], a methylenedioxy group [δ_H 6.07 s; δ_C 101.9], and methoxyl group [δ_H 4.20 s; δ_C 61.8]. The furan ring was also

corroborated at the same positions, C-7 and C-8, as in **4** deduced from HMBC correlations of H-2"/C-7, H-2"/C-8, H-3"/C-7, and H-3"/C-8. Similarly, the methylenendioxy group was attached to C-3' and C-4' as in **4**, which was confirmed by HMBC correlations of the singlet methylene at δ_H 6.07 to C-3' and C-4'. Thus, compounds **4** and **13** shared the same skeleton, but the difference must be the position of the methoxyl group. Observed HMBC correlation of the methoxyl proton to C-5 helped to place it on the C-5 position. Based on the above data and comparison of its ^{1}H NMR data with those in literature (Table 4.14) indicated that compound **13** was 5-Methoxy-3',4'-methylenedioxy (8,7-4",5")flavone [32].

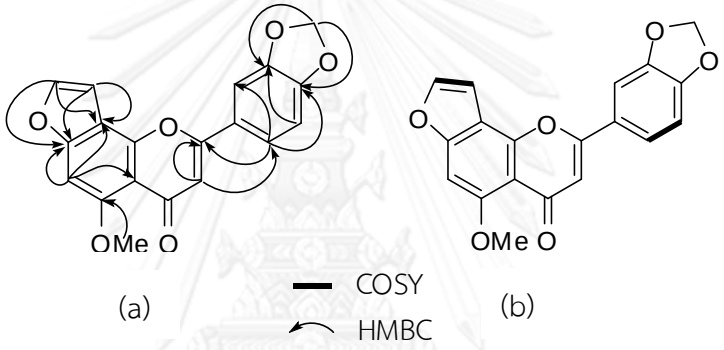

Figure 4.28 HMBC (a) and COSY (b) correlations of compound **13**

Table 4.14 NMR spectroscopic data of compound **13** and 5-Methoxy-3',4'-methylenedioxy(8,7-4",5")flavone

Position	5-Methoxy-3',4'-methylenedioxy (8,7-4",5")flavone[a]	Compound **13**[b]	
	δ_H (mult, *J* in Hz)	δ_H (mult, *J* in Hz)	δ_C
2			161.0
3	6.87 (s)	6.57 (s)	106.9
4			178.3
5			153.6
6	7.33 (d, *J* = 1.0 Hz)	7.36 (d, *J* = 0.8 Hz)	95.4
7			157.9
8			117.4
9			155.7
10			112.8
1'			125.6
2'	7.73 (brs)	7.35 (d, *J*= 1.6 Hz)	106.2
3'			148.4
4'			150.4
5'	7.13 (dd, *J*= 9.0, 1.0 Hz)	6.93 (dd, *J*= 8.0, 0.8 Hz)	108.7
6'	7.78 (dd, *J*= 9.0, 2.0 Hz)	7.48 (dd, *J*= 8.0, 1.6 Hz)	121.2
2''	8.09 (d, *J*= 2.0 Hz)	7.61 (d, *J*= 2.4 Hz)	145.2
3''	7.51 (dd, *J*= 2.0, 1.0 Hz)	7.05 (dd, *J*= 2.4, 1.2 Hz)	105.4
-OCH_2O-	6.18 (s)	6.07 (s)	101.9
5-OMe	3.91 (s)	4.20 (s)	61.8

[a] recorded in DMSO-d_6 on 90 MHz NMR spectrometer.

[b] recorded in $CDCl_3$ on 400 MHz NMR spectrometer.

4.2 Biological activities of isolated compounds

4.2.1 Anti-inflammatory

Nitric oxide (NO) is synthesized from the precursor L-arginine by inducible nitric oxide synthase (iNOS) which is a chemical mediator in inflammatory cells. [59] Upon inflammatory processes, macrophages are activated and release nitric oxide as well as pro-inflammatory cytokines such as tumor necrosis factor-α (TNF-α), interleukin-1β (IL-1β), and interleukin-6 (IL-6). Over production of these inflammatory mediators and cytokines are involved in the causation of many diseases including rheumatoid arthritis, asthma, atherosclerosis, and endotoxin-induced multiple organ injury [60].

All isolated compounds were tested for their anti-inflammatory activity by measuring the inhibition of NO production in LPS-activated murine macrophage J774.A1 cell lines. The results were presented as the half maximal inhibitory concentration (IC_{50}). Desmethoxy kanugin (**1**), derrisin B (**9**) and pongaflavone (**12**) showed anti-inflammatory activity on murine macrophage J774.A1 cells, while the remaining compounds did not display any significant activity at Table 4.15. After that, they were assessed for their cytotoxicity by using MTT colorimetric method. The results expressed as cell viability are shown in Figure 4.29. Neither desmethoxy kanugin (**1**) nor pongaflavone (**12**) displayed significant toxicity on macrophage J774.A1 cells. This result supported both compounds inhibited nitrite levels without causation of cell death. In the case of derrisin B (**9**), it was relatively toxic at the higher dose as shown, the NO production inhibitory effect of **9** was possibly due to its cyctotoxicity. When compared with indomethacin, a positive control, (IC_{50} = 28.42 ± 3.51 μM), both desmethoxy kanugin (1) and pongaflavone (12) displayed stronger inhibitory activity than indomethacin. As the result, these two compounds might potentially be applied as lead compound for development of an anti-inflammatory drug.

Table 4.15 Inhibitory effects of isolated compounds on nitric oxide production in LPS-stimulated macrophages.

Compound	IC_{50} (μM)*
Desmethoxy kanugin (**1**)	22.83 ± 0.75
Derrisin B (**9**)	11.24 ± 0.24
Pongaflavone (**12**)	14.59 ± 0.30
Indomethacin (positive control)	28.42 ± 3.51

* Results were presented as mean ± SEM (n=3)

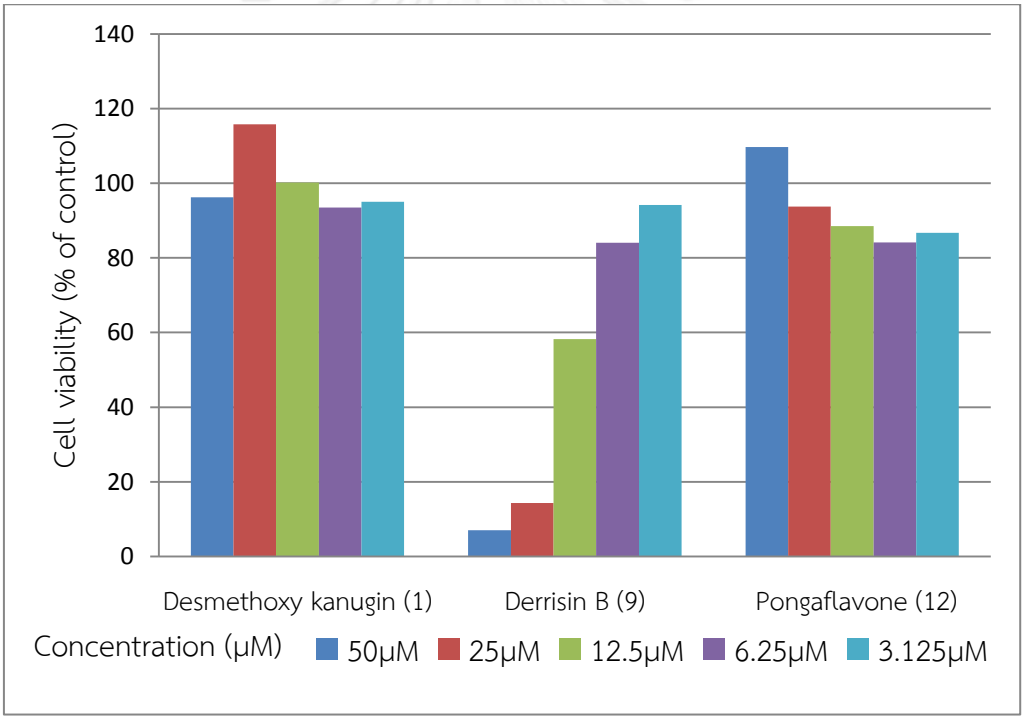

Figure 4.29 Cytotoxicity of desmethoxy kanugin (**1**), derrisin B (**9**), pongaflavone (**12**) at various dose.

4.2.2 Inhibition of advanced glycation end products

Glycation (also known as nonenzymatic protein glycation) is a reaction between reducing sugar such as fructose or glucose with proteins [61]. This results in the formation of advanced glycation endproducts (AGEs). AGEs can react with thiol groups of cysteine and induce crosslinking of extracellular and intracellular proteins [62]. Moreover, that can be a factor in the development or complications of diabetes.

All pure compounds, except for derrisin A (**5**), were evaluated for inhibition of AGEs by using antiglycation assay in BSA-MGO model. Methylglyoxal (MGO) is formed as a side-product of metabolic pathways and intermediate in the formation of AGEs. The results of inhibition of AGEs of isolated compounds are shown in Table 4.16. It was found that derrisin B (**9**) showed the most potent activity on the formation of AGEs by 84.45% of inhibition at a screening dose (100 μM). After that, BSA was incubated with MGO and various concentrations of derrisin B (**9**) (100, 50, 25, 12.5 and 6.25 μM) for 1 week to determine the IC_{50} and the percentage of AGEs inhibition at each concentration as shown in Figure 4.30. Aminoguanidine was used as a positive control and the results are depicted in Figure 4.31. The % AGEs inhibition of derrisin B (**9**) and aminoguanidine were found to be a dose-dependent manner (Figure 4.30 and 4.31) by using Sigmaplot, and their IC_{50} were calculated. Derrisin B (**9**) displayed inhibitory activity on the formation of AGEs with an IC_{50} value of 18.00 ± 0.35 μM, and its activity was 26.5-fold higher than aminoguanidinec (Table 4.17). Therefore, derrisin B (**9**) could suppress the formation of AGEs *in vitro* model. This compound might be applied as a lead for development of antiglycative agent for inhibiting protein glycation in diabetic patients.

Table 4.16 Inhibitory effects of isolated compound (100 μM) on formation of fluorescent advanced glycation end products (AGEs) in BSA incubated with MGO for 1 **week.**

Compounds	% AGEs inhibition*
Desmethoxy kanugin (**1**)	N.A.
Pongaglabrone (**2**)	N.A.
Pongachromene (**3**)	N.A.
Pongapin (**4**)	18.46 ±12.50
Karanjin (**6**)	14.05 ±1.37
3,7,4' – Trimethoxyflavone (**7**)	N.A.
Fisetin tetramethyl ether (**8**)	N.A.
Derrisin B (**9**)	84.45 ±4.43
Pongaglabol methyl ether (**10**)	N.A.
Lacheolatin B (**11**)	8.78 ±4.51
Pongaflavone (**12**)	N.A.
5-Methoxy-3',4'-methylenedioxy(8,7-4'',5'')flavone (**13**)	N.A.

*Each value represents the mean ± SEM (n=3)

N.A. = No activity

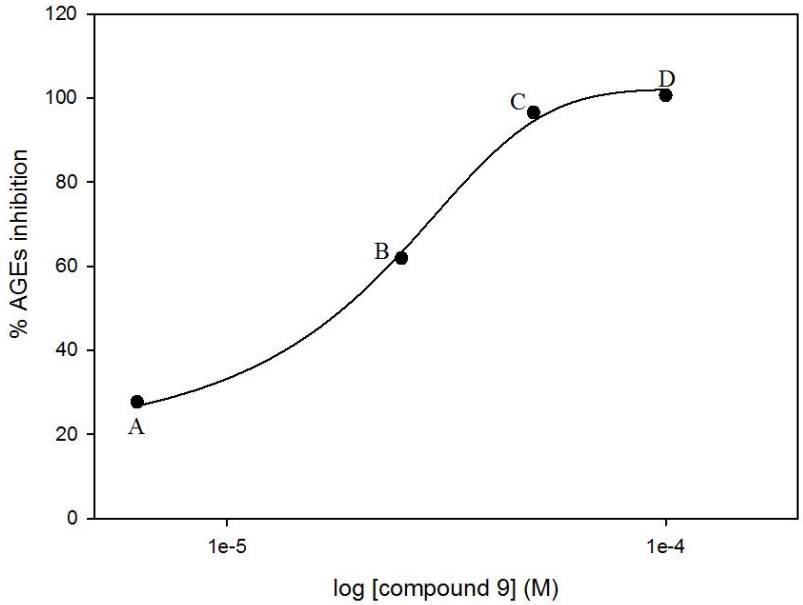

Figure 4.30 % AGEs inhibition of derrisin B (**9**) in BSA-MGO model. Each value represents mean ± SEM (n=3), (A) 27.72% ± 2.24 at concentration of 6.25 μM, (B) 61.89% ± 1.82 at concentration of 25 μM, (C) 96.53% ± 2.22 at concentration of 50 μM, (D) 100.65% ± 4.22 at concentration of 100 μM.

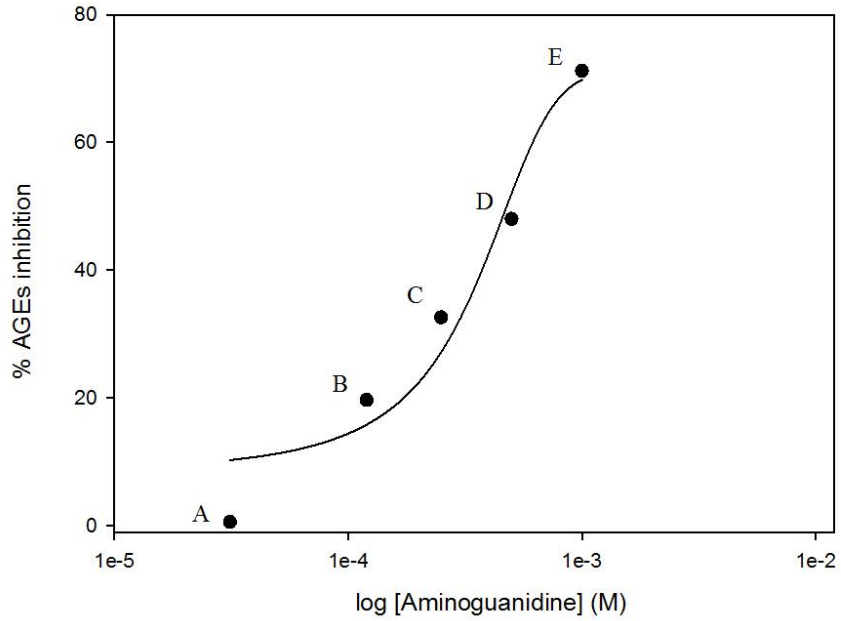

Figure 4.31 % AGEs inhibition of aminoguanidine in BSA-MGO model. Each value represent mean ± SEM (n=3), (A) 0.59% ± 2.31 at concentration of 31.25 μM, (B) 19.67% ± 0.39 at concentration of 125 μM, (C) 32.62% ± 2.27 at concentration of 250 μM, (D) 48.02% ± 0.46 at concentration of 500 μM, (E) 71.18% ± 2.84 at concentration of 1000 μM.

Table 4.17 Inhibitory effects of derrisin B (9) and aminoguanidine on formation of fluorescent advanced glycation end products (AGEs) in BSA incubated with MGO for 1 week.

Compound	IC_{50} (μM)*
Aminoguanidine (AG)	477.11 ± 10.02
Derrisin B (9)	18.00 ± 0.35

* Results were presented as mean ± SEM (n=3)

CHAPTER V

CONCLUSION

The EtOAc crude extract from stem bark of *D. indica* (Lamk.) Bennet. was purified by chromatographic techniques to afford thirteen flavonoids. These included two new flavonoids, derrisins A (**5**) and B (**9**), together with 11 known flavones namely flavone demethoxykanugin (**1**), pongaglabrone (**2**), pongachromene (**3**), pongapin (**4**), karajin (**6**), 3,7,4' –trimethoxyflavone (**7**), fisetin tetramethyl ether (**8**), pongaglabol methyl ether (**10**), lanceolatin B (**11**), pongaflavone (**12**) and, 5-methoxy-3',4'-methylenedioxy(8,7-4",5")flavone (**13**). Their structures were determined on the basis of their spectroscopic (NMR and MS) data analysis, and single-crystal X-Ray diffraction analysis. Moreover, the structures of known compounds were confirmed by comparison of their spectroscopic data with those reported in literature.

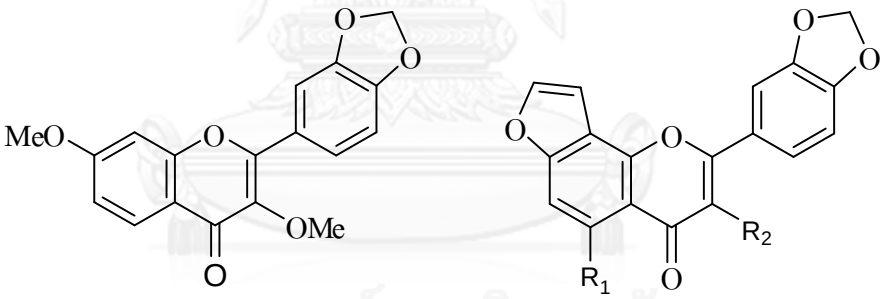

1

2: $R_1 = R_2$=H
4: R_1 =H R_2=OMe
13: R_1 = OMe R_2=H

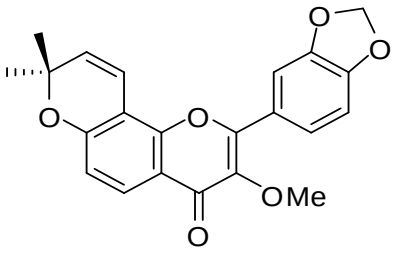

3

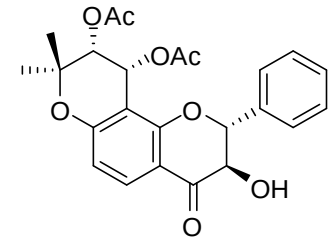

5

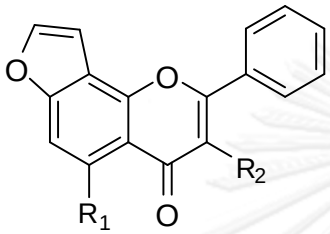

6: R_1 = H R_2 = OMe
10: R_1 = OMe R_2 = H
11: R_1 = R_2 = H

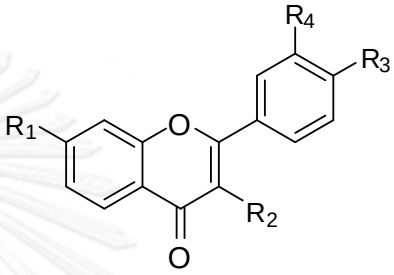

7: R_1 = R_2 = R_3 =OMe R_4 = H
8: R_1 = R_2 = R_3 = R_4 = OMe

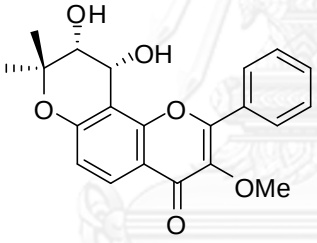

9

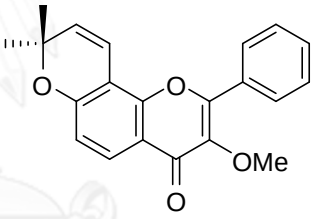

12

All flavonoids were evaluated for anti-inflammatory activity (NO inhibitory assay) and inhibition of advanced glycation end products (AGEs) activity. The anti-inflammatory effects of pure compounds were determined by suppressing nitric oxide production in LPS-activated murine macrophage J774.A1 cells. Desmethoxy kanugin (**1**), derrisin B (**9**) and pongaflavone (**12**) showed anti-inflammatory activity on macrophage cells, with IC_{50} value of 22.83 ± 0.75, 11.24 ± 0.24 and 14.59 ± 0.30 μM, respectively. However, it is possible that the inhibitory activity of derrisin B (**9**) is caused by the cytotoxic activity, determined by MTT colorimetric method. Desmethoxy kanugin (**1**) and pongaflavone (**12**) did not exhibit any significant toxicity on macrophage cells. This suggested both compounds inhibited nitrite levels

themselves without exerting the cell death. Moreover, both desmethoxy kanugin (**1**) and pongaflavone (**12**) were more active than indomethacin, a positive control, againt the production of NO in LPS activated macrophages. Therefore, these compounds might be applied for anti-inflammatory drugs. Additionally, isolated flavonoids were subjected to the antiglycation assay in BSA-MGO model to assess their inhibitory effect on AGEs formation. Only derrisin B (**9**), a new chromenoflavones, exhibited the potent activity with IC_{50} value of 18.00 ± 0.35 μM. Most importantly, its activity was 26.5-fold higher than a positive control, aminoguanidine (IC_{50} = 477.11 ± 10.02 μM). Hence, derrisin B (**9**) might be utilized as a lead compound for inhibitory protein glycation in diabetic patients.

In the present study, it was found that some flavonoids isolated from *D. indica* stem bark displayed interesting biological activities, but only in *in vitro* model. In order to develop then as lead compounds, the action mechanism on those activities should further be investigated.

REFERENCES

1. Brahmachari, G. Natural Products in Drug Discovery: Impacts and Opportunities — An Assessment. In Bioactive Natural Products : Opportunities and Challenges in Medicinal Chemistry. Singapore: World Scientific Publishing Company, 2011. p. 1-7.
2. WHO. WHO traditional medicine strategy 2002-2005. Geneva: World Health Organization, 2002. p 1-2.
3. Newman, D.J., Cragg, G.M. and Snader, K.M. Natural products as sources of new drugs over the period 1981-2002. Journal of Natural Products 66 (2003): 1022-1037.
4. Karkare, S.S. Isolation and structure elucidation of antiproliferative agents from Madagascar rainforests. Master's Thesis, Chemistry, Faculty of Science, Virginia Polytechnic Institute and State University; 2007, p. 7-8.
5. Badole, S.L., Jadhav, S.B., Wagh, N.K. and Menaa, F. General Beneficial Effects of *Pongamia pinnata* (L.) Pierre on Health. In Bioactive Food as Dietary Interventions for the Aging Population: Elsevier Inc, 2013. p. 445-455.
6. Koshia Hemant, G. Studies on effect of medicated oil formulations of Karanj Oil (*Derris Indica*). Doctoral dissertation, Faculty of medicine, Saurashtra University; 2010, p. 5-13.
7. Scott, P.T., Pregelj, L., Chen, N., Hadler, J.S., Djordjevic, M.A. and Gresshoff, P.M. *Pongamia pinnata*: An untapped resource for the biofuels industry of the future. Bioenergy Research 1 (2008): 2-10.
8. Sangwan, S., Rao, D.V. and Sharma, R.A. A Review on *Pongamia Pinnata* (L.) Pierre: A Great Versatile Leguminous Plant. Nature and Science 8 (2010): 130-138.
9. Al Muqarrabun, L.M.R., Ahmat, N., Ruzaina, S.A.S., Ismail, N.H. and Sahidin, I. Medicinal uses, phytochemistry and pharmacology of *Pongamia pinnata* (L.) Pierre. Journal of ethnopharmacology 150 (2013): 395-420.
10. Aiman, R. Recent research on indigenous antidiabetic medicinal plants an overall assessment. Indian journal of physiology and pharmacology 14 (1970): 65-76.
11. Koysomboon, S., van Altena, I., Kato, S. and Chantrapromma, K. Antimycobacterial flavonoids from *Derris indica*. Phytochemistry 67(10) (2006): 1034-1040.
12. Wagh, P., Rai, M., Deshmukh, S.K. and Durate, M.C.T. Bio-activity of oils of *Trigonella foenumgraecum* and *Pongamia pinnata*. African journal of biotechnology 6 (2007): 1592-1596.
13. Arote, S.R. and Yeole, P.G. *Pongamia pinnata* L: A comprehensive review. International Journal of PharmTech Research 2 (2010): 2283-2290.

14.Baral, S.R. and Kurmi, P.P. A Compendium of Medicinal Plants Nepal. Nepal: Mrs Rachana Publishers, 2006. p 534.
15.Bhattacharjee, S.K. Handbook of Medicinal Plants.IIIrd edition. India: Pointer Publishers, 2001. p 478.
16.Oommen, S., Ved, D.K. and Krishan, R. Tropical Indian Medicinal Plants: Oregon. USA, 2000. p 599.
17.GoN. Medicinal Plants of Nepal. In Bulletin of the Department of Plant Resources. 28. Nepal: Ministry of Forest and Soil Conservation, 2007. p. 402.
18.Joshi, S.G. Medicinal Plants. India: Oxford & IBH Publishing, 2006.
19.Krishnamurthi, A. The Wealth of India-Raw Materials. India: Council of Scientific and Industrial Research, 1998. p 206-211.
20.Ahmad, G., Yadav, P.P. and Maurya, R. Furanoflavonoid glycosides from *Pongamia pinnata* fruits. Phytochemistry 65(7) (2004): 921-924.
21.Talapatra, S.K., Mallik, A.K. and Talapatra, B. Pongaglabol, a new hydroxyfuranoflavone, and aurantiamide acetate, a dipeptide from the flowers of *Pongamia glabra*. Phytochemistry 19 (1980): 1199-1202.
22.Yadav, P.P., Ahmad, G. and Maurya, R. Furanoflavonoids from *Pongamia pinnata* fruits. Phytochemistry 65(4) (2004): 439-443.
23.González-Gallego, J., García-Mediavilla, M.V., Sánchez-Campos, S. and Tuñón, M. Anti-Inflammatory and immunomodulatory properties of dietary flavonoids. In Polyphenols in Human Health and Disease: Elsevier Inc, 2013. p. 435.
24.Higdon, J. and Drake, J. Flavonoids [Online]. 2008. Available from: http://lpi.oregonstate.edu/infocenter/phytochemicals/flavonoids/index.html [2014, February 27]
25.Sabir, A. Using flavonoids as a natural products with high prarmacological potency to improving oral health [Online]. 2010. Available from: http://www.academia.edu/2494588/USING_FLAVONOIDS_AS_A_NATURAL_PRODUCTS_WITH_HIGH_PHARMACOLOGICAL_POTENCY_TO_IMPROVING_ORAL_HEALTH [2014, February 27]
26.Saha, M.M., Mallik, U.K. and Mallik, A.K. A chromenoflavone and two caffeicesters from *Pongamia glabra* Phytochemistry 30 (1991): 3834-3836.
27.Tanaka, T., Iinuma, M., Yuki, K., Fujii, Y. and Mizuno, M. Flavonoids in root bark of *Pongamia pinnata*. Phytochemistry 31 (1992): 993-998.
28.Li, L., and other. Pongamone A-E, five flavonoids from the stems of a mangrove plant, *Pongamia pinnata*. Phytochemistry 67(13) (2006): 1347-1352.
29.Ranga Rao, R., and other. New furanoflavanoids, intestinal alpha-glucosidase inhibitory and free-radical (DPPH) scavenging, activity from antihyperglycemic root

extract of *Derris indica* (Lam.). Bioorganic & medicinal chemistry 17(14) (2009): 5170-5175.

30. Marzouk, M.S.A., Ibrahim, M.T., El-Gindi, O.R. and Bakr, M.S.A. Isoflavonoids glycosides and rotenoids from *Pongamia pinnata* leaves. Zeitschrift für Naturforschung 63c (2008): 1-7.
31. Yin, H., Zhang, S. and Wu, J. Study on flavonoids from stem bark of *Pongamia pinnata*. Zhong Yao Cai 27 (2004): 493-495.
32. Talapatra, S.K., Mallik, A.K. and Talapatra, B. Isopongaglabol and 6-methoxyisopongaglabol, two new hydroxyfuranoflavones from *Pongamia glabra*. Phytochemistry 21 (1982): 761-766.
33. Minakawa, T., and other. Constituents of *Pongamia pinnata* isolated in a screening for activity to overcome tumor necrosis factor-related apoptosis-inducing ligand-resistance. Chemical and Pharmaceutical Bulletin 58 (2010): 1549-1551.
34. Pathak, V.P., Saini, T.R. and Khanna, R.N. Isopongachromene, a chromenoflavone from *Pongamia glabra* seeds. Phytochemistry 22 (1983a): 308-309.
35. Carcache-Blanco, E.J., and other. Constituents of the stem bark of *Pongamia pinnata* with the potential to induce quinone reductase. Journal of Natural Products 66 (2003): 1197-1202.
36. Kanungo, P.D., Ganguly, A., Guha, A., Bhattacharyya, A. and Adityachaudhury, N. Glabone, a new furanoflavone from *Pongamia glabra*. Phytochemistry 26 (1987): 3373-3374.
37. Rashid, N., Abbasi, M.S.A., Tahir, M.K., Yusof, N.M. and Yamin, B.M. Isolation and crystal structure of karanjachromene. Analytical Sciences 24 (2008): 21-22.
38. Yin, H., and other. Pongaflavanol: a prenylated flavonoid from *Pongamia pinnata* with a modified ring A. Molecules 11 (2006b): 786-791.
39. Semalty, A., Semalty, M., Kumar, P., Mir, S.R., Ali, M. and Amin, S. Isolation and hypoglycemic activity of a novel pongamiaflavonyl flavonol from *Pongamia pinnata* pods. International Journal of Pharmacology 8 (2012): 265-270.
40. Yin, H., Zhang, S., Wu, J. and Nan, H. Dihydropyranoflavones from *Pongamia pinnata*. Journal of Brazilian Chemical Society 17 (2006a): 1432-1435.
41. Kitagawa, I., Zhang, R.S., Hori, K., Tsuchiya, K. and Shibuya, H. Indonesia medicinal plants. II. Chemical structures of pongapinones A and B, two new phenylpropanoids from the bark of Pongamia pinnata (Papilionaceae). Chemical and Pharmaceutical Bulletin 40 (1992): 2041-2043.

42.Gandhidasan, R., Neelakantan, S., Raman, P.V. and Devaraj, S. Components of the galls on the leaves of *Pongamia glabra*: structures of pongagallone-A and pongagallone-B. Phytochemistry 26 (1987): 281-283.

43.Srinivasan, K., Muruganandan, S., Lal, J., Chandra, S., Tandan, S. and Raviprakash, V. Evaluation of anti-inflammatory activity of Pongamia pinnata leaves in rats. Journal of Ethanopharmacology 78 (2001): 151-157.

44.Ganesh, M., and other. Anti-inflammatory and Analgesic Effects of *Pongamia glabra* Leaf Gall Extract. Pharmacologyonline 1 (2008): 497-512.

45.Sagar, M.K., Kumar, P.A. and Upadhyaya, K.K. Anti-inflammatory and analgesic activities of methanolic extract of *Pongamia pinnata* stem bark. International Journal of Pharma Professional's Research 1 (2010): 5-9.

46.Badole, S.L., Zanwar, A.A., Ghule, A.E., Ghosh, P. and Bodhankar, S.L. Analgesic and anti-inflammatory activity of alcoholic extract of stem bark of *Pongamia pinnata* (L.) Pierre. Biomedicine & Aging Pathology 2(1) (2012): 19-23.

47.Kesari, V., Das, A. and Rangan, L. Physico-chemical characterization and anti-microbial activity from seed oil of *Pongamia pinnata*, a potential biofuel crop. Biomass and Bioenergy 34 (2010): 108-115.

48.Rani, M.S., Dayanand, C.D., Shetty, J., Vegi, P.K. and Kutty, A.V.M. Evaluation of Antibacterial Activity of *Pongamia pinnata linn* on Pathogens of Clinical Isolates. American Journal of Phytomedicine and Clinical Therapeutics 1 (2013): 645-651.

49.Chinnasamy, A., Subramanian, V. and Gajendran, B. Anticancer activity of *Pongamia glabra* V. seed oil extract against selected human cancer cell lines. International Research Journal of Pharmacy 3 (2012): 131-134.

50.Punitha, R. and Manoharan, S. Antihyperglycemic and antilipidperoxidative effects of *Pongamia pinnata* (Linn.) Pierre flowers in alloxan induced diabetic rats. Journal of ethnopharmacology 105(1-2) (2006): 39-46.

51.Tamrakar, A.K., Yadav, P.P., Tiwari, P., Maurya, R. and Srivastava, A.K. Identification of pongamol and karanjin as lead compounds with antihyperglycemic activity from *Pongamia pinnata* fruits. Journal of ethnopharmacology 118(3) (2008): 435-439.

52.Das, B., Chakravarty, A.K., Masuda, K., Suzuki, H. and Ageta, H. A diterpenoid from roots of *Gelonium multiflorum*. Phytochemistry 37 (1994): 1363-1366.

53.Mittal, O.P. and Seshadri, T.R. Demethoxykanugin: a new crystalline compound from *Pongamia glabra*. Journal of the Chemical Society (1956): 2176-2178.

54.Garcez, F.R., Scramin, S., Nascimento, M.C.D. and Mors, W.B. Prenylated flavonoids as evolutionary indicators in the genus *Dahlstedtia*. Phytochemistry 27 (1988): 1079-1083.

55.Gupta, S.C., Singh, F.P., Cook, I.B. and Ternai, B. Carbon-13 NMR studies of some complex natural oxygen heterocycles. V. Carbon-13 NMR spectra of furanoflavones. Organic magnetic resonance 20 (1982): 221-223.

56.Vismaya, Sapna Eipeson, W., Manjunatha, J.R., Srinivas, P. and Sindhu Kanyaa, T.C. Extraction and recovery of karanjin: A value addition to karanja (*Pongamia pinnata*) seed oil. Industrial Crops and Products 32 (2010): 118-122.

57.Lee, J.I. and Park, S.B. An effective synthesis of 3-methoxyflavones via 1-(2-hydroxyphenyl)-2-methoxy-3-phenyl-1,3-propanediones. Bulletin of the Korean Chemical Society 33 (2012): 1379-1382.

58.Yoshioka, T., Inokuchi, T., Fujioka, S. and Kimura, Y. Phenolic compounds and flavonoids as plant growth regulators from fruit and leaf of *Vitex rotundifolia*. Zeitschrift fuer Naturforschung 59c (2004): 509-514.

59.Moncada, S. and Higgs, A. The L-arginine-nitric oxide pathway. The New England Journal of Medicine 329 (1993): 2002-2012.

60.Lee, S.J., Bai, S.K., Lee, S.K., Namkoong, S. and other. Astaxanthin Inhibits Nitric Oxide Production and Inflammatory Gene Expression by Suppressing I**κ**B Kinase-dependent NF-**κ**B Activation. Molecules and Cells 16 (2003): 97-105.

61.Hiro, M., and other. Experimental Models for Advanced Glycation End Product Formation Using Albumin, Collagen, Elastin,Keratin and Proteoglycan. . Anti-Aging Medicine 9 (2012): 125-134.

62.Kaewnarin, K., Shank, L., Niamsup, H. and Rakariyatham, N. Inhibitory effects of Lamiaceae plant on the formation of Advanced Glycation Endproducts (AGEs) in Model Proteins. Journal of Medical and Bioengineering 2 (2013): 224-227.

APPENDIX

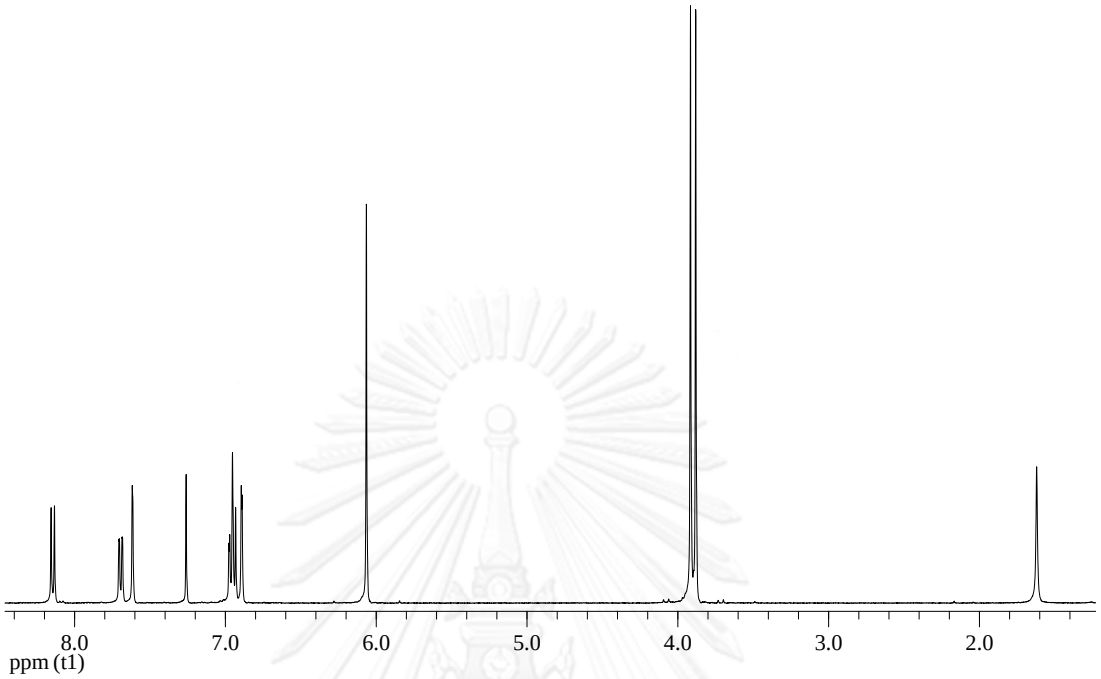

Figure A.1 ^{1}H NMR (400 MHz) spectrum of compound **1** ($CDCl_3$)

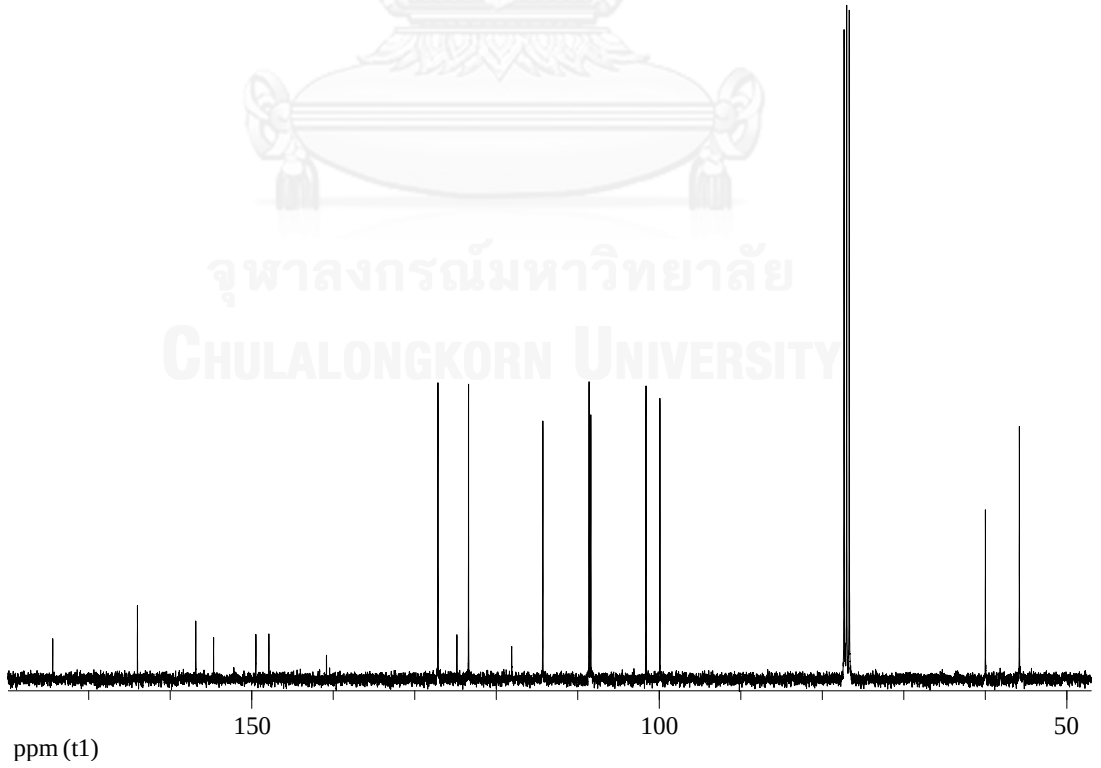

Figure A.2 ^{13}C NMR (100 MHz) spectrum of compound **1** ($CDCl_3$)

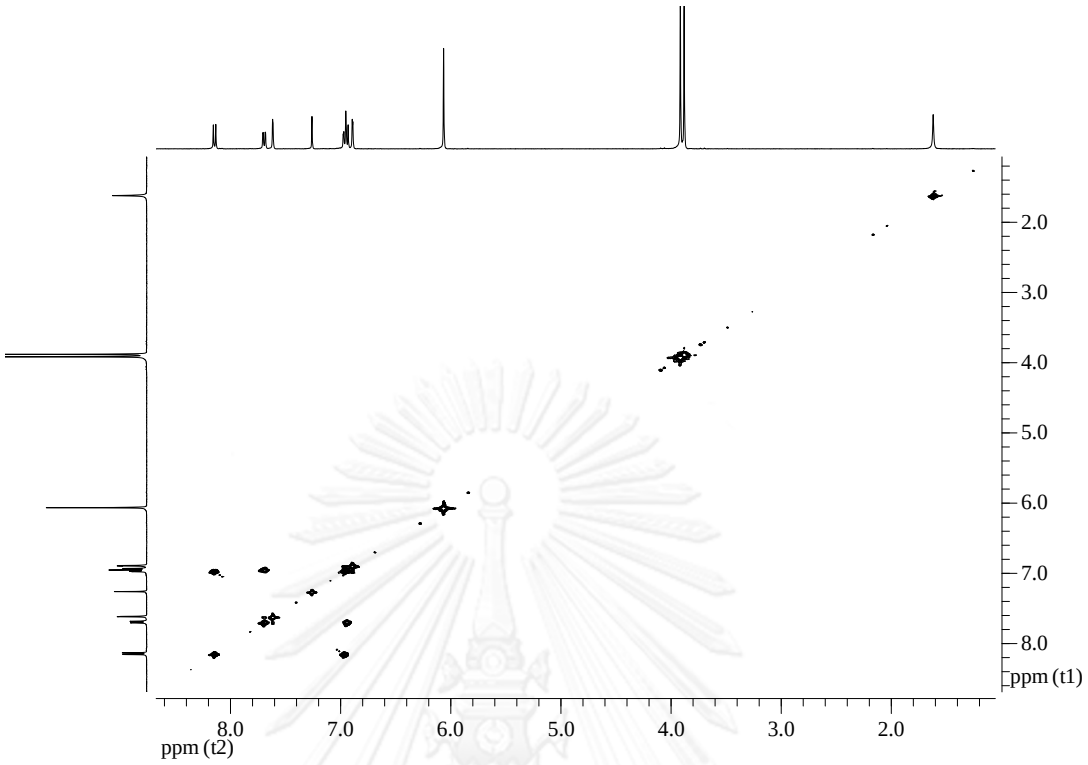

Figure A.3 ^{1}H-^{1}H COSY spectrum of compound **1** ($CDCl_3$)

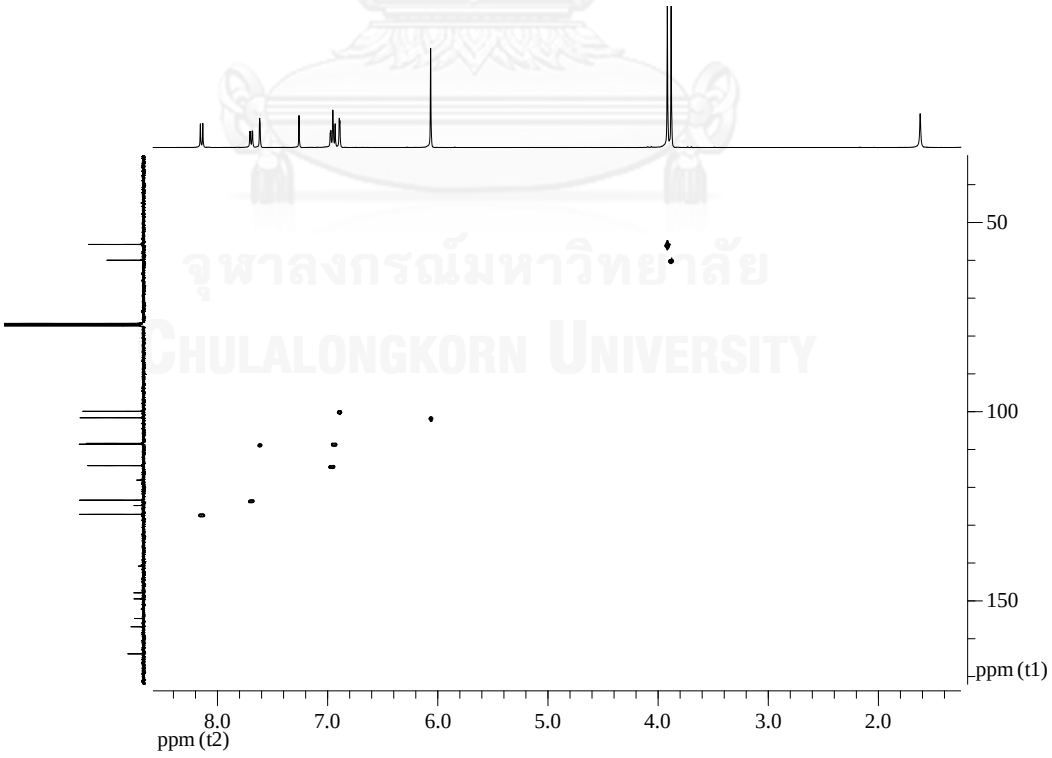

Figure A.4 HSQC spectrum of compound **1** ($CDCl_3$)

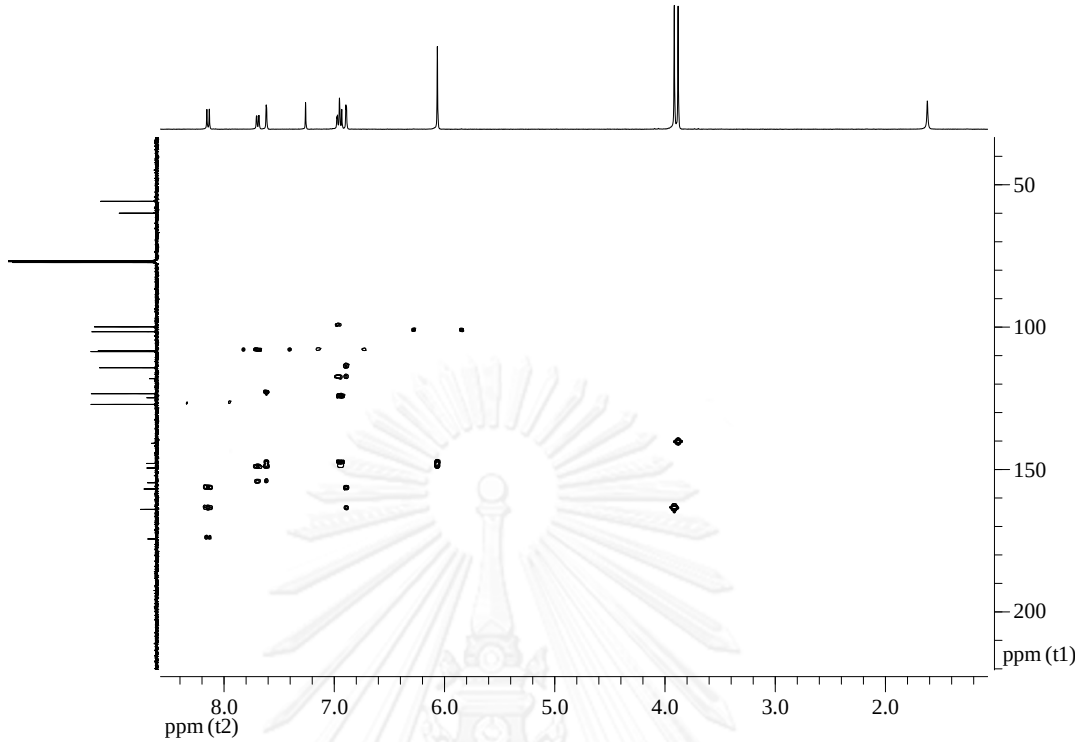

Figure A.5 HMBC spectrum of compound **1** ($CDCl_3$)

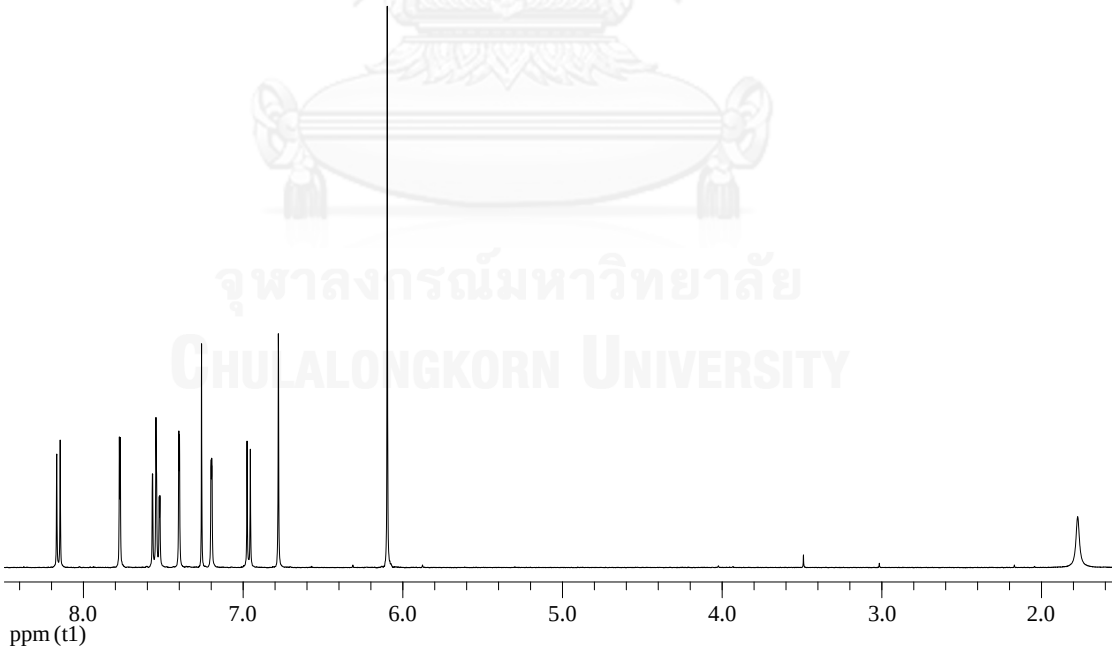

Figure A.6 ^{1}H NMR (400 MHz) spectrum of compound **2** ($CDCl_3$)

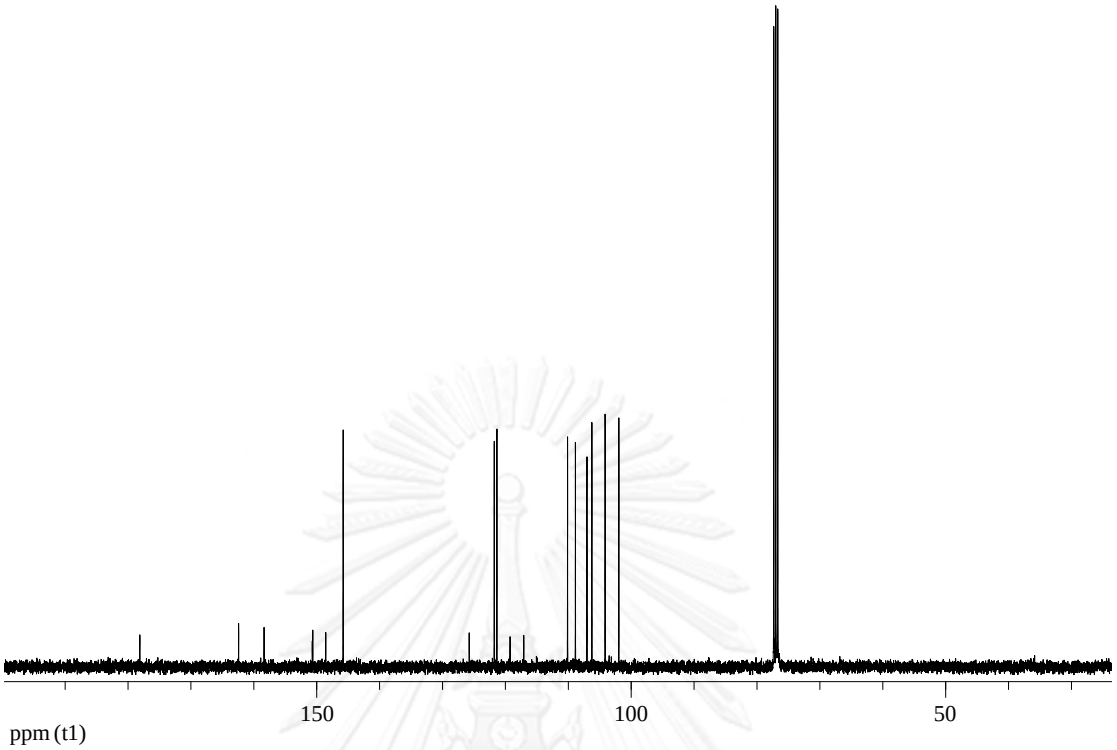

Figure A.7 ^{13}C NMR (100 MHz) spectrum of compound **2** ($CDCl_3$)

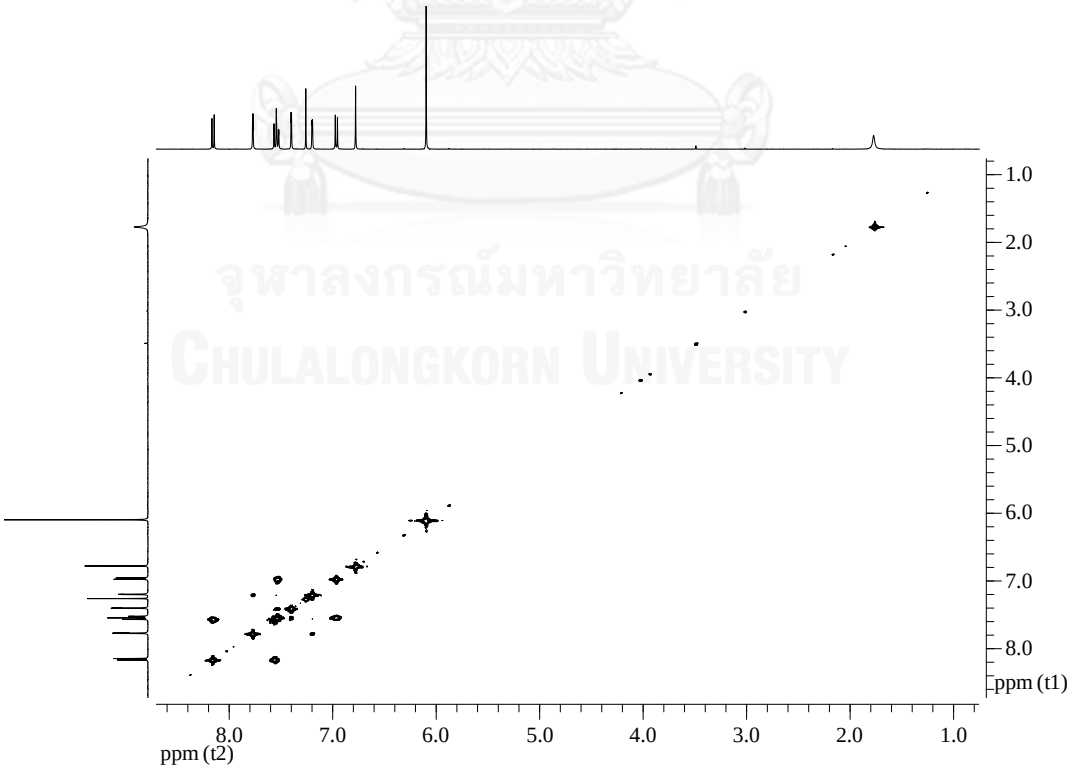

Figure A.8 ^{1}H-^{1}H COSY spectrum of compound **2** ($CDCl_3$)

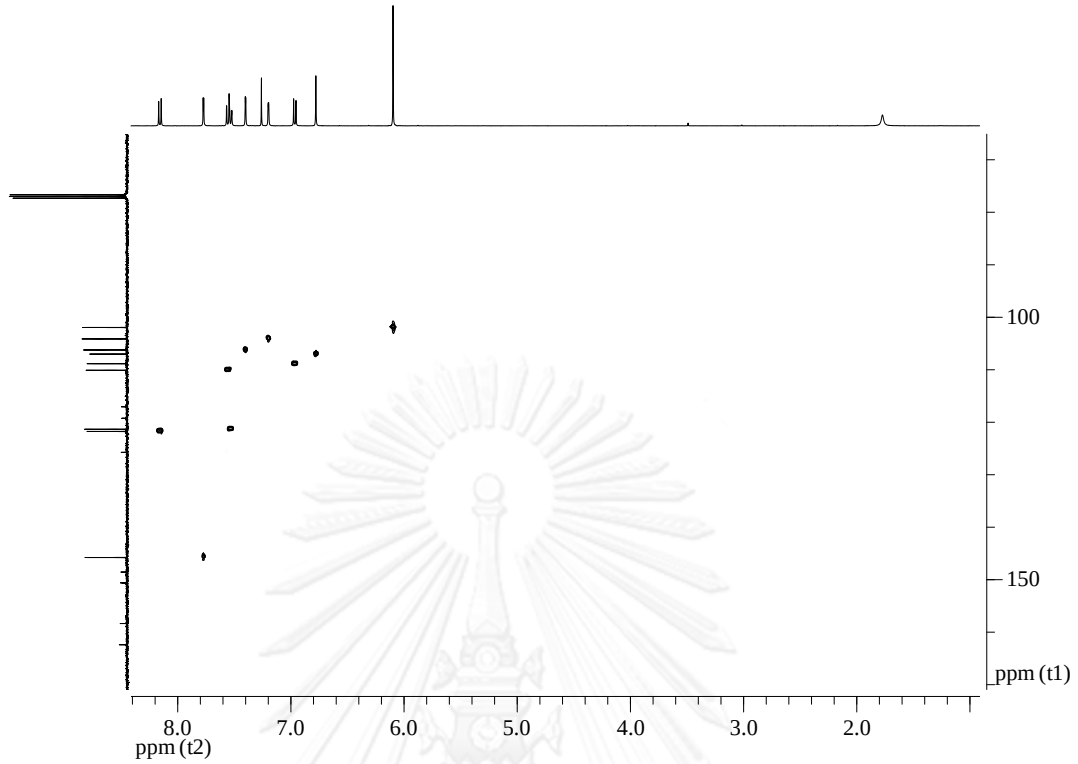

Figure A.9 HSQC spectrum of compound **2** ($CDCl_3$)

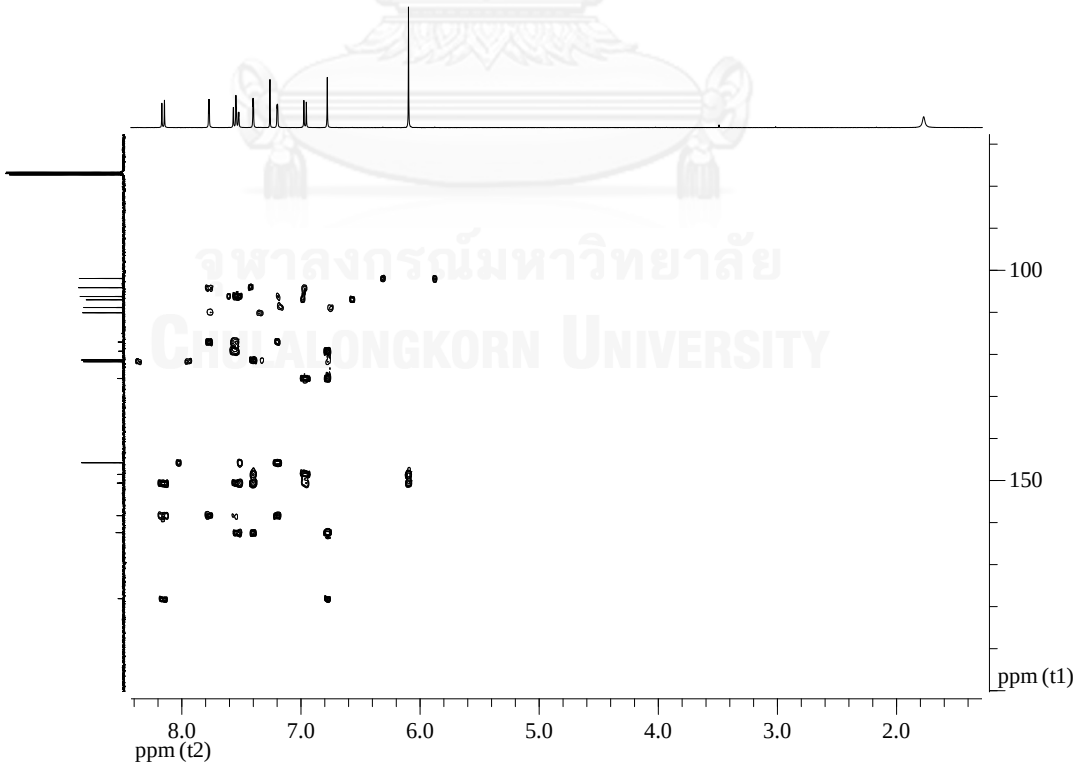

Figure A.10 HMBC spectrum of compound **2** ($CDCl_3$)

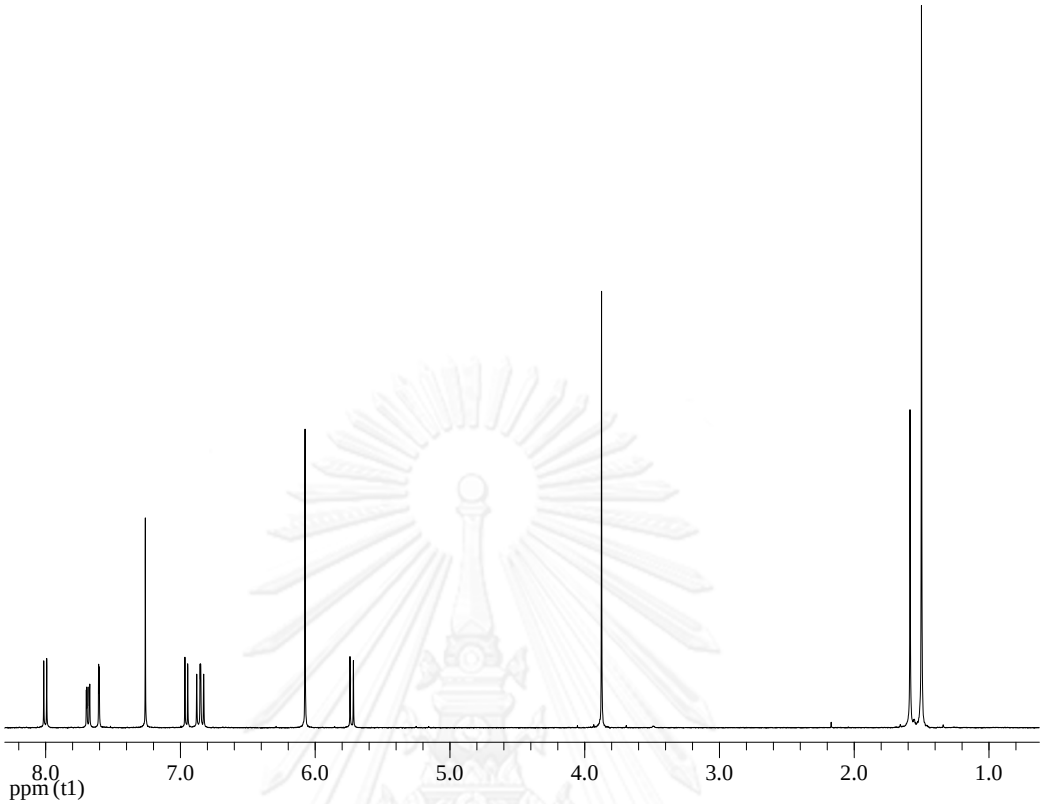

Figure A.11 ^{1}H NMR (400 MHz) spectrum of compound **3** ($CDCl_3$)

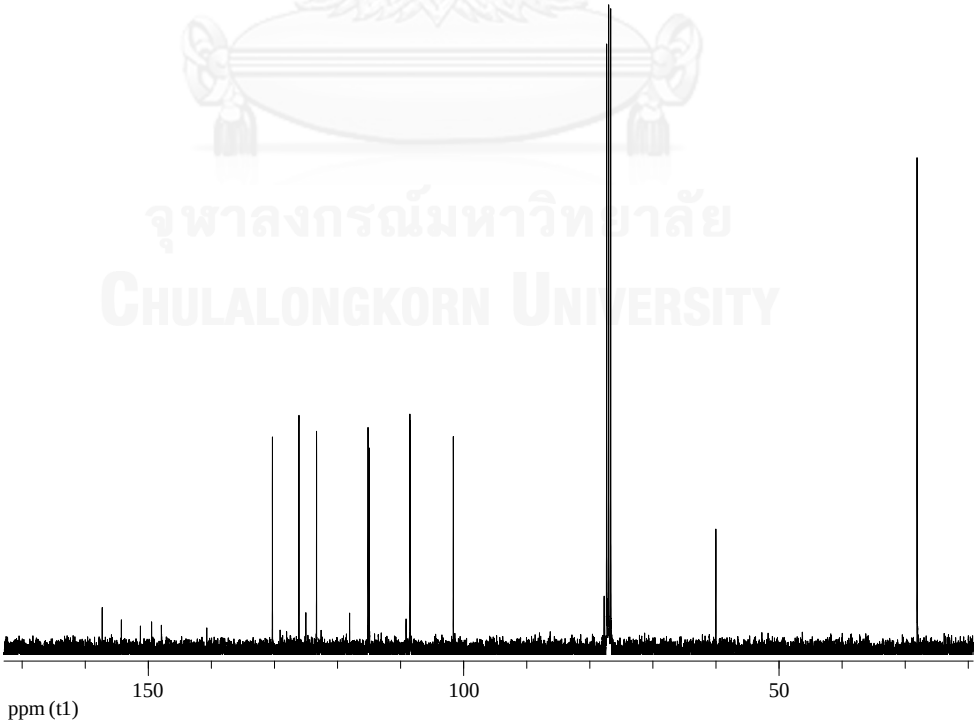

Figure A.12 ^{13}C NMR (100 MHz) spectrum of compound **3** ($CDCl_3$)

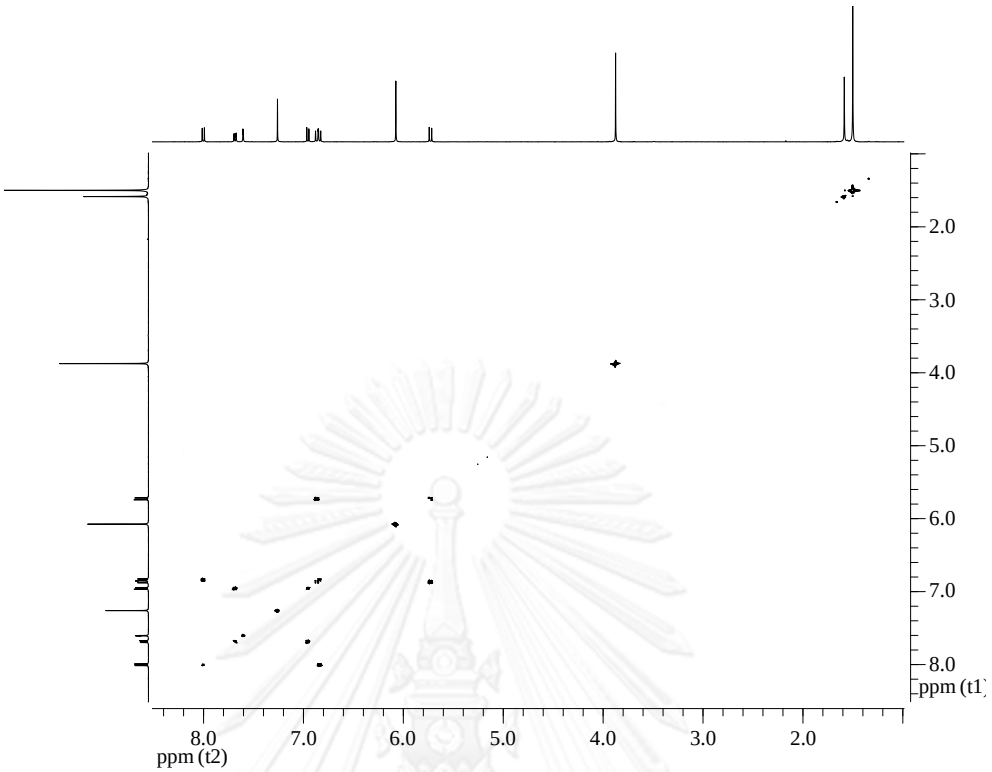

Figure A.13 ^{1}H-^{1}H COSY spectrum of compound **3** ($CDCl_3$)

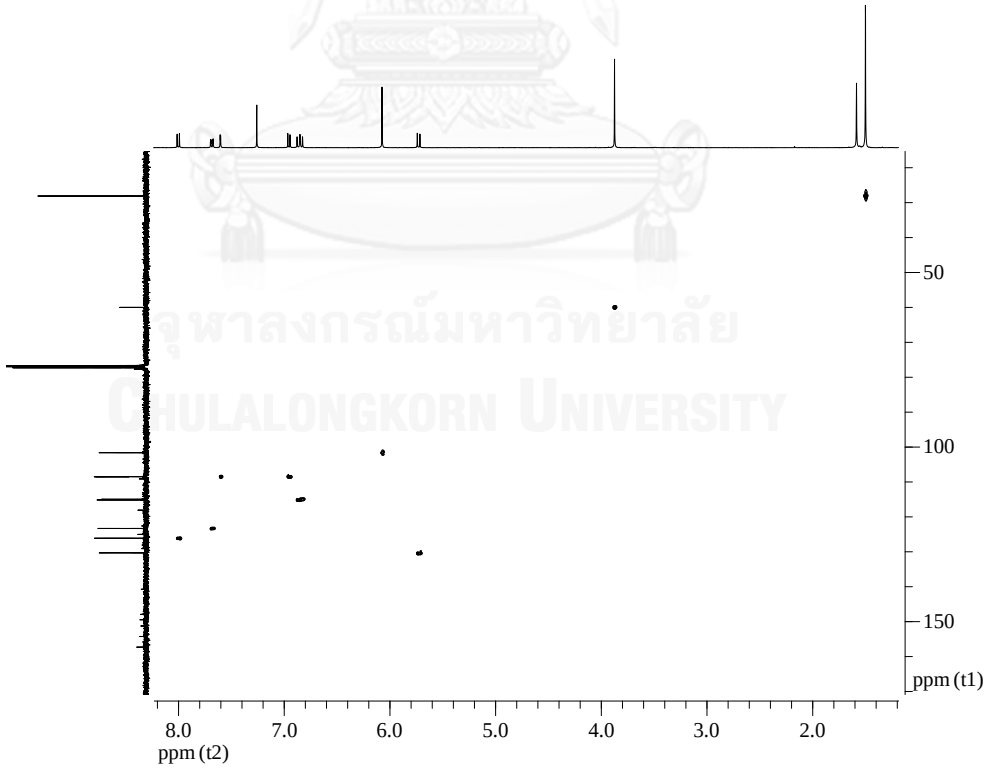

Figure A. 14 HSQC spectrum of compound **3** ($CDCl_3$)

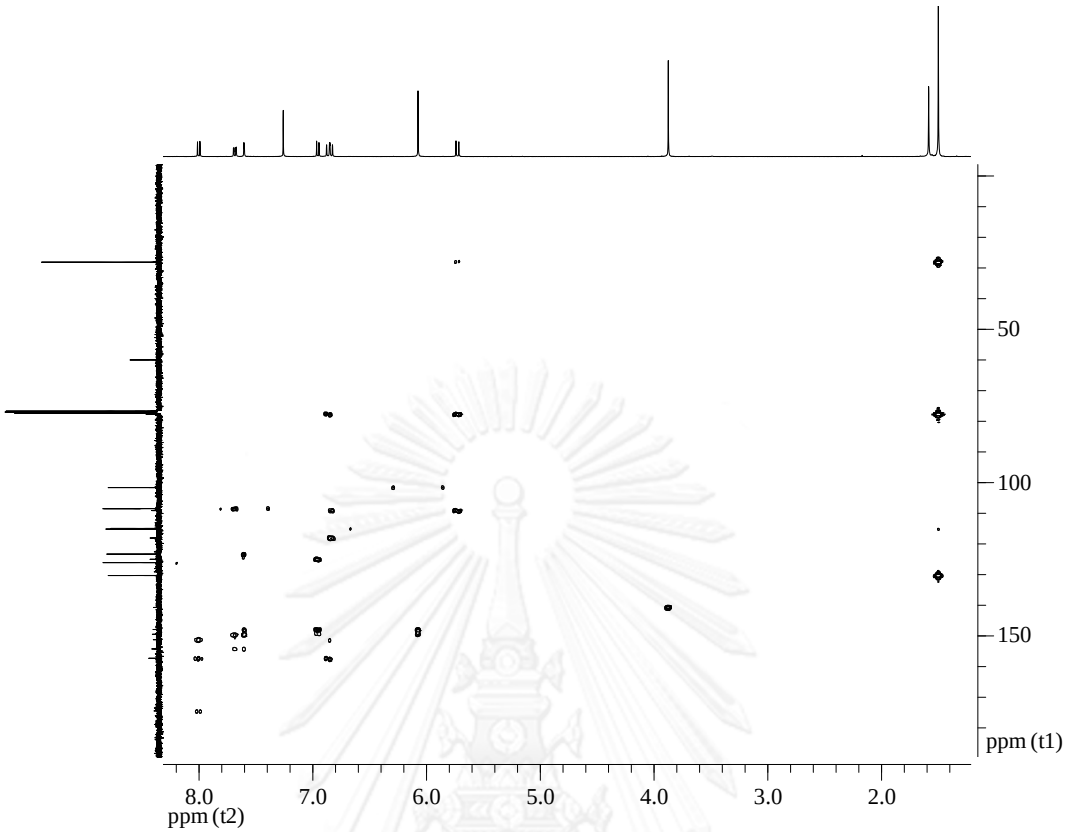

Figure A.15 HMBC spectrum of compound **3** ($CDCl_3$)

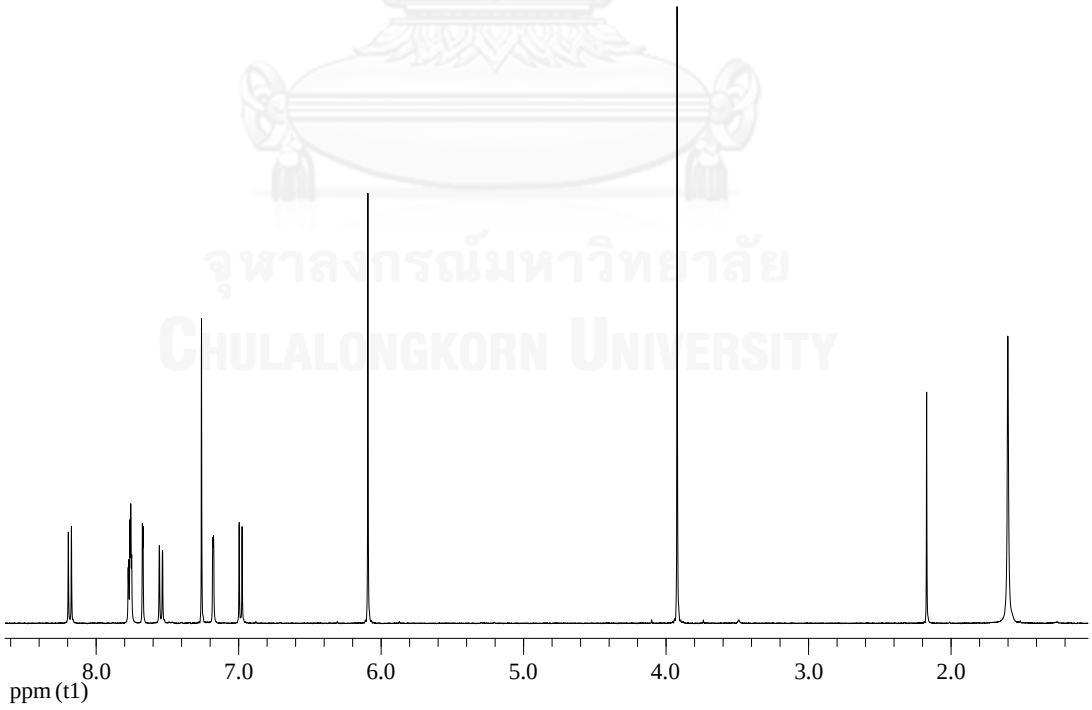

Figure A.16 ^{1}H NMR (400 MHz) spectrum of compound **4** ($CDCl_3$)

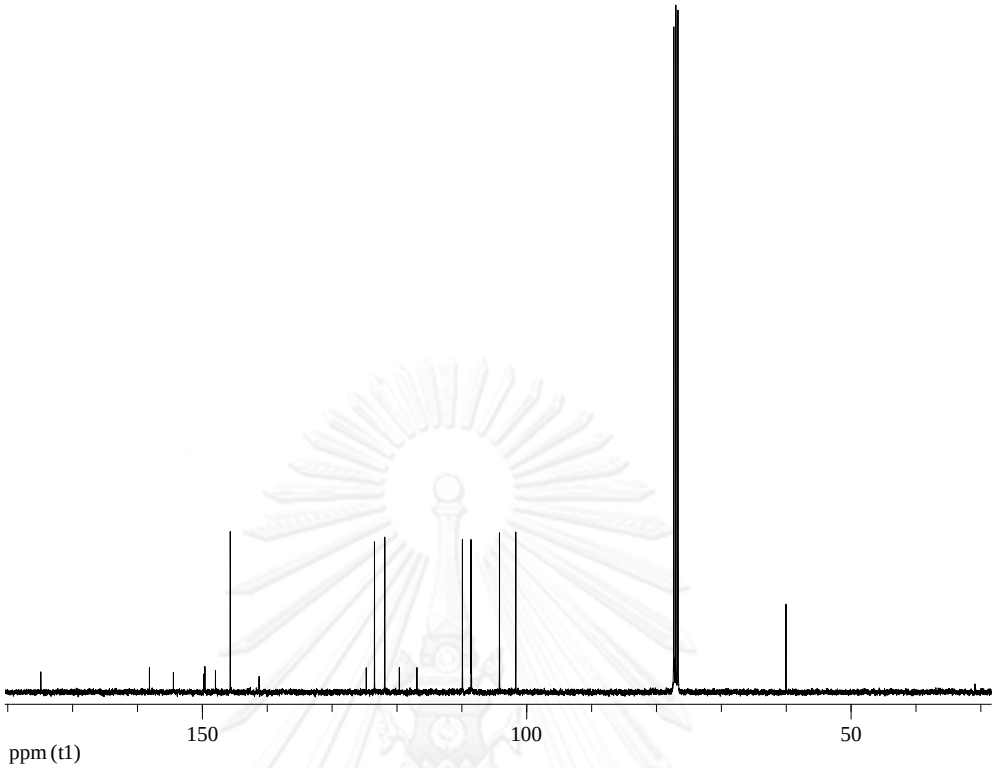

Figure A.17 ^{13}C NMR (100 MHz) spectrum of compound **4** ($CDCl_3$)

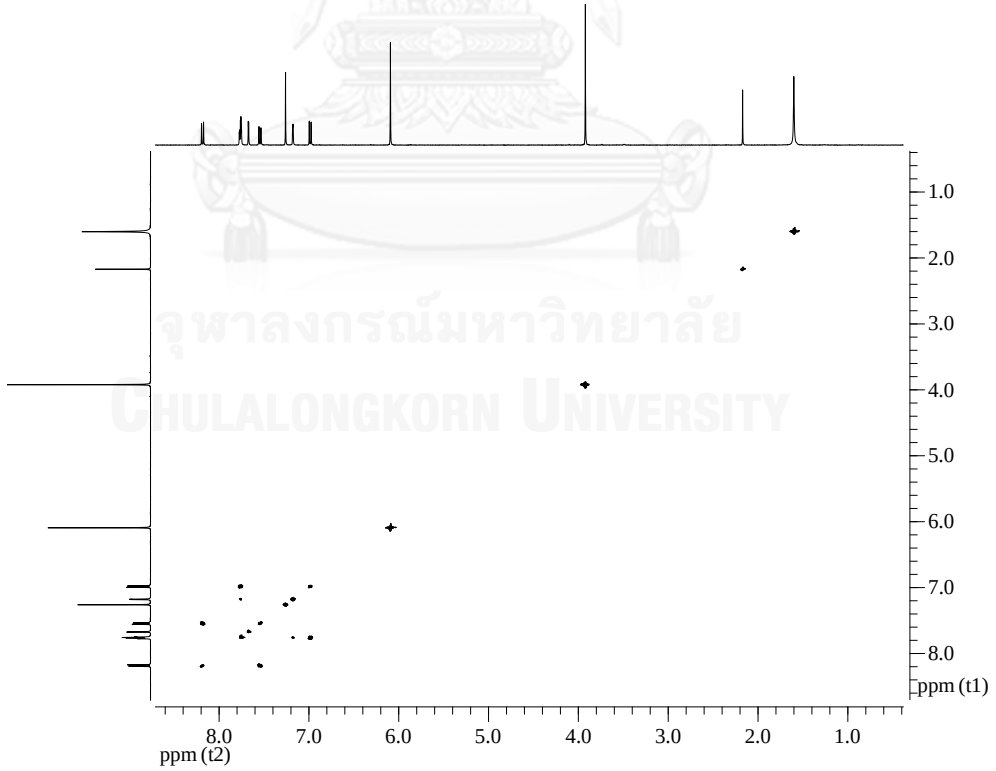

Figure A.18 ^{1}H-^{1}H COSY spectrum of compound **4** ($CDCl_3$)

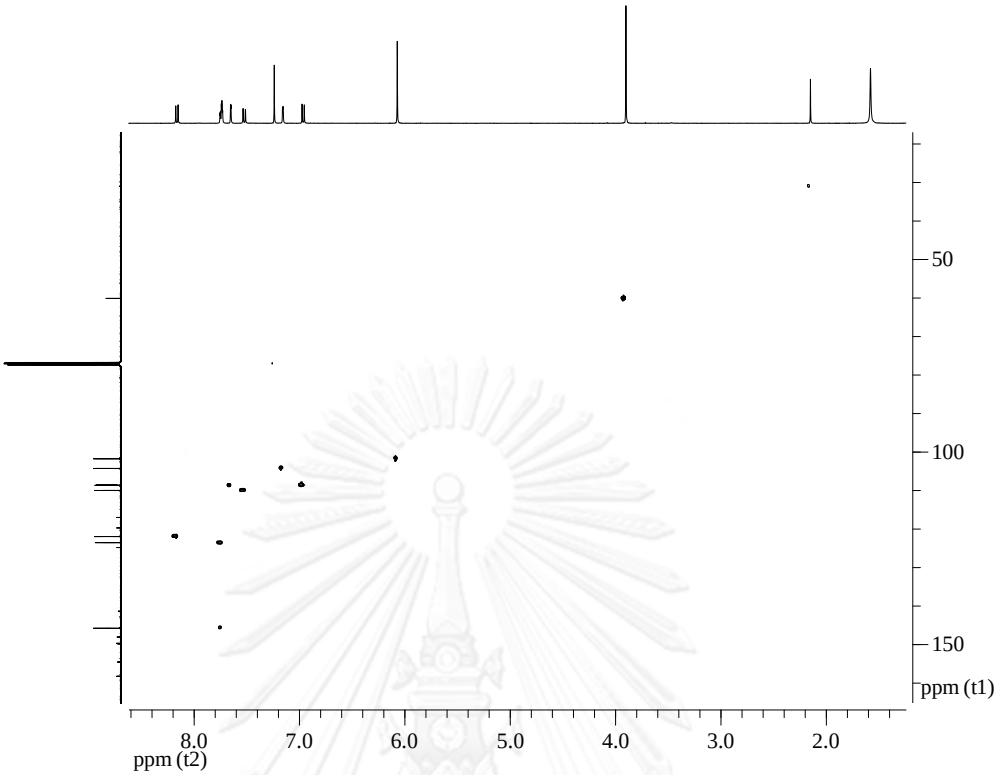

Figure A.19 HSQC spectrum of compound **4** ($CDCl_3$)

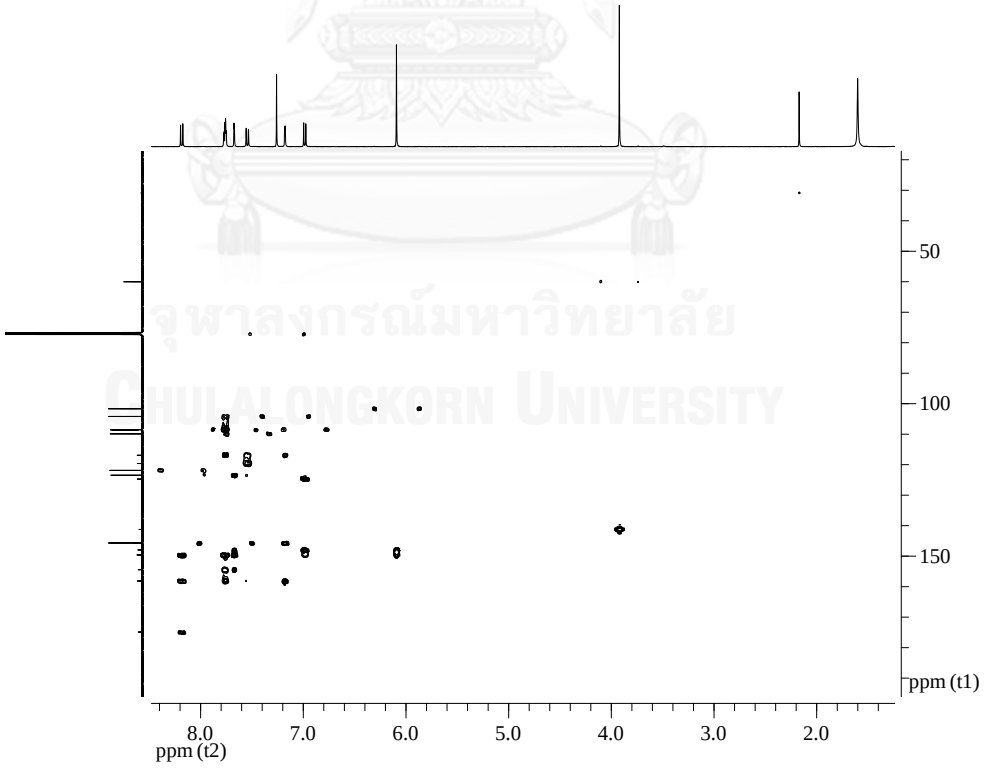

Figure A.20 HMBC spectrum of compound **4** ($CDCl_3$)

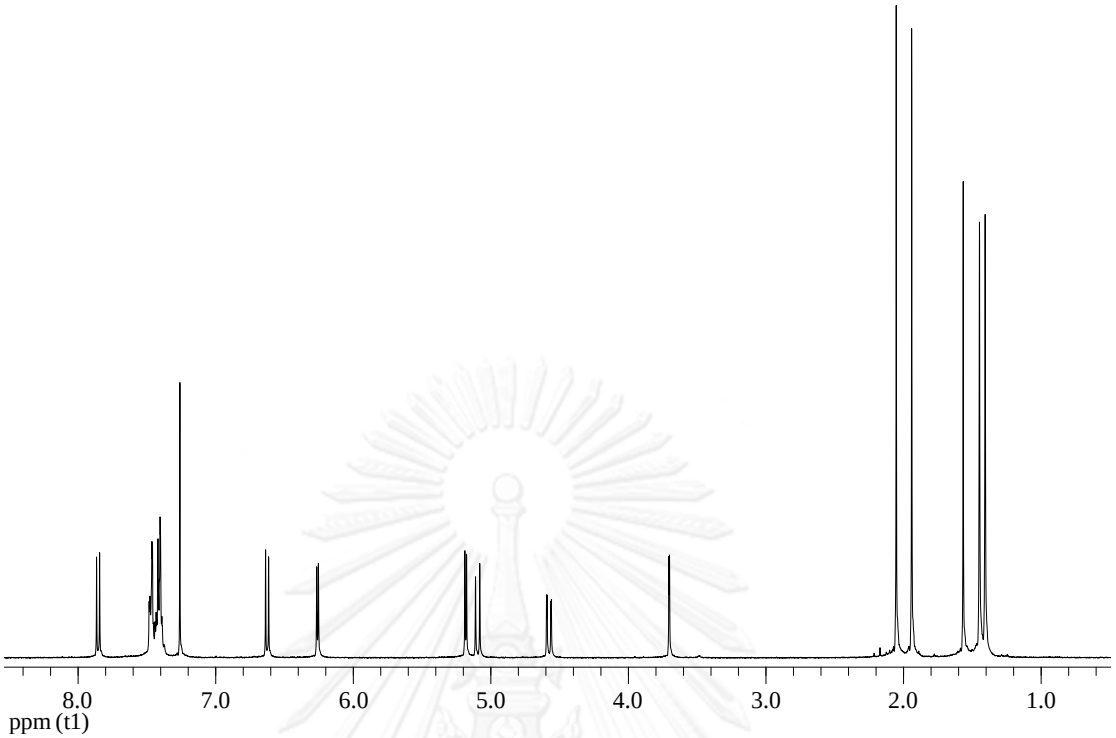

Figure A.21 ^{1}H NMR (400 MHz) spectrum of compound **5** ($CDCl_3$)

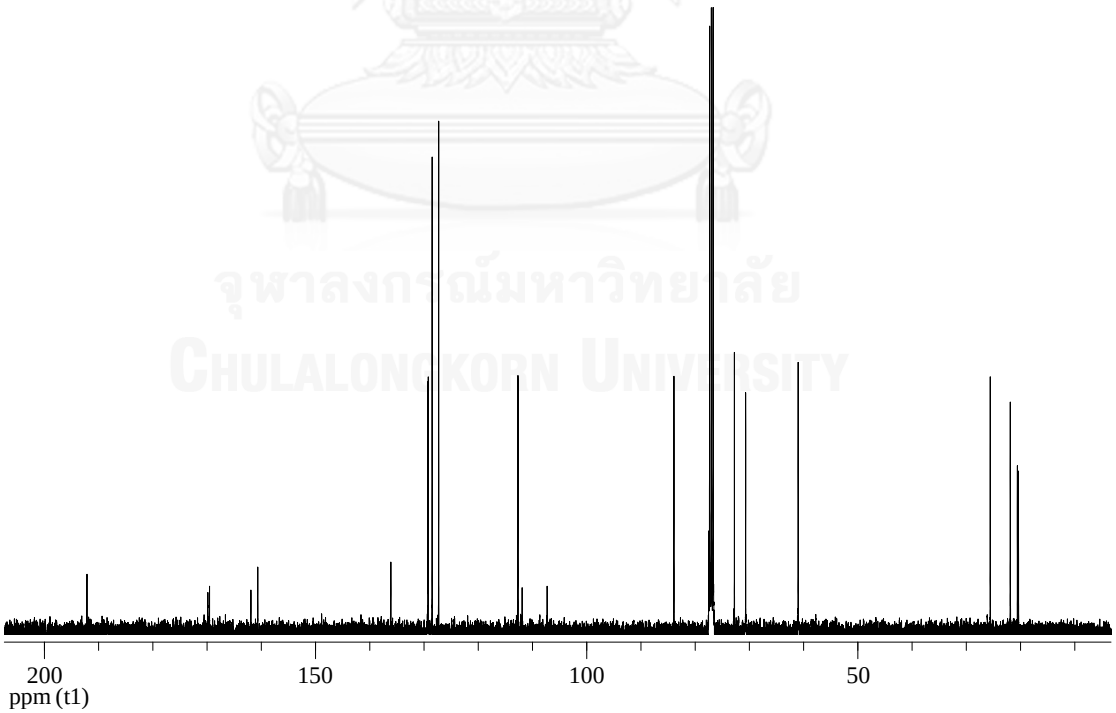

Figure A.22 ^{13}C NMR (100 MHz) spectrum of compound **5** ($CDCl_3$)

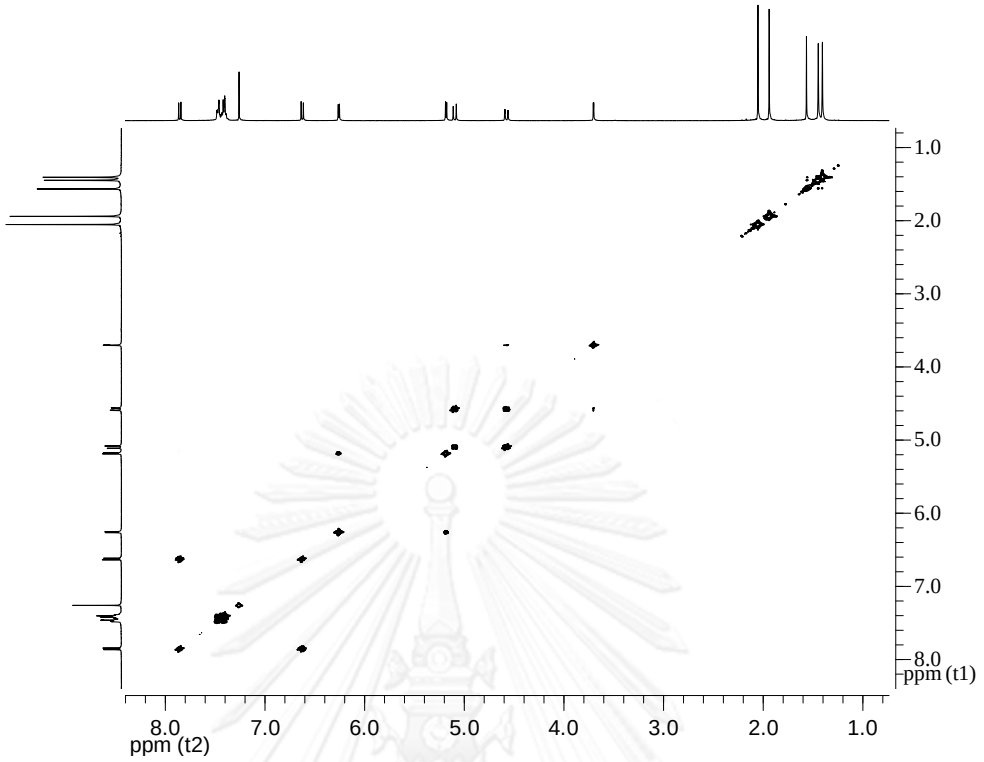

Figure A.23 ^{1}H-^{1}H COSY spectrum of compound **5** ($CDCl_3$)

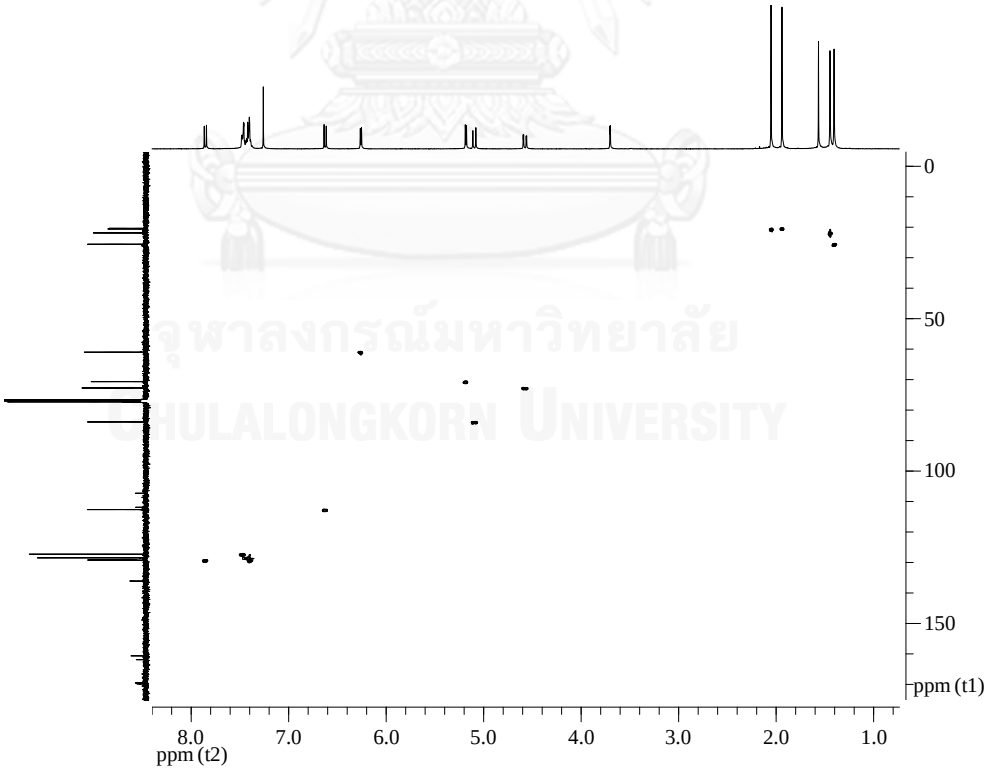

Figure A.24 HSQC spectrum of compound **5** ($CDCl_3$)

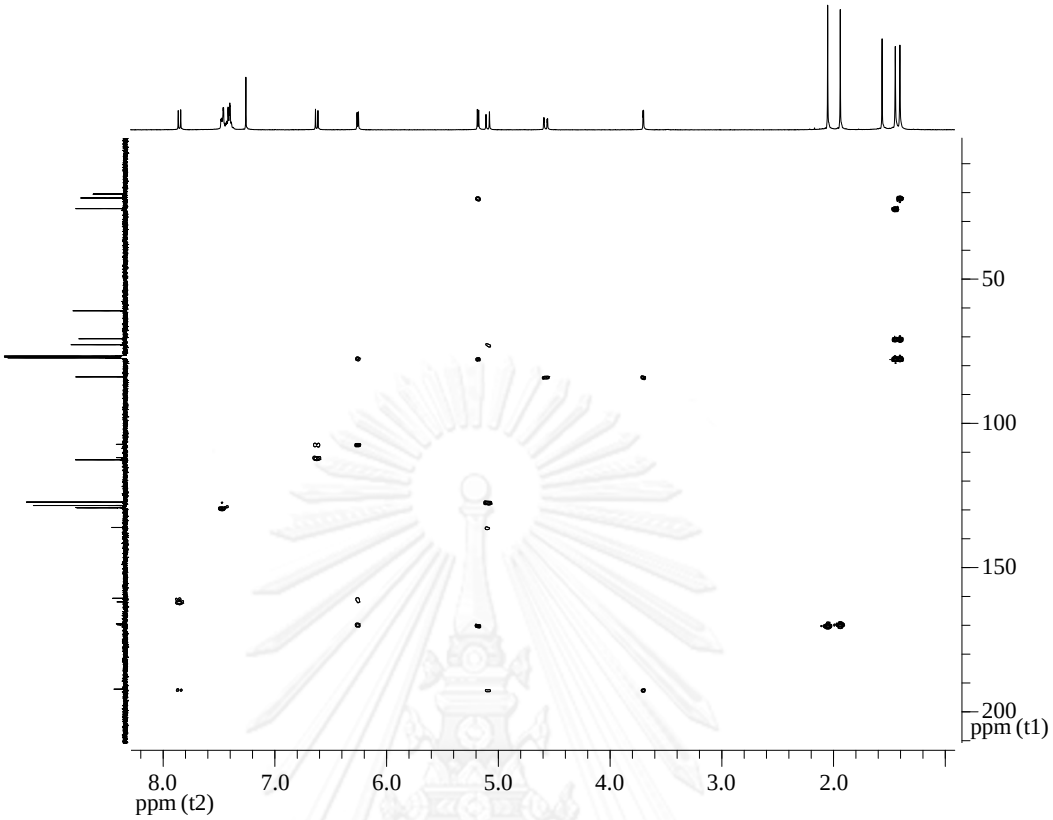

Figure A.25 HMBC spectrum of compound **5** ($CDCl_3$)

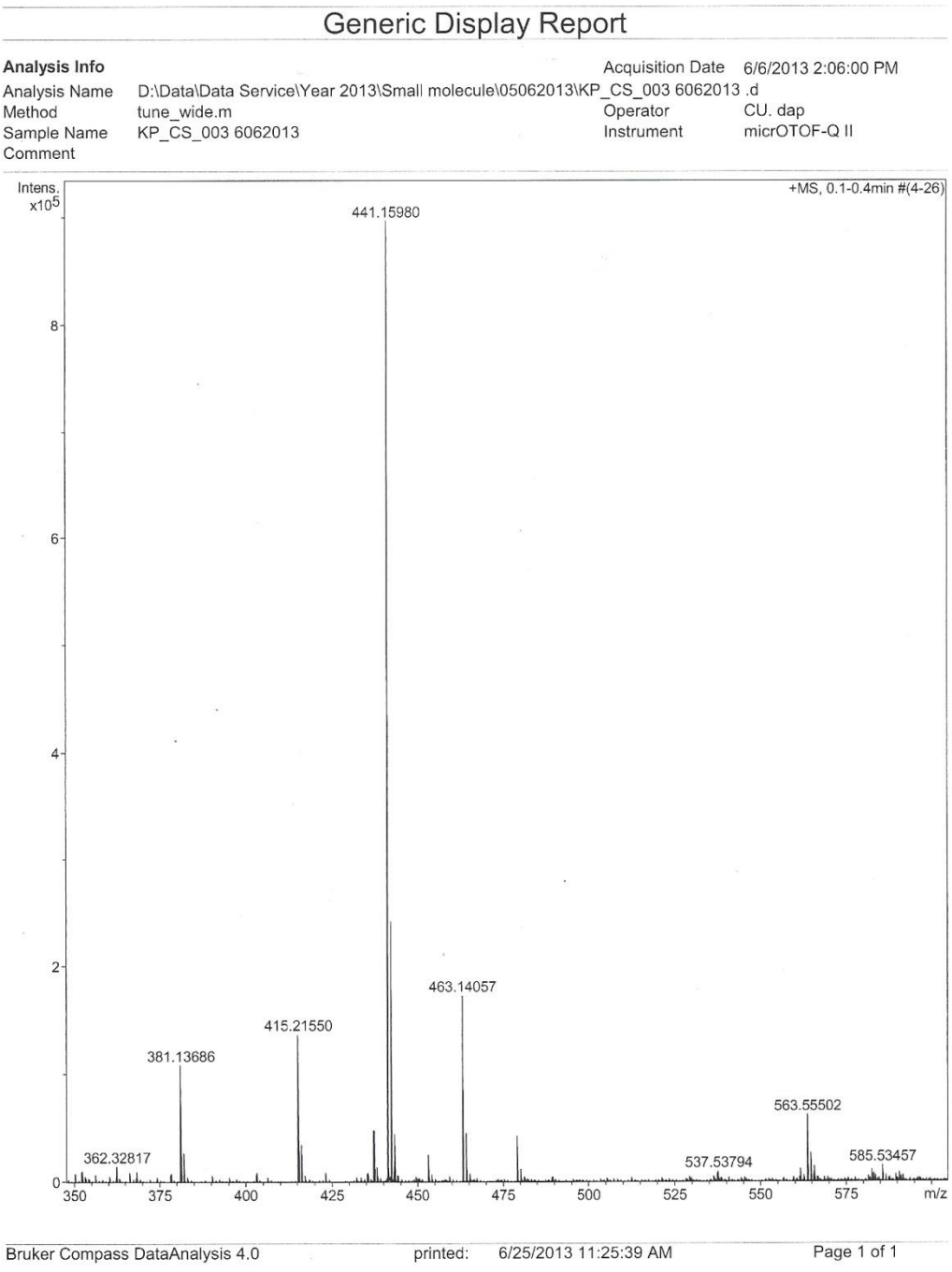

Figure A.26 HRESIMS mass spectrum of compound **5**

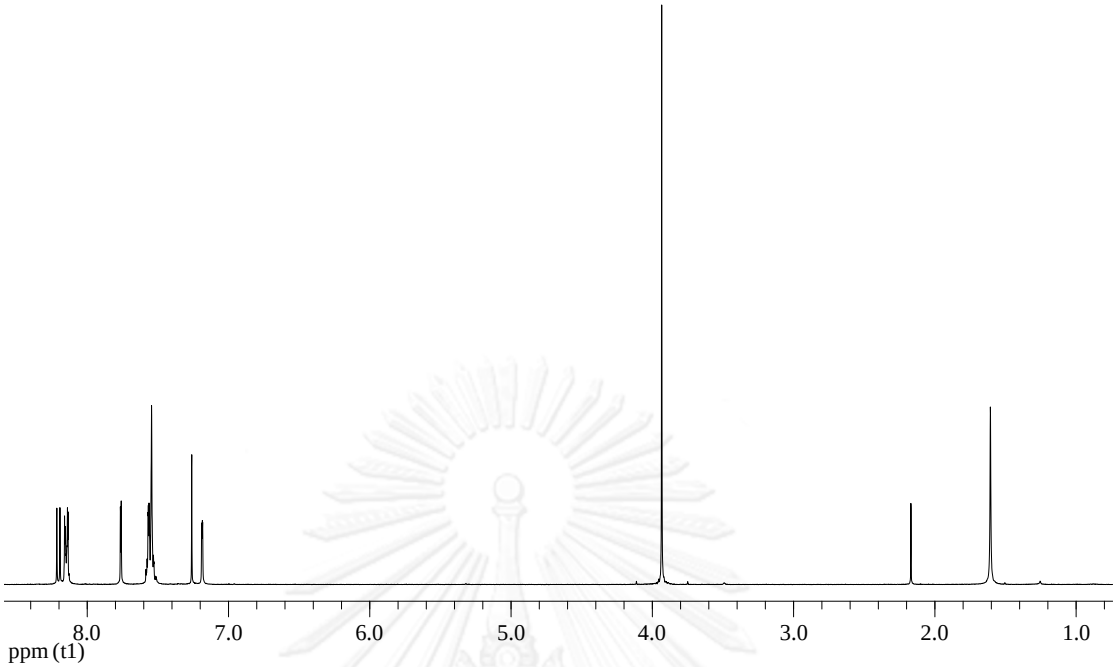

Figure A.27 ^{1}H NMR (400 MHz) spectrum of compound **6** ($CDCl_3$)

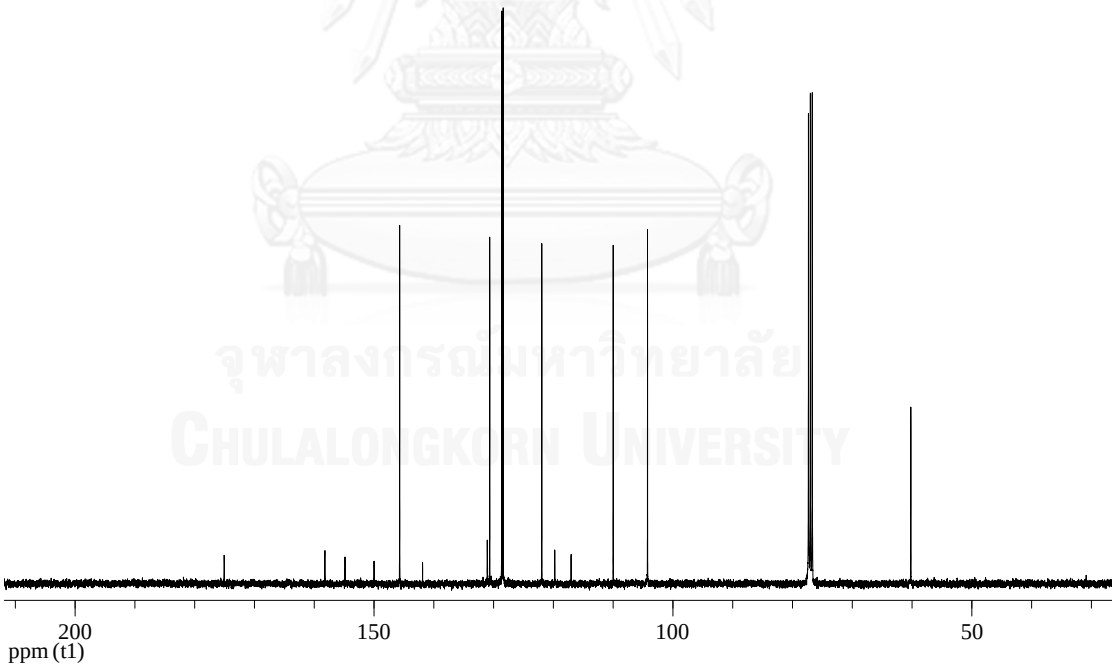

Figure A.28 ^{13}C NMR (100 MHz) spectrum of compound **6** ($CDCl_3$)

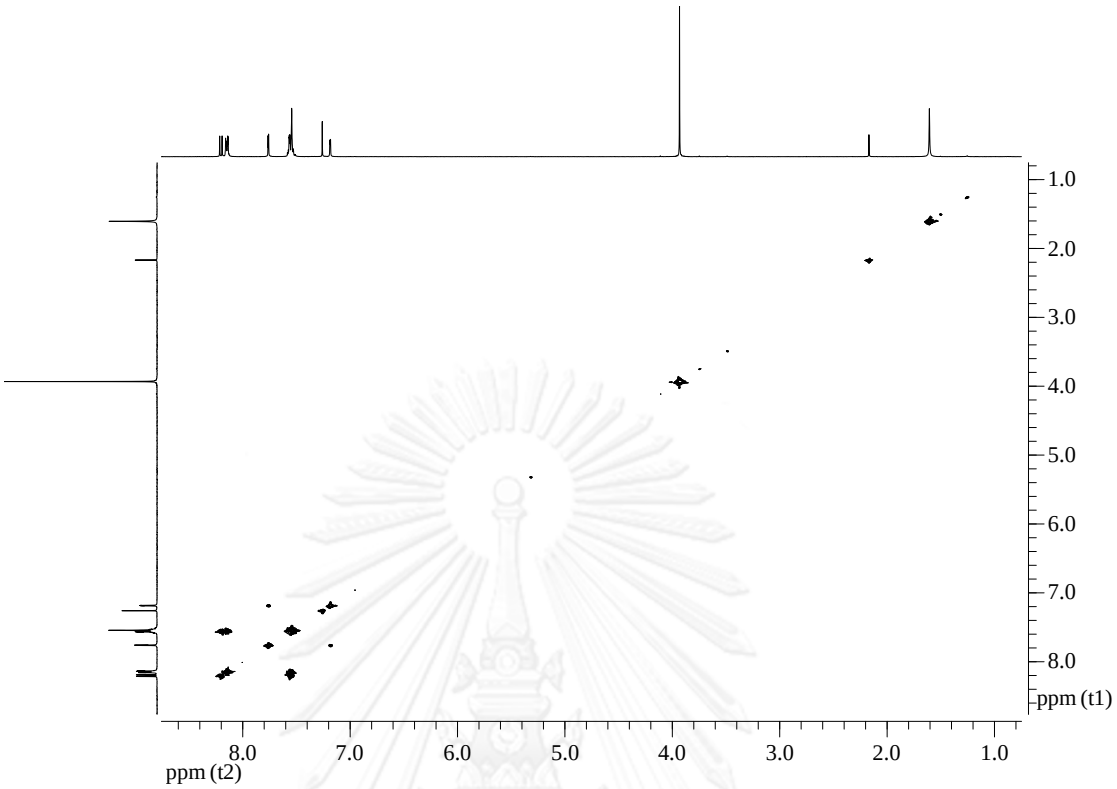

Figure A.29 ^{1}H-^{1}H COSY spectrum of compound **6** ($CDCl_3$)

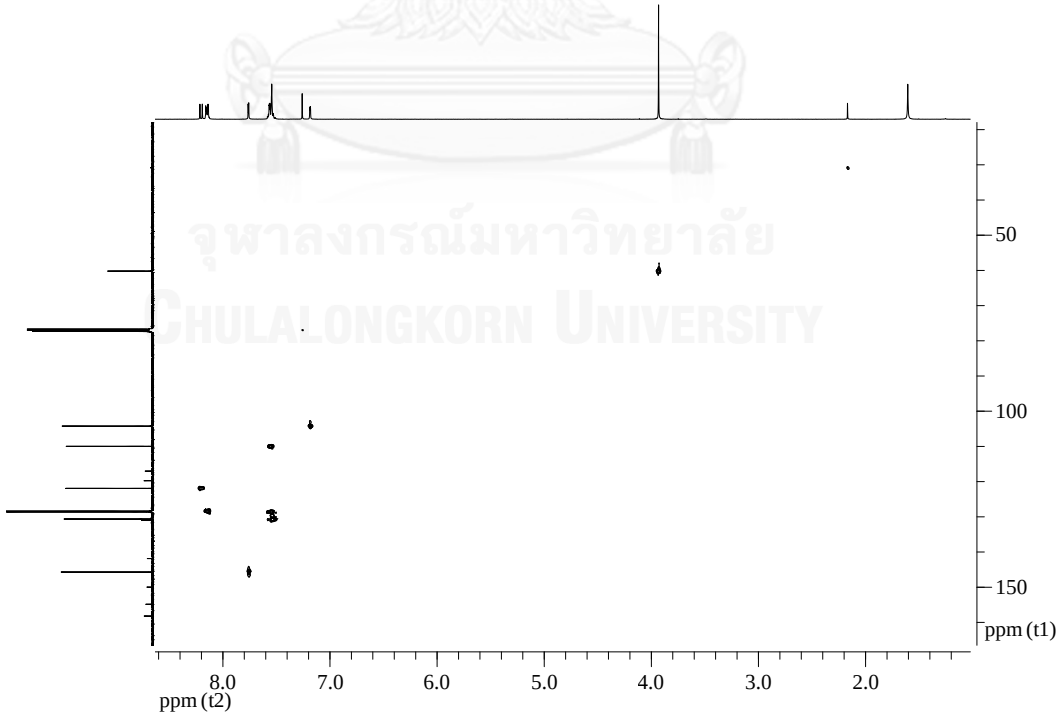

Figure A.30 HSQC spectrum of compound **6** ($CDCl_3$)

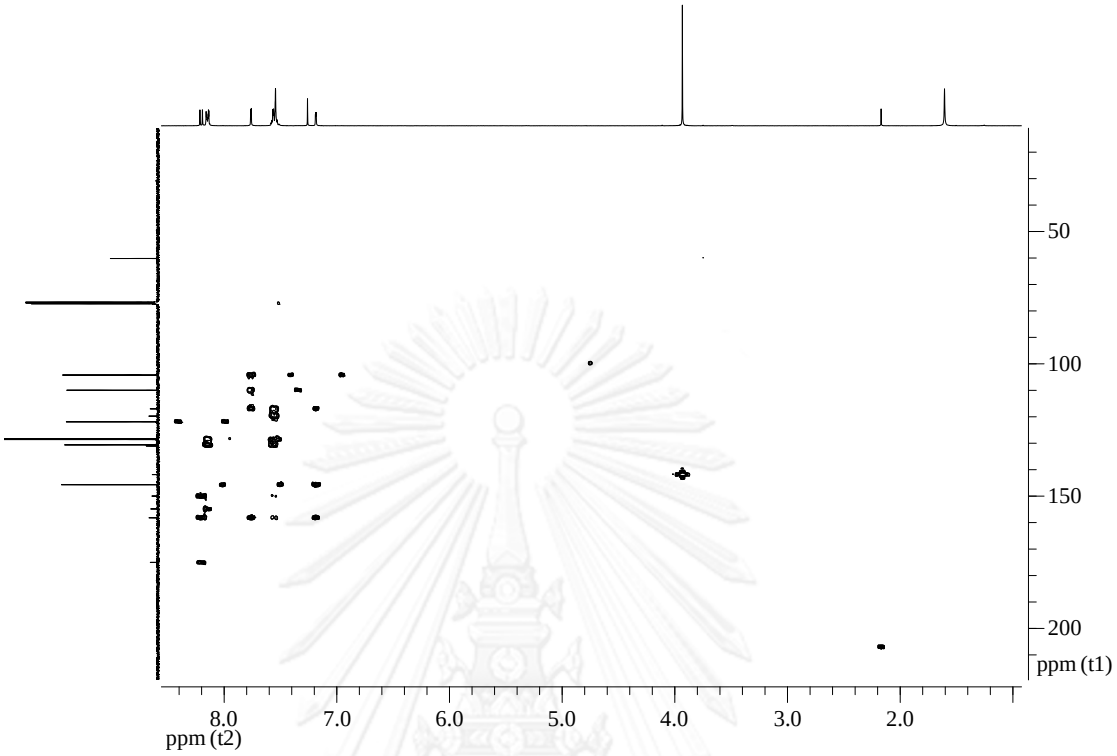

Figure A.31 HMBC spectrum of compound **6** ($CDCl_3$)

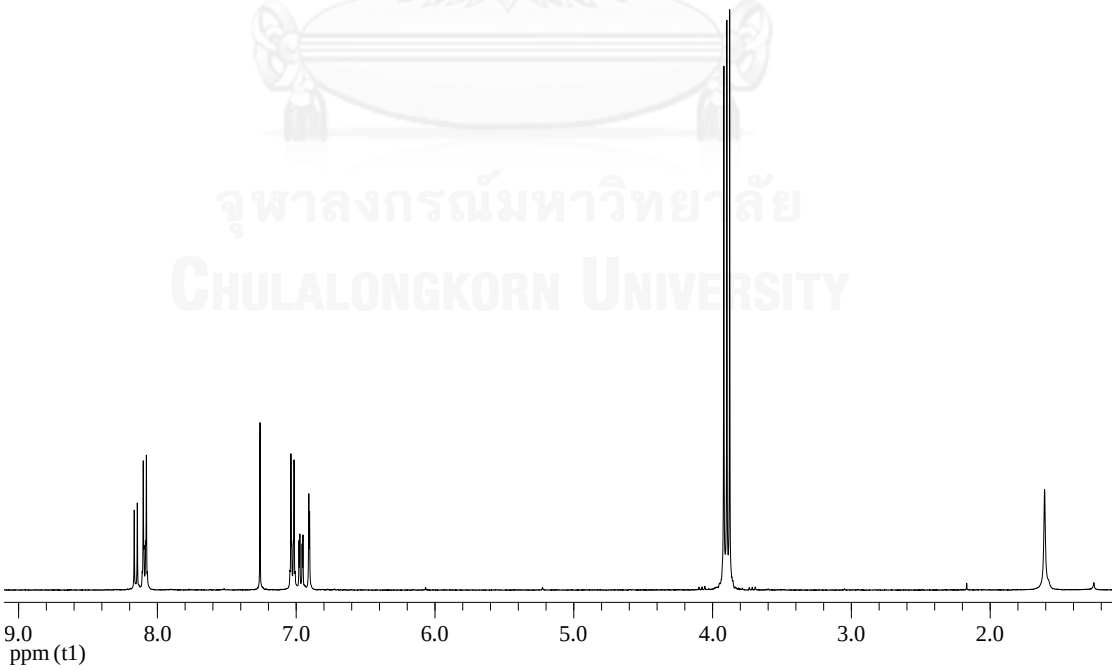

Figure A.32 ^{1}H NMR (400 MHz) spectrum of compound **7** ($CDCl_3$)

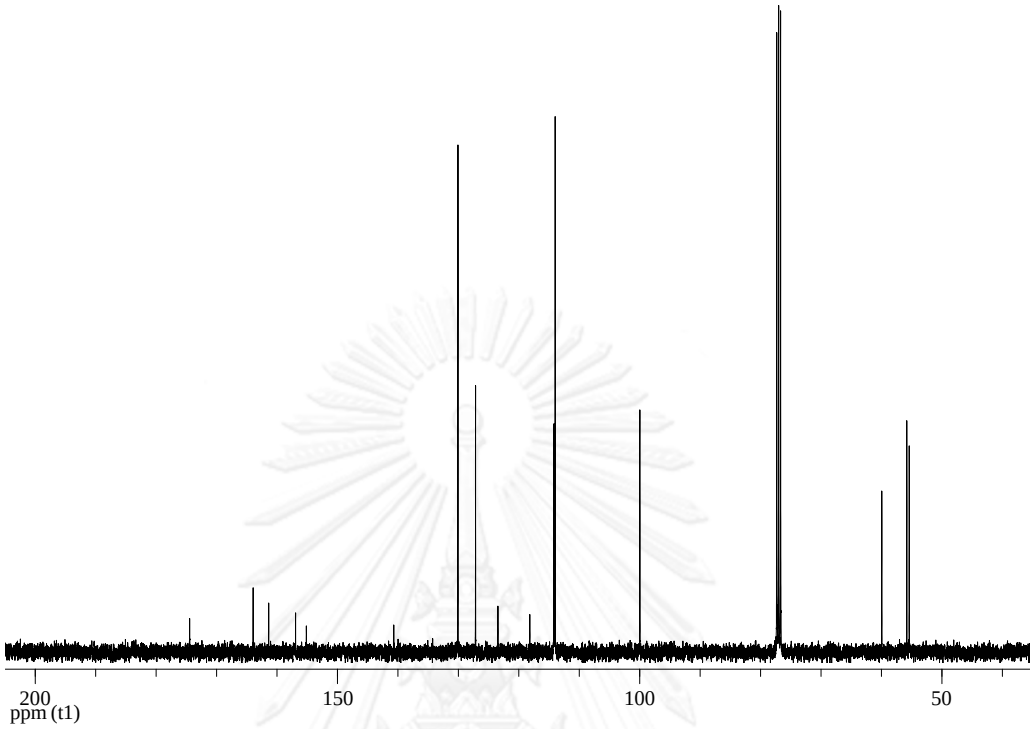

Figure A.33 ^{13}C NMR (100 MHz) spectrum of compound **7** ($CDCl_3$)

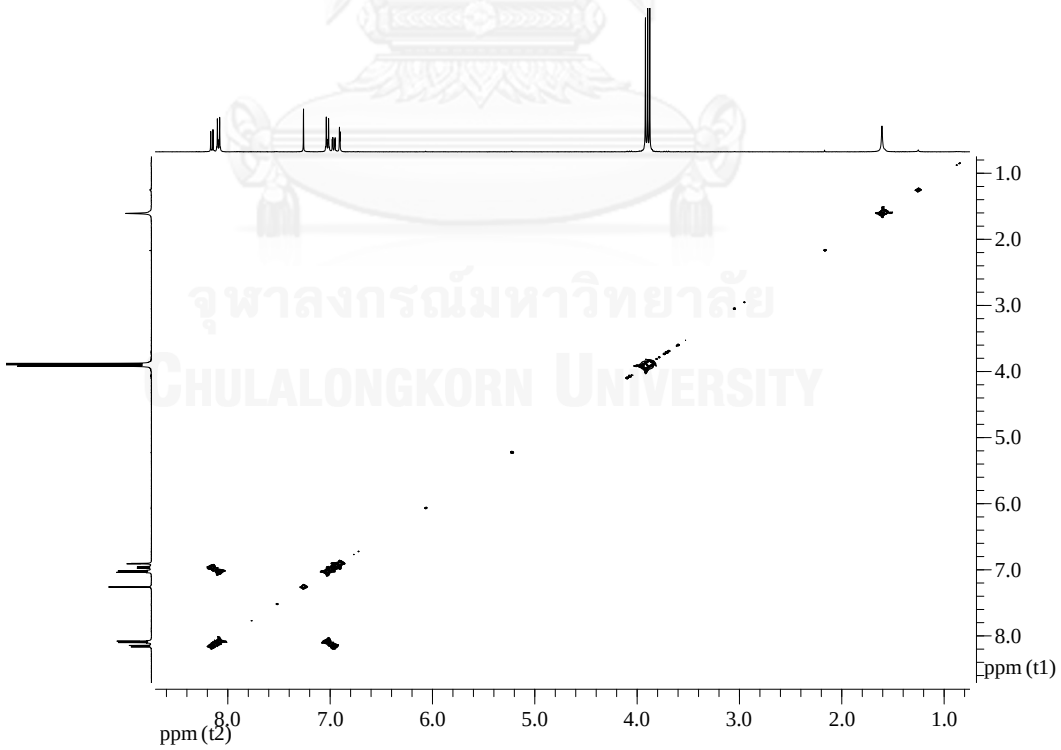

Figure A.34 ^{1}H-^{1}H COSY spectrum of compound **7** ($CDCl_3$)

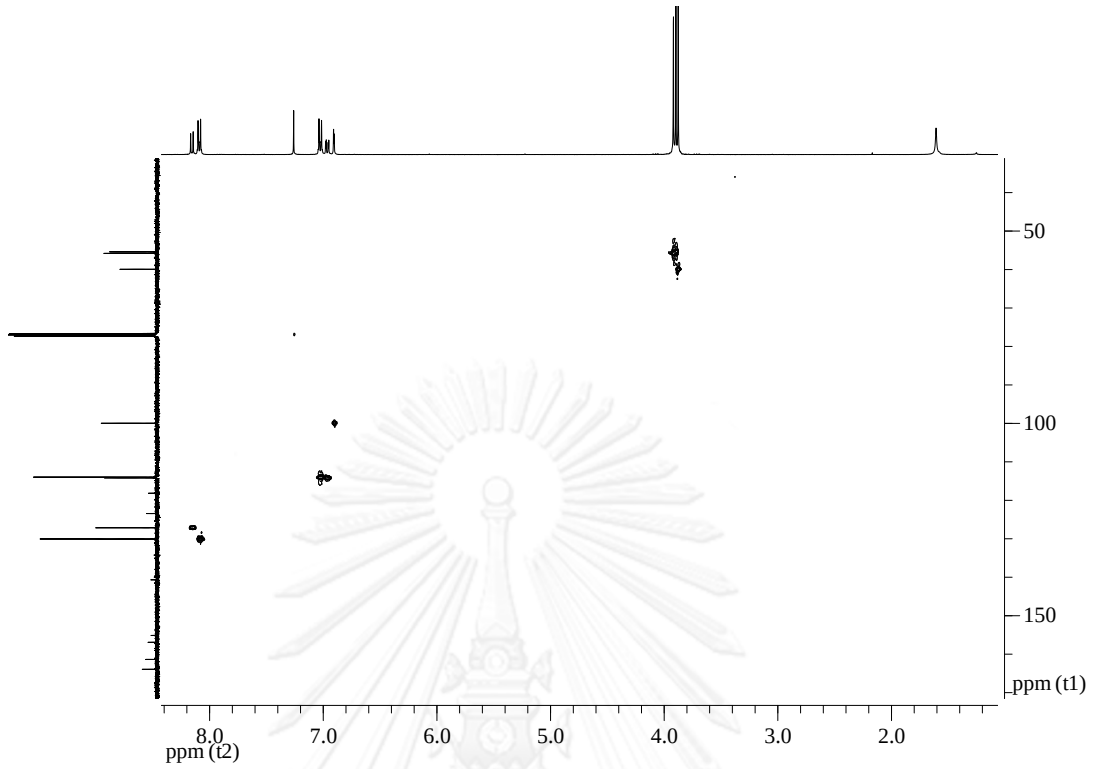

Figure A.35 HSQC spectrum of compound **7** ($CDCl_3$)

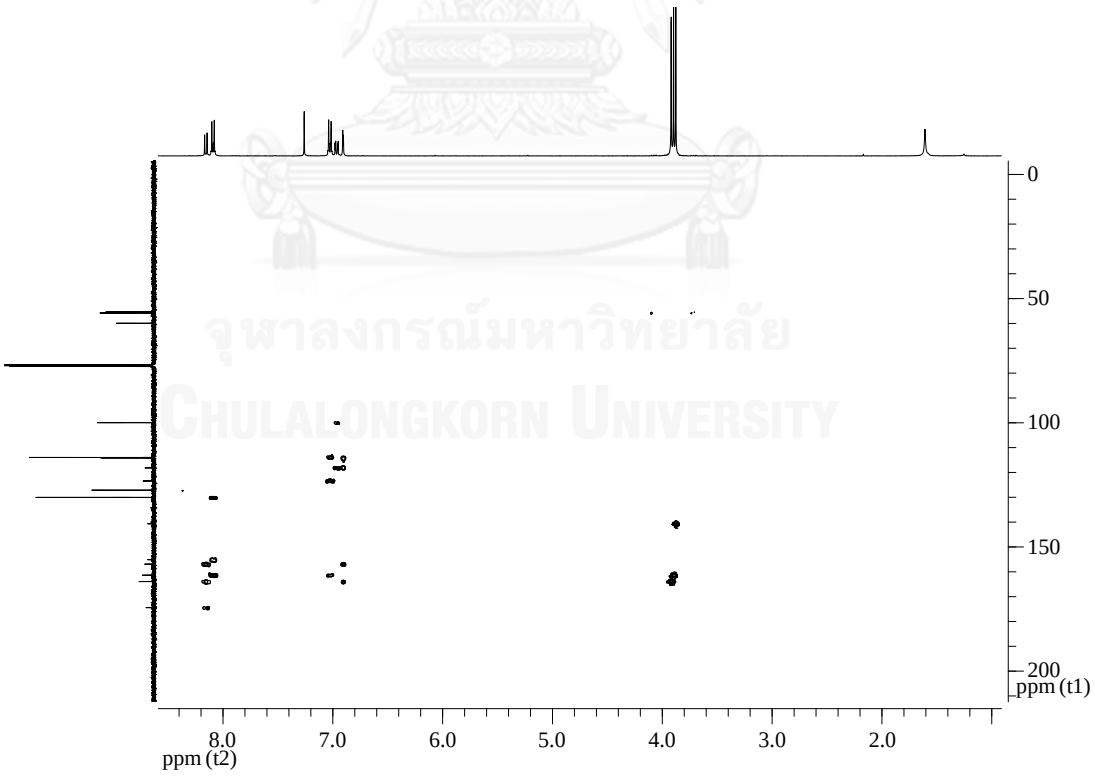

Figure A.36 HMBC spectrum of compound **7** ($CDCl_3$)

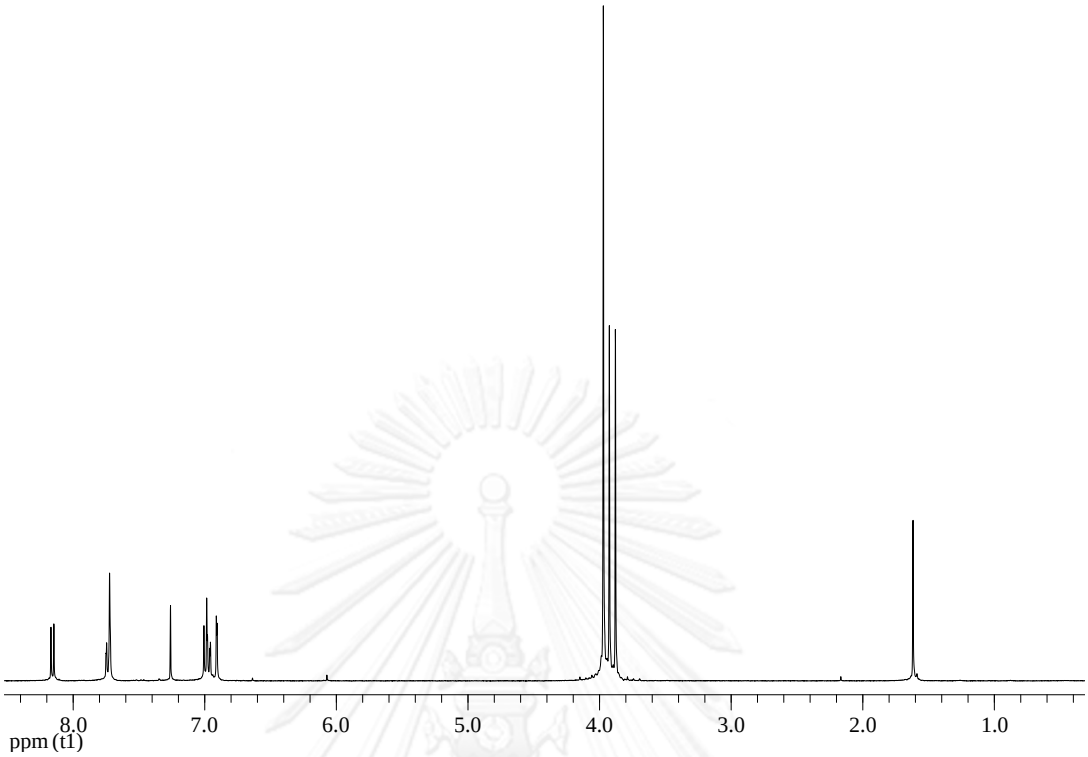

Figure A.37 ^{1}H NMR (400 MHz) spectrum of compound **8** ($CDCl_3$)

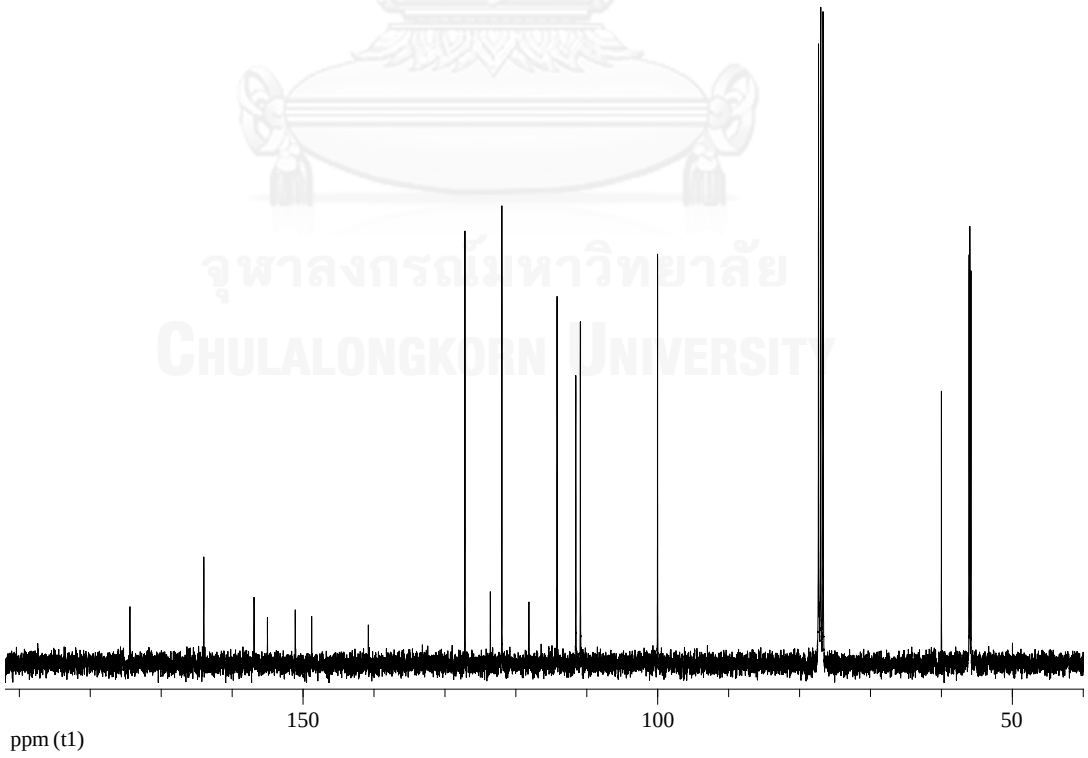

Figure A.38 ^{13}C NMR (100 MHz) spectrum of compound **8** ($CDCl_3$)

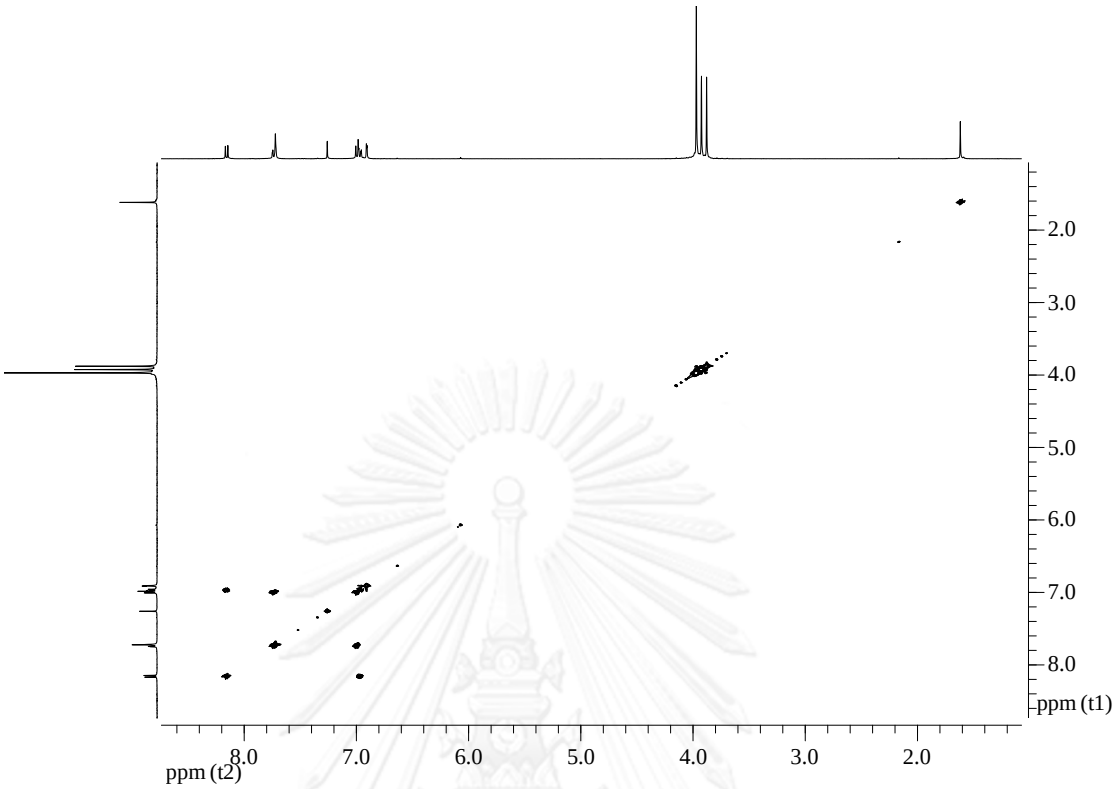

Figure A.39 ^{1}H-^{1}H COSY spectrum of compound **8** ($CDCl_3$)

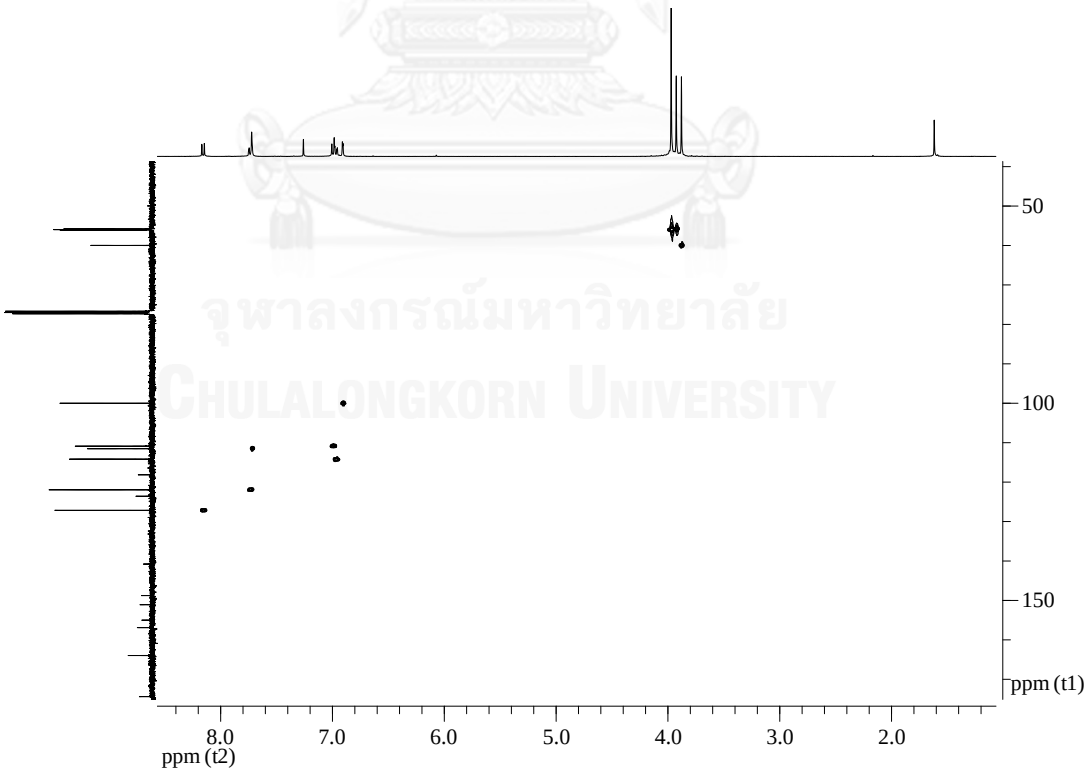

Figure A.40 HSQC spectrum of compound **8** ($CDCl_3$)

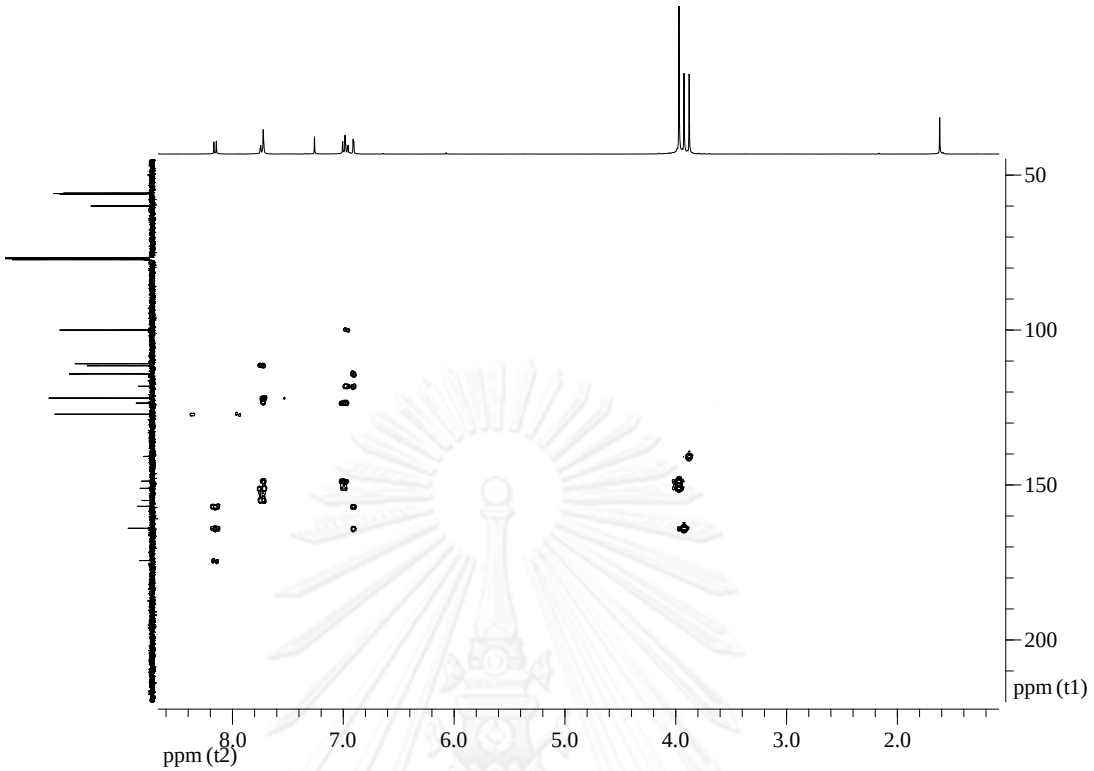

Figure A.41 HMBC spectrum of compound **8** ($CDCl_3$)

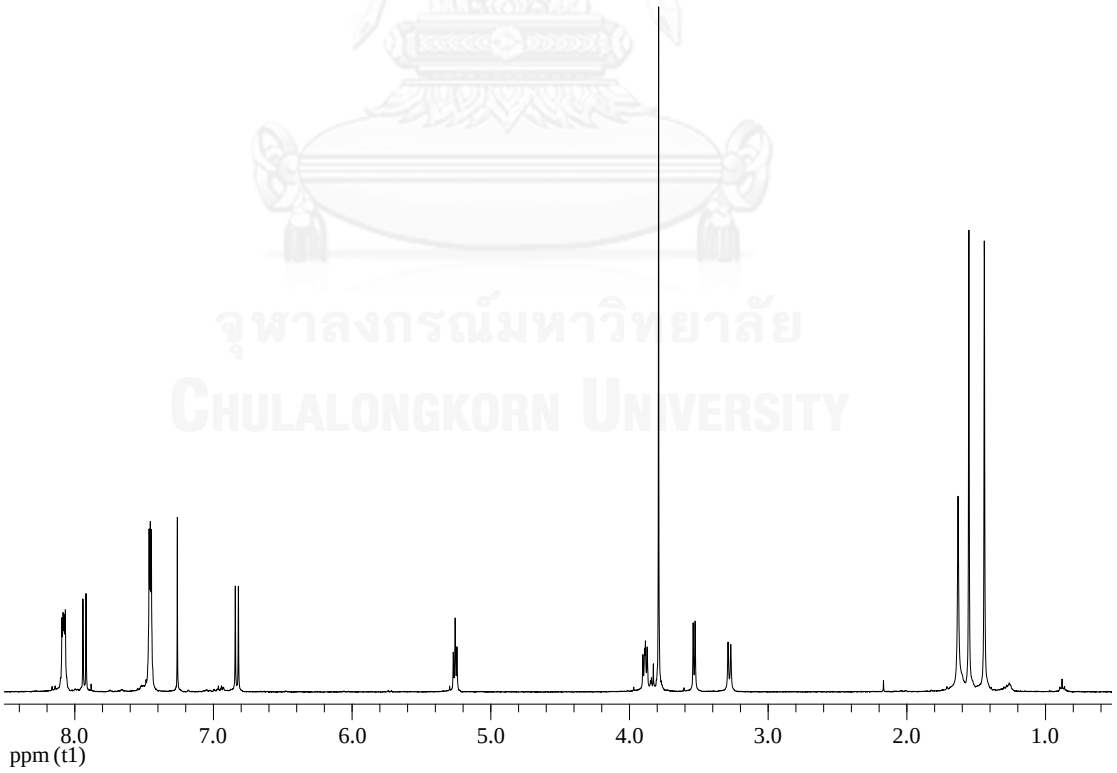

Figure A.42 ^{1}H NMR (400 MHz) spectrum of compound **9** ($CDCl_3$)

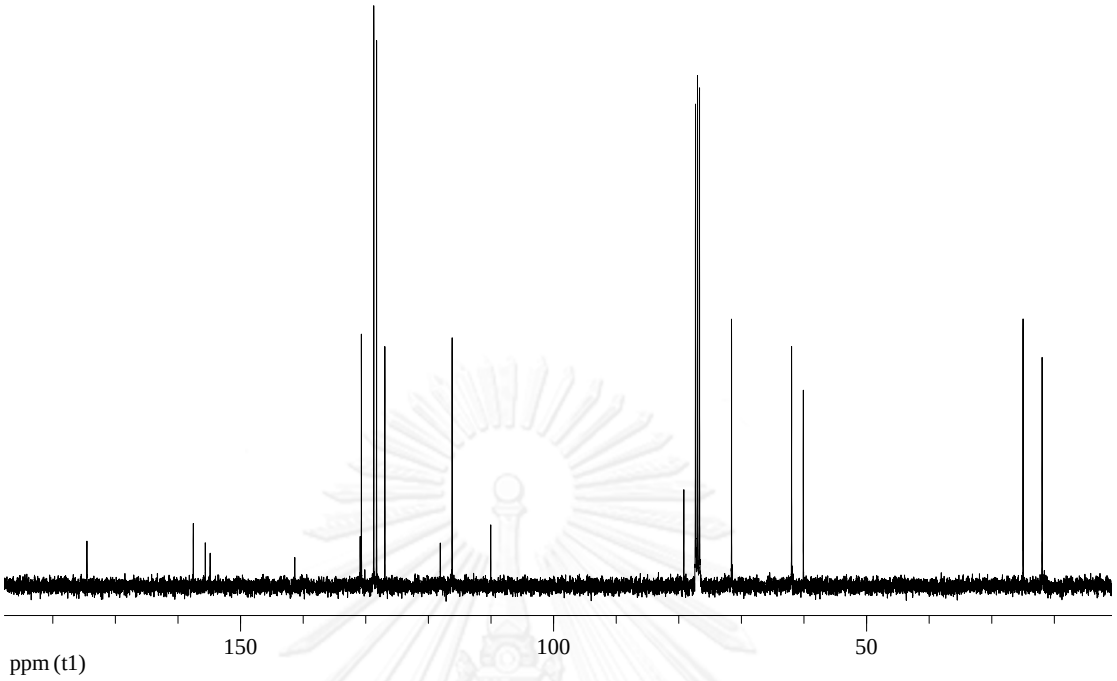

Figure A.43 ^{13}C NMR (100 MHz) spectrum of compound **9** ($CDCl_3$)

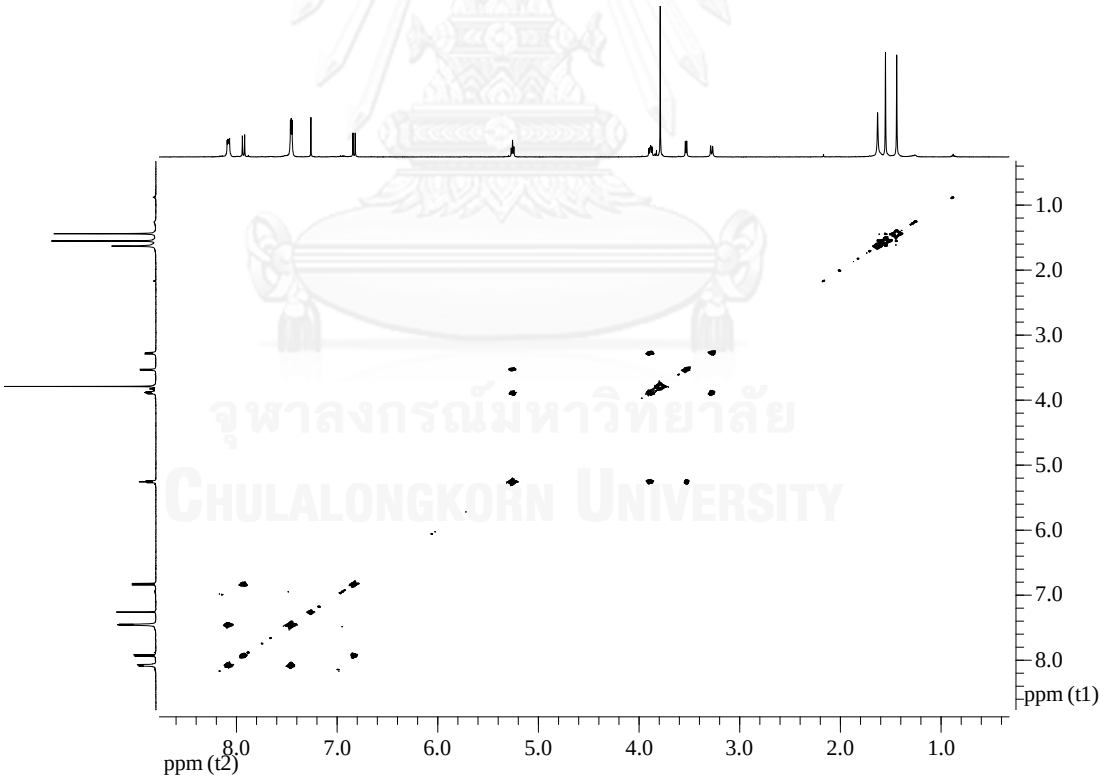

Figure A.44 ^{1}H-^{1}H COSY spectrum of compound **9** ($CDCl_3$)

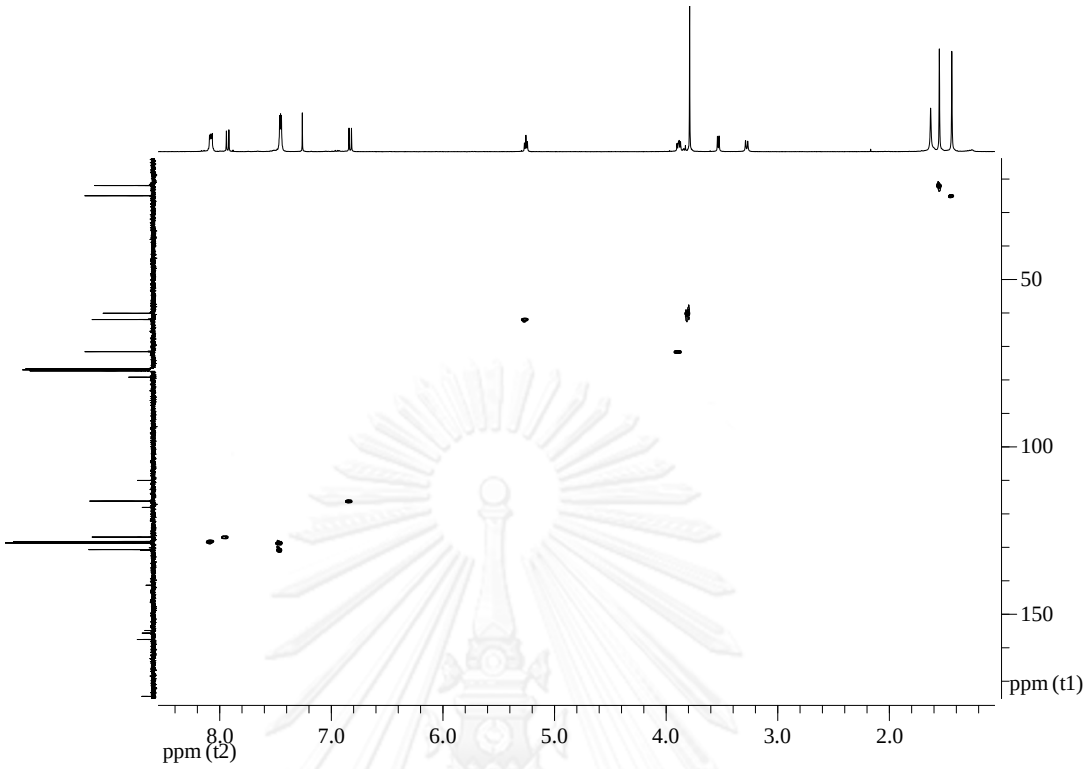

Figure A.45 HSQC spectrum of compound **9** ($CDCl_3$)

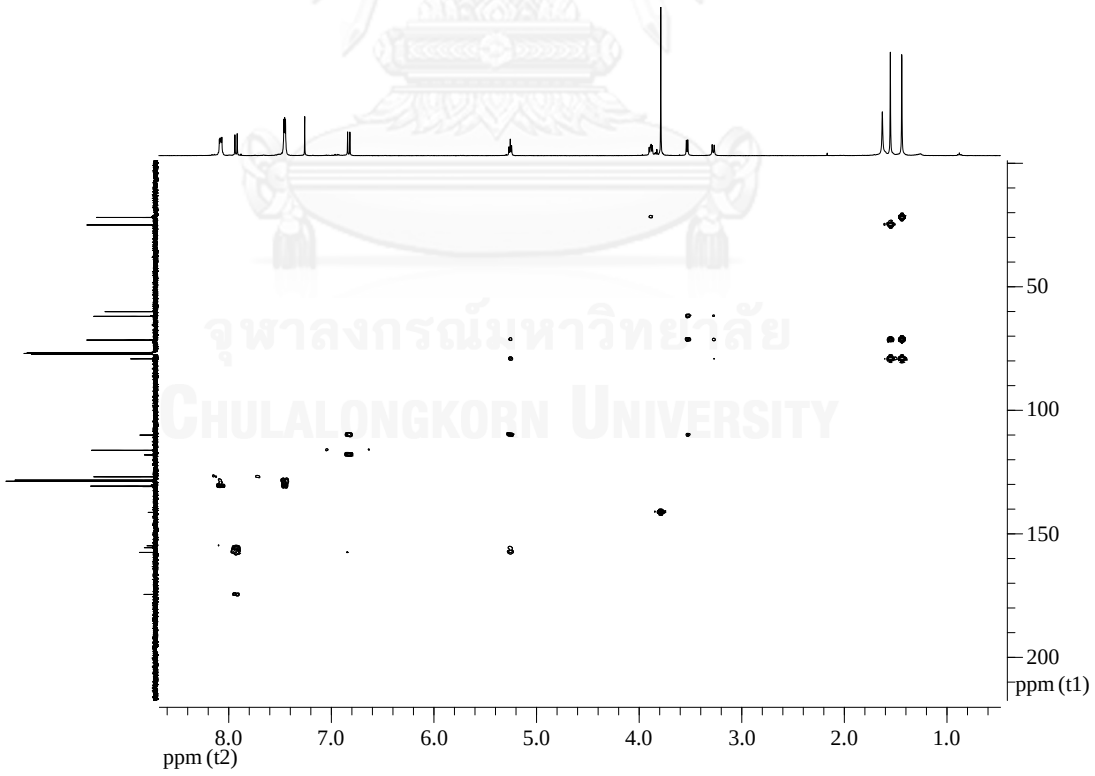

Figure A.46 HMBC spectrum of compound **9** ($CDCl_3$)

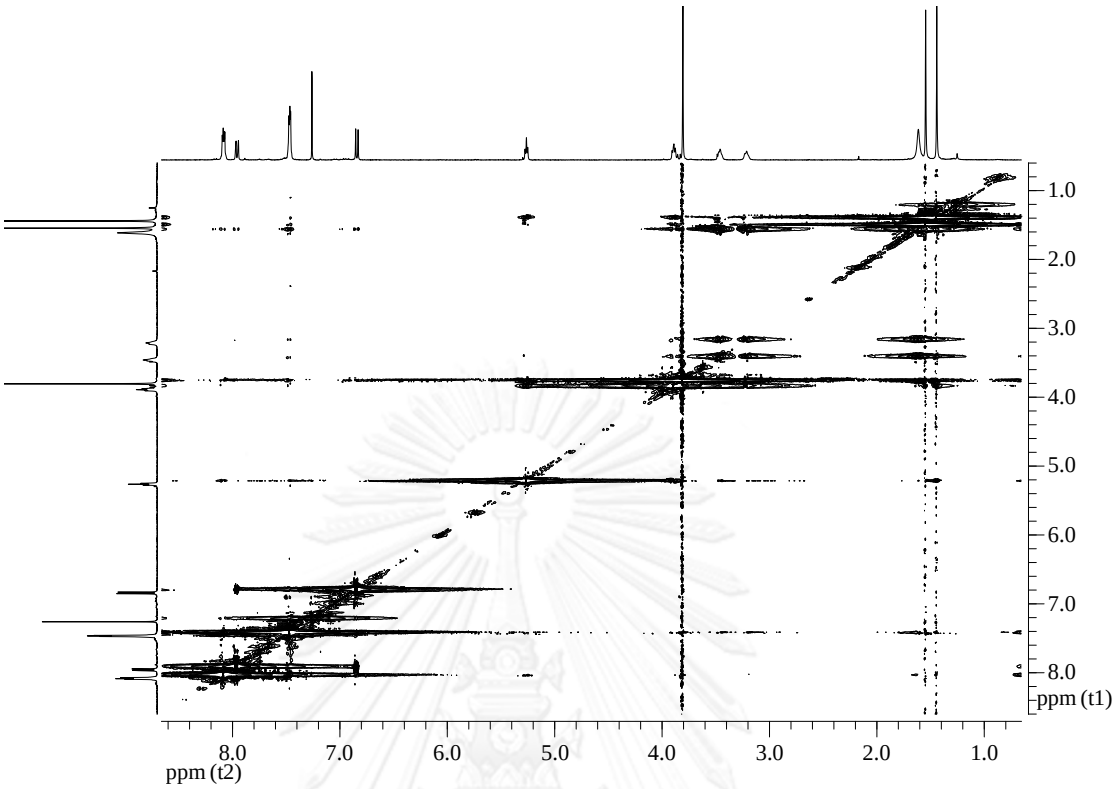

Figure A.47 NOESY spectrum of compound **9** ($CDCl_3$)

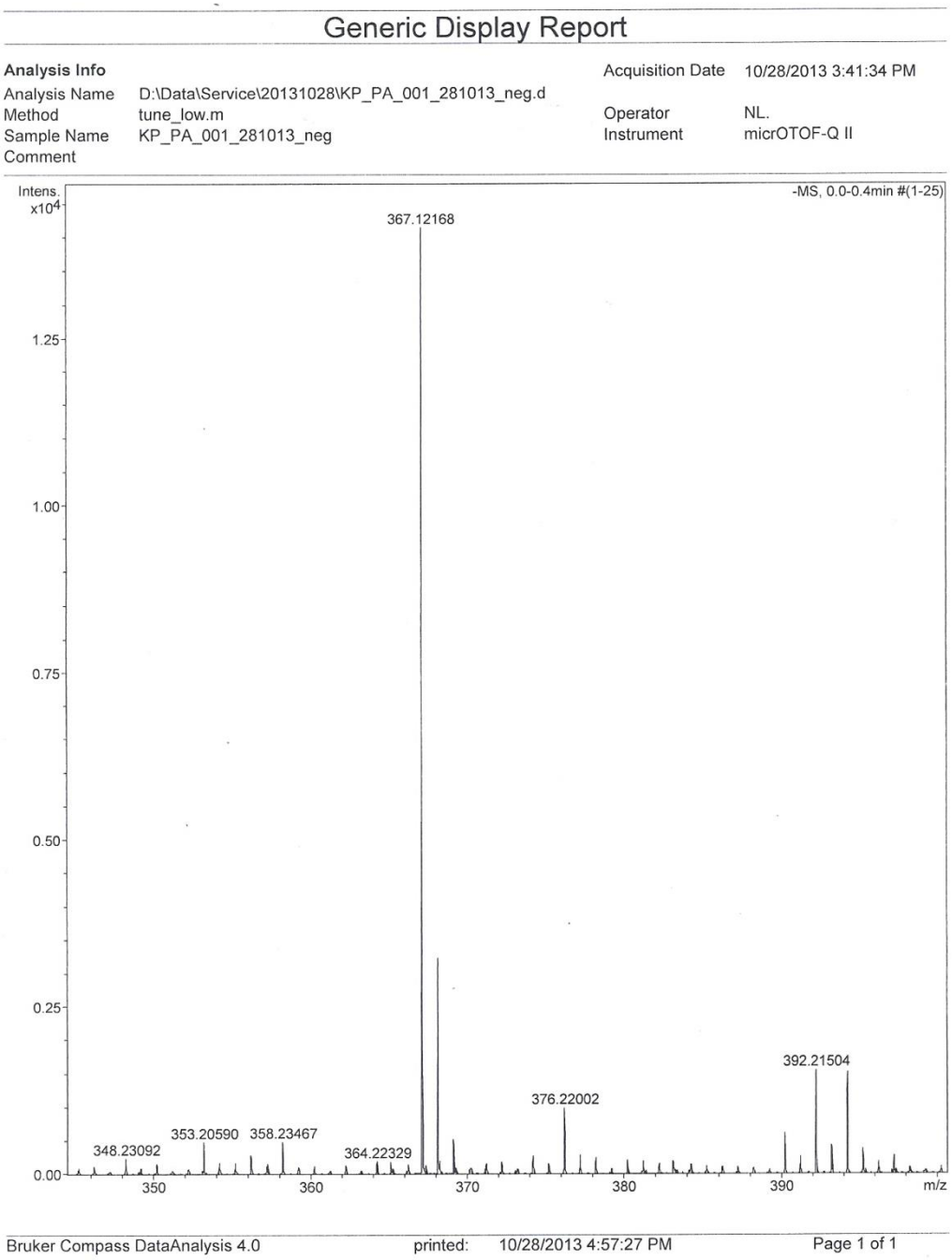

Figure A.48 HRESIMS mass spectrum of compound **9**

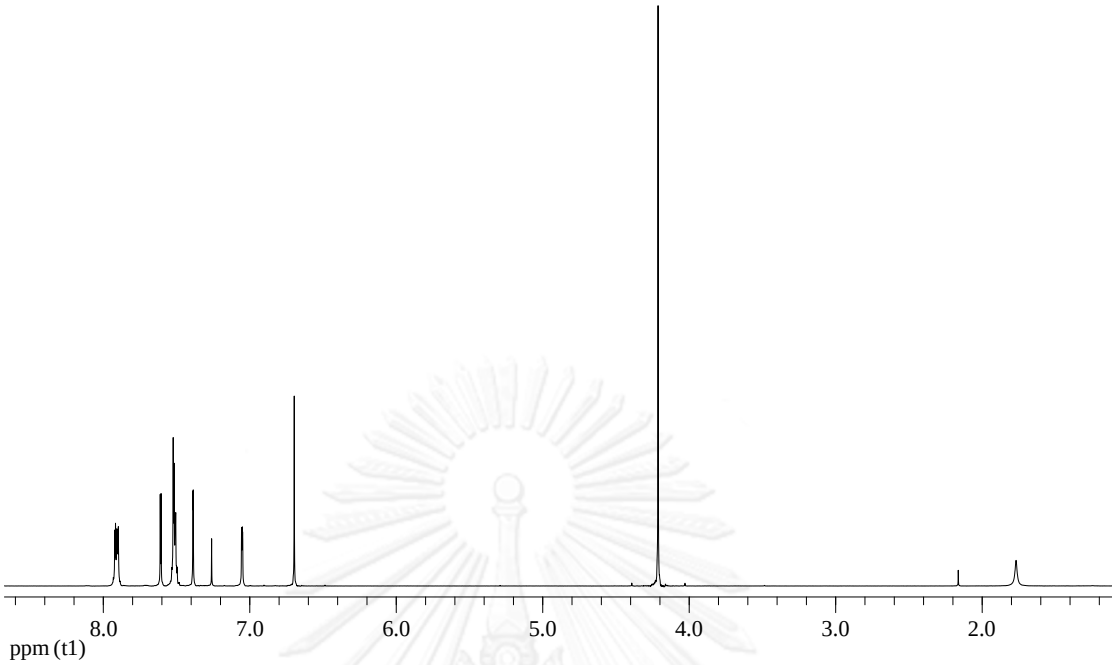

Figure A.49 ^{1}H NMR (400 MHz) spectrum of compound **10** ($CDCl_3$)

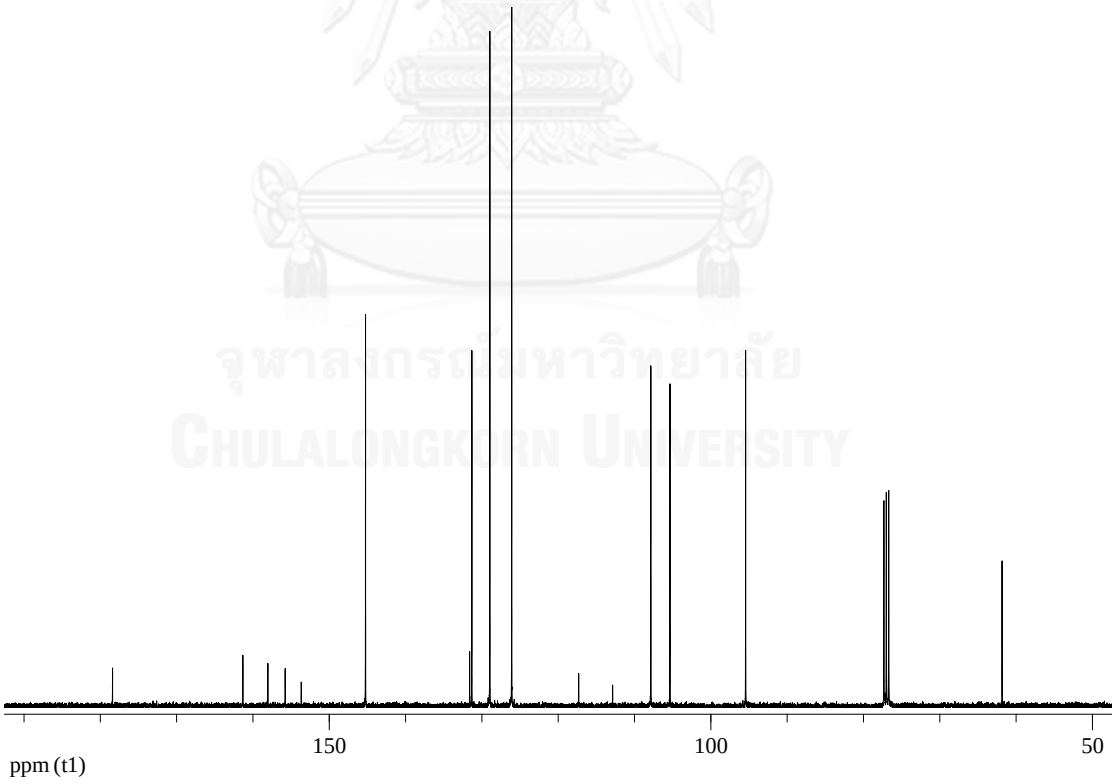

Figure A.50 ^{13}C NMR (100 MHz) spectrum of compound **10** ($CDCl_3$)

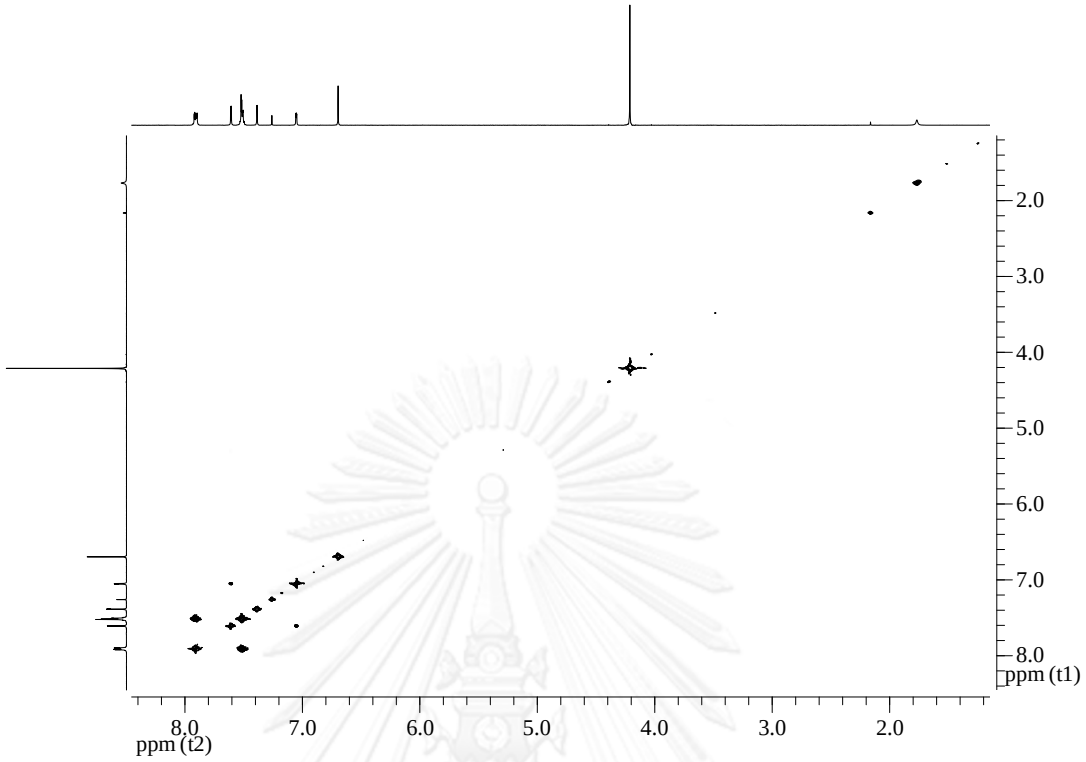

Figure A.51 ^{1}H-^{1}H COSY spectrum of compound **10** ($CDCl_3$)

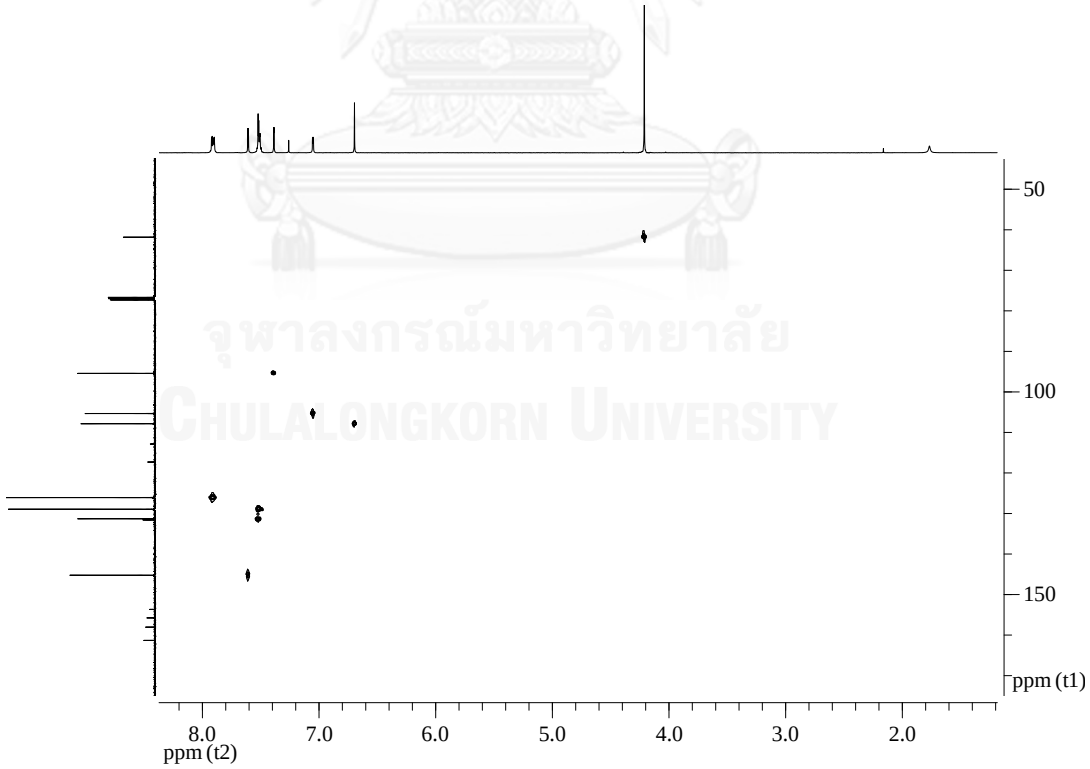

Figure A.52 HSQC spectrum of compound **10** ($CDCl_3$)

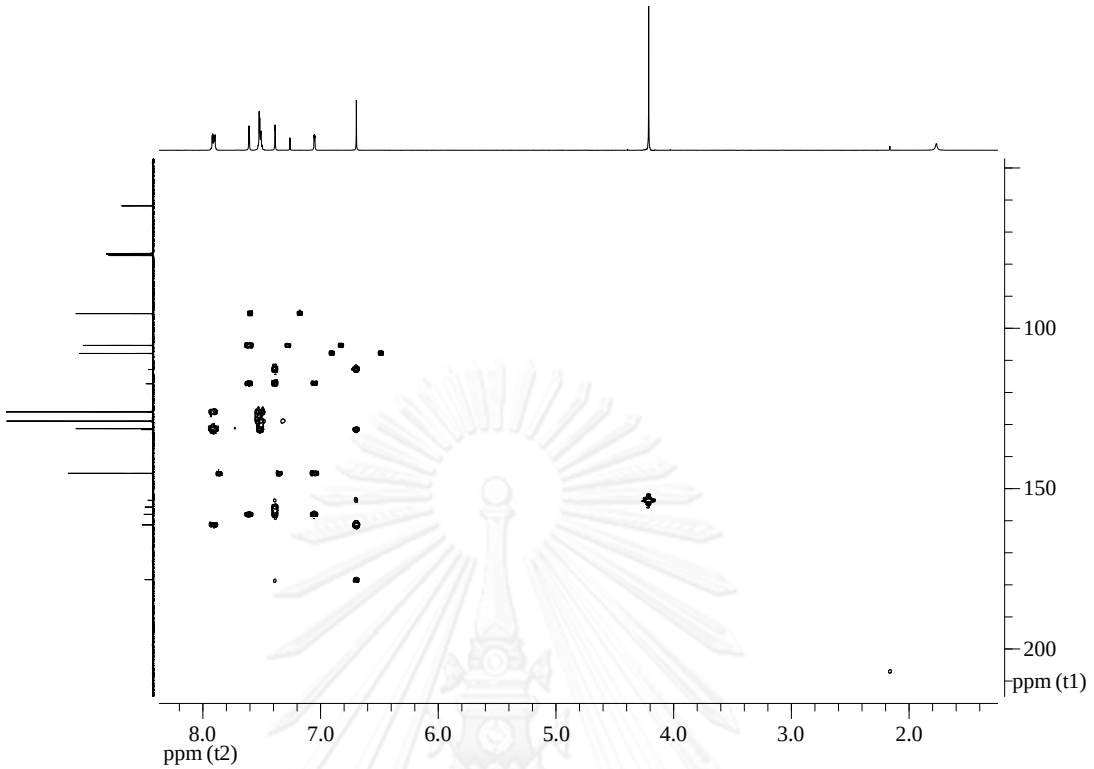

Figure A.53 HMBC spectrum of compound **10** ($CDCl_3$)

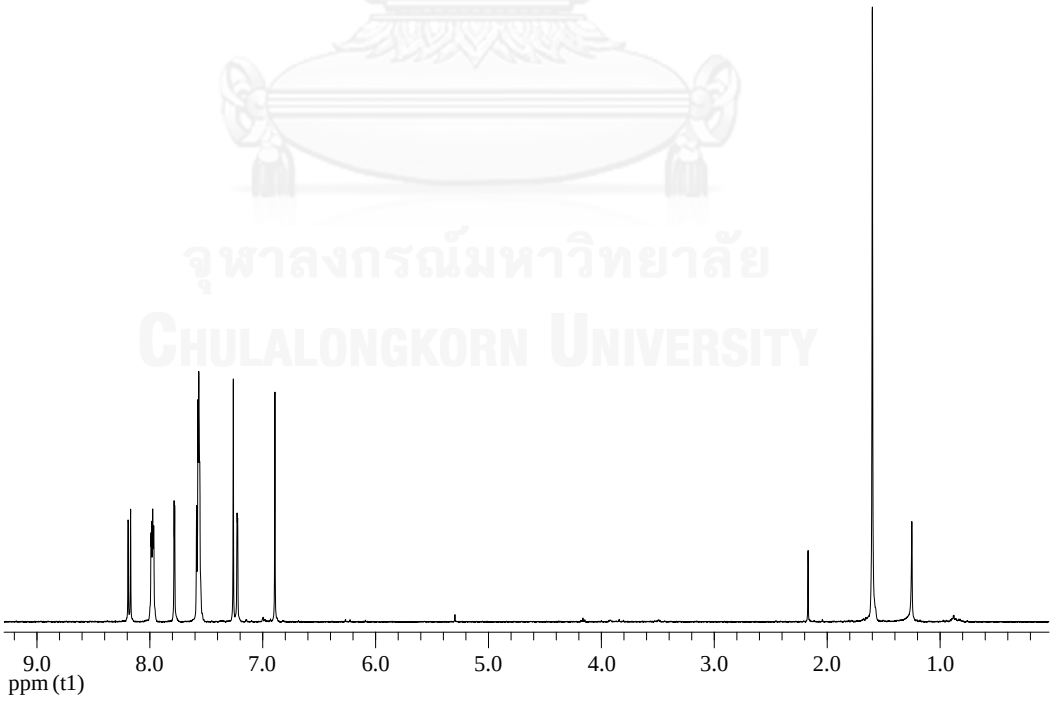

Figure A.54 ^{1}H NMR (400 MHz) spectrum of compound **11** ($CDCl_3$)

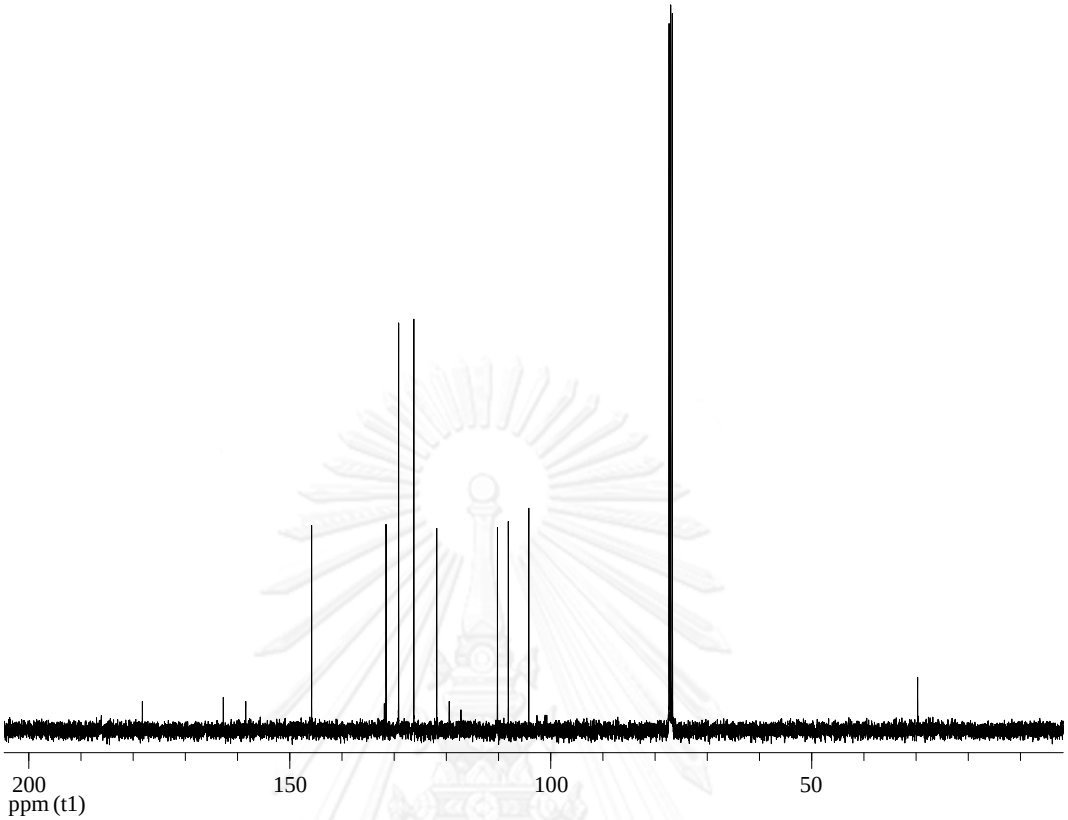

Figure A.55 ^{13}C NMR (100 MHz) spectrum of compound **11** ($CDCl_3$)

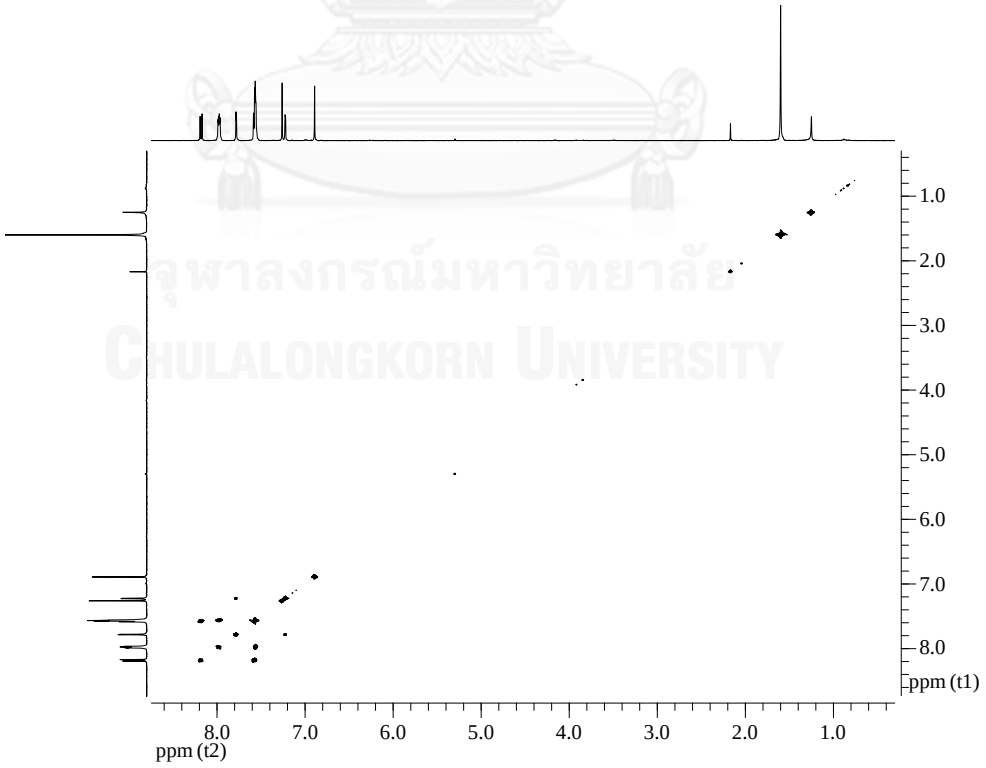

Figure A.56 ^{1}H-^{1}H COSY spectrum of compound **11** ($CDCl_3$)

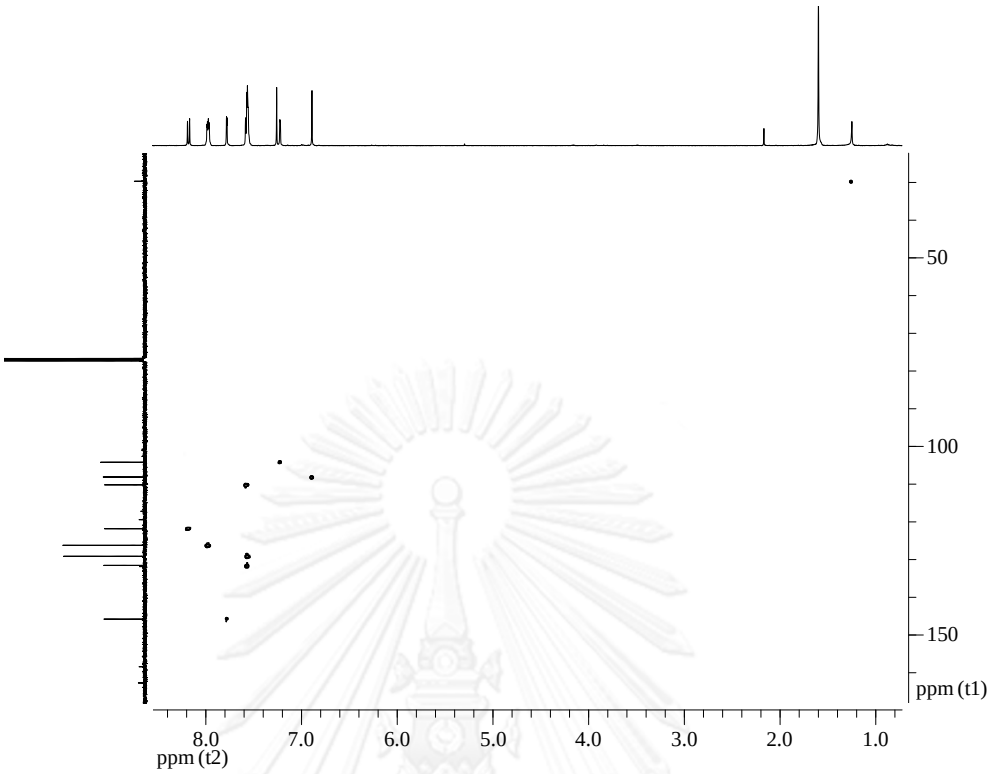

Figure A.57 HSQC spectrum of compound **11** ($CDCl_3$)

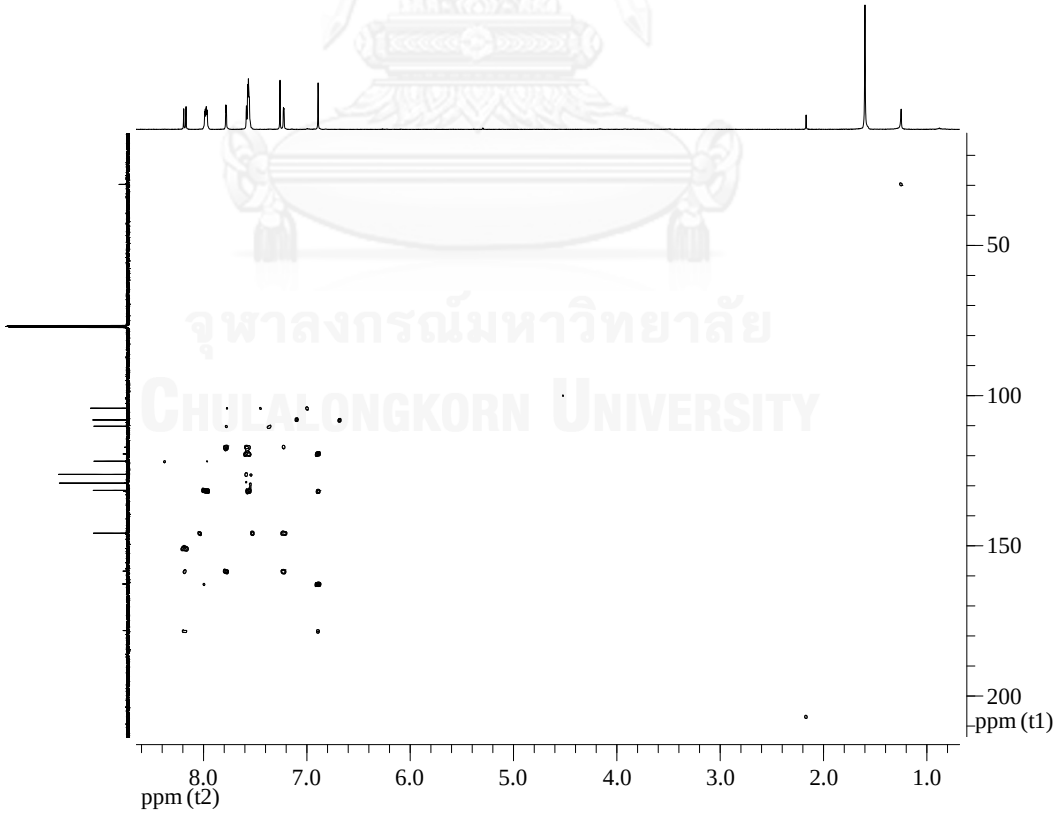

Figure A.58 HMBC spectrum of compound **11** ($CDCl_3$)

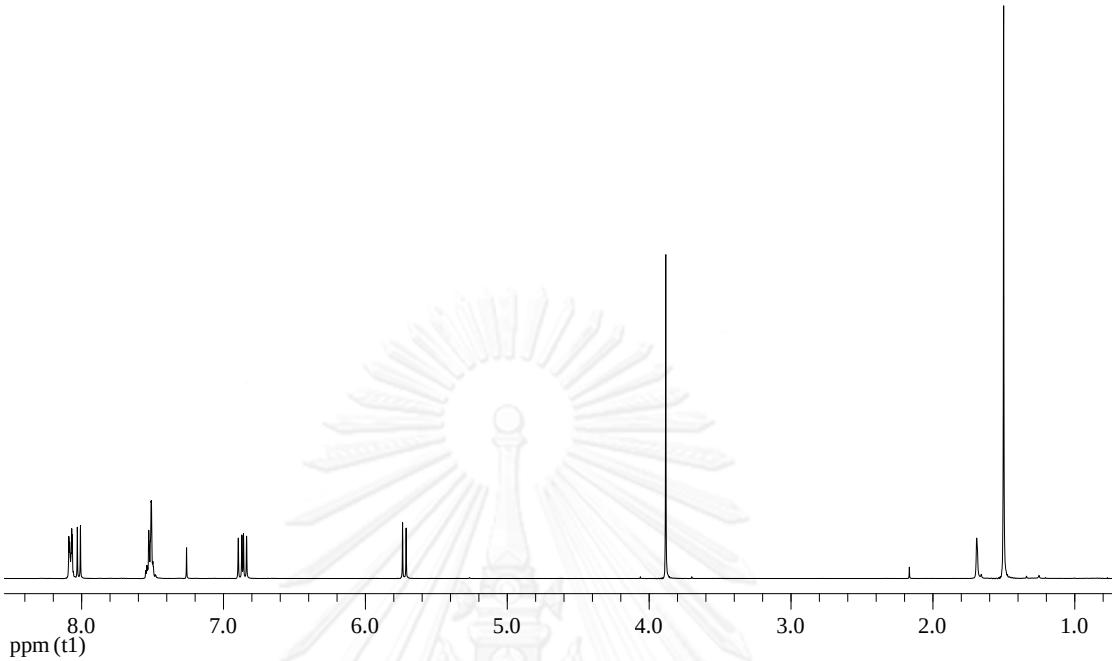

Figure A.59 ^{1}H NMR (400 MHz) spectrum of compound **12** ($CDCl_3$)

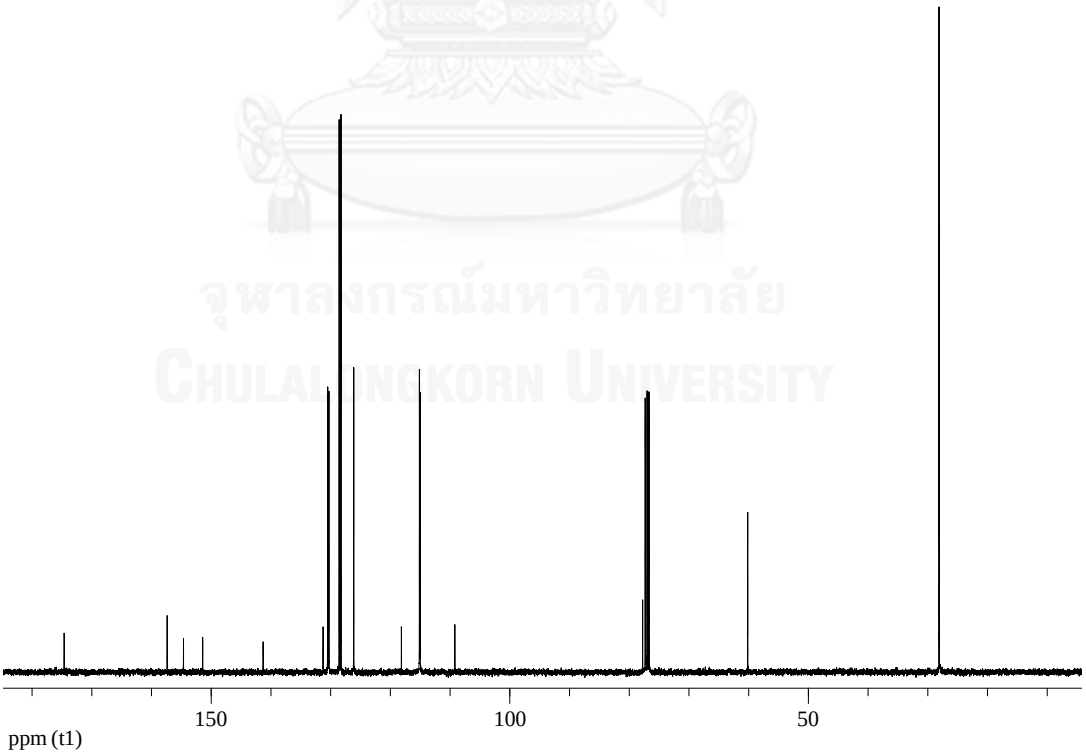

Figure A.60 ^{13}C NMR (100 MHz) spectrum of compound **12** ($CDCl_3$)

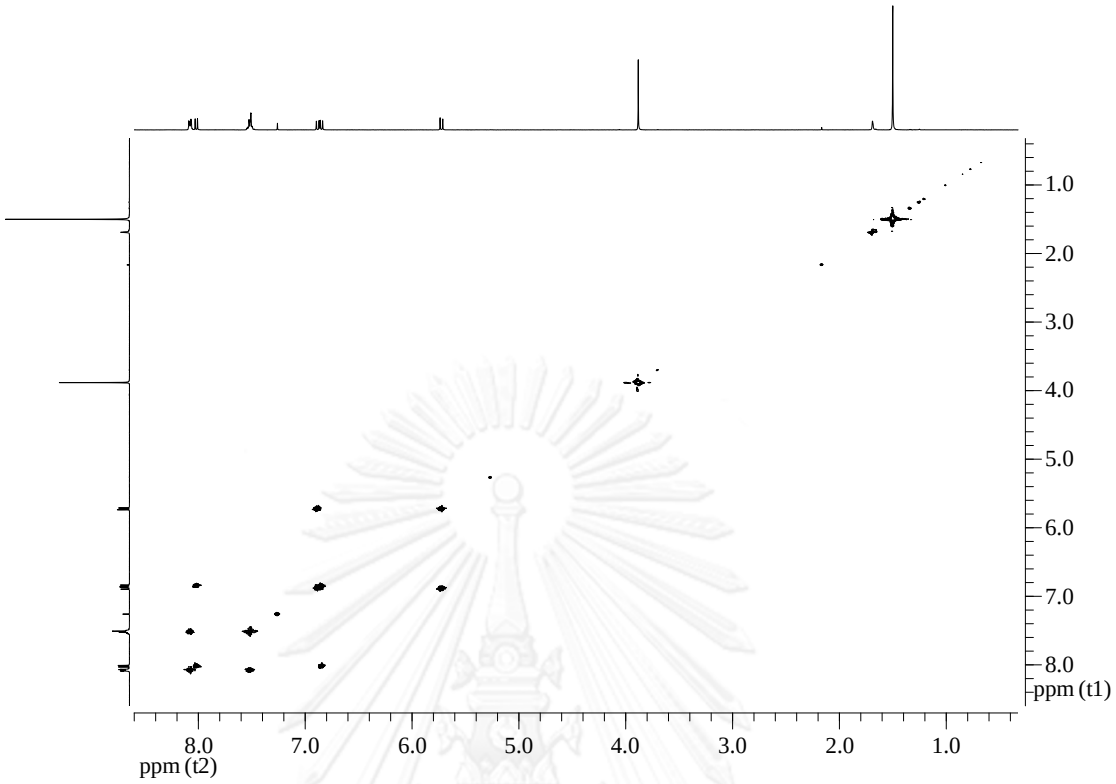

Figure A.61 ^{1}H-^{1}H COSY spectrum of compound **12** ($CDCl_3$)

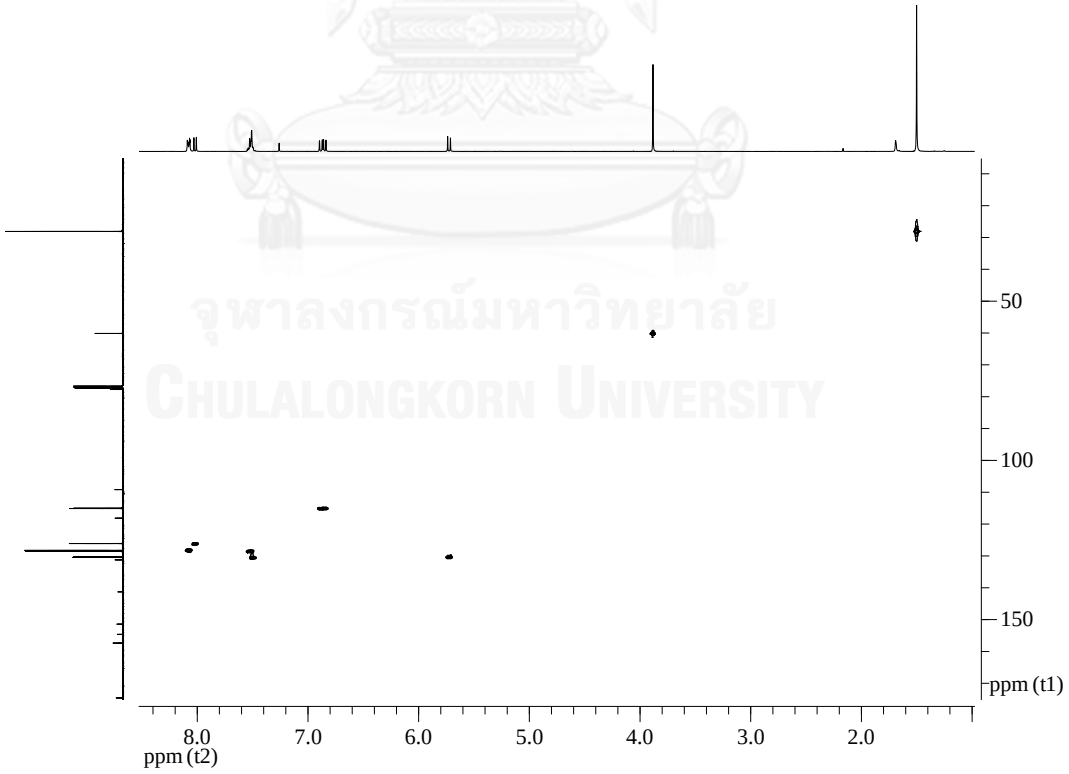

Figure A.62 HSQC spectrum of compound **12** ($CDCl_3$)

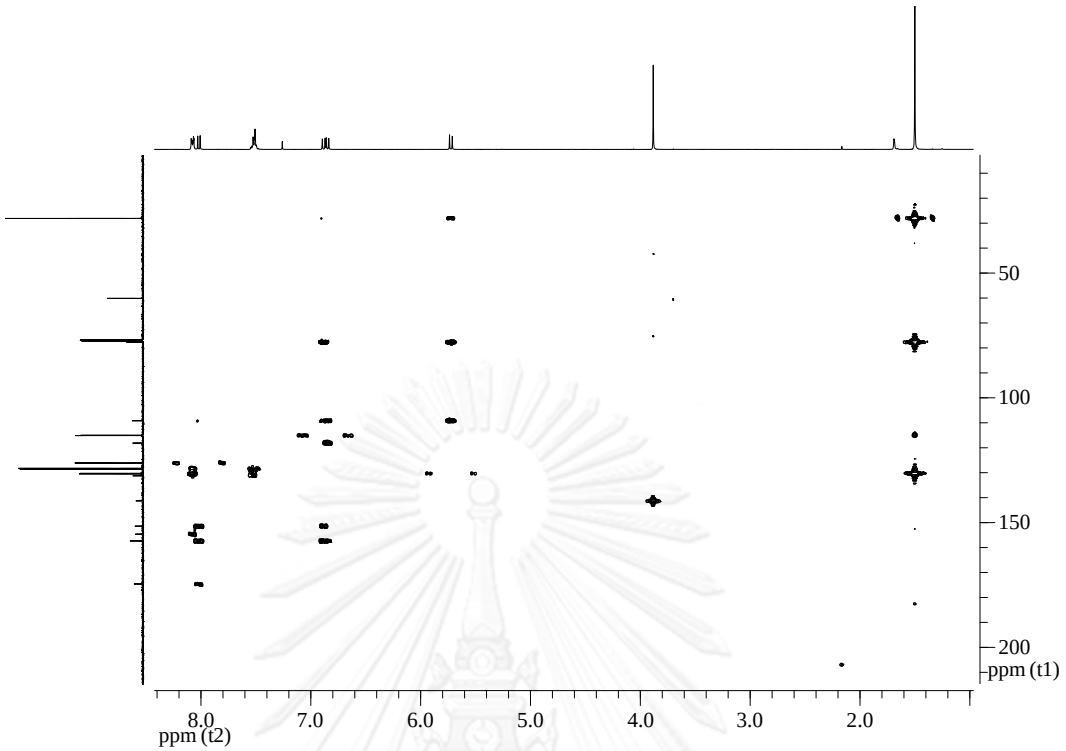

Figure A.63 HMBC spectrum of compound **12** ($CDCl_3$)

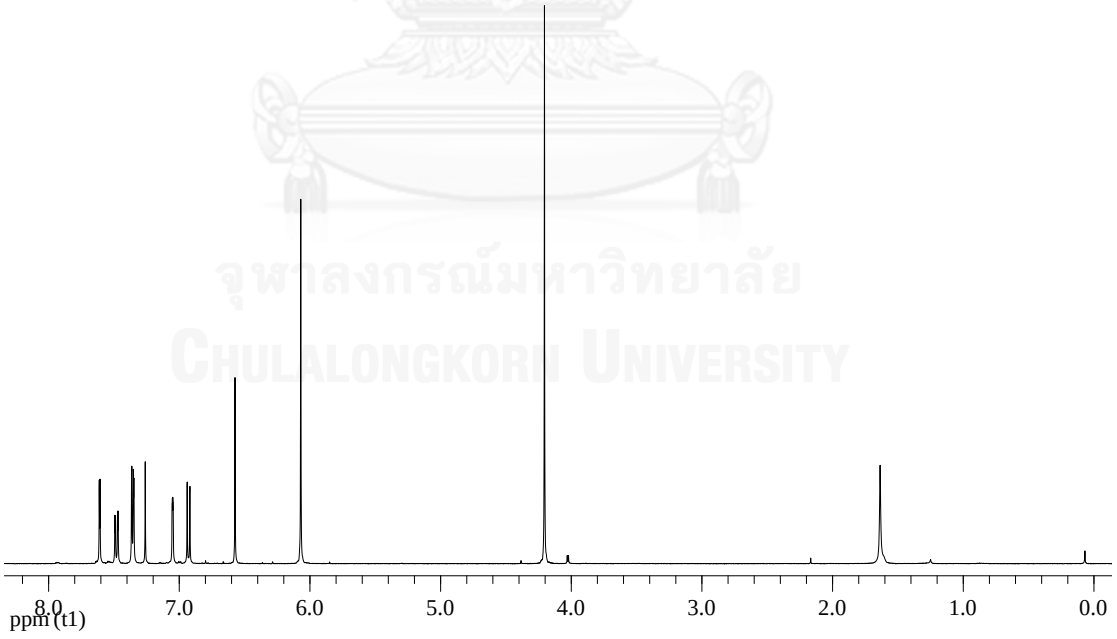

Figure A.64 ^{1}H NMR (400 MHz) spectrum of compound **13** ($CDCl_3$)

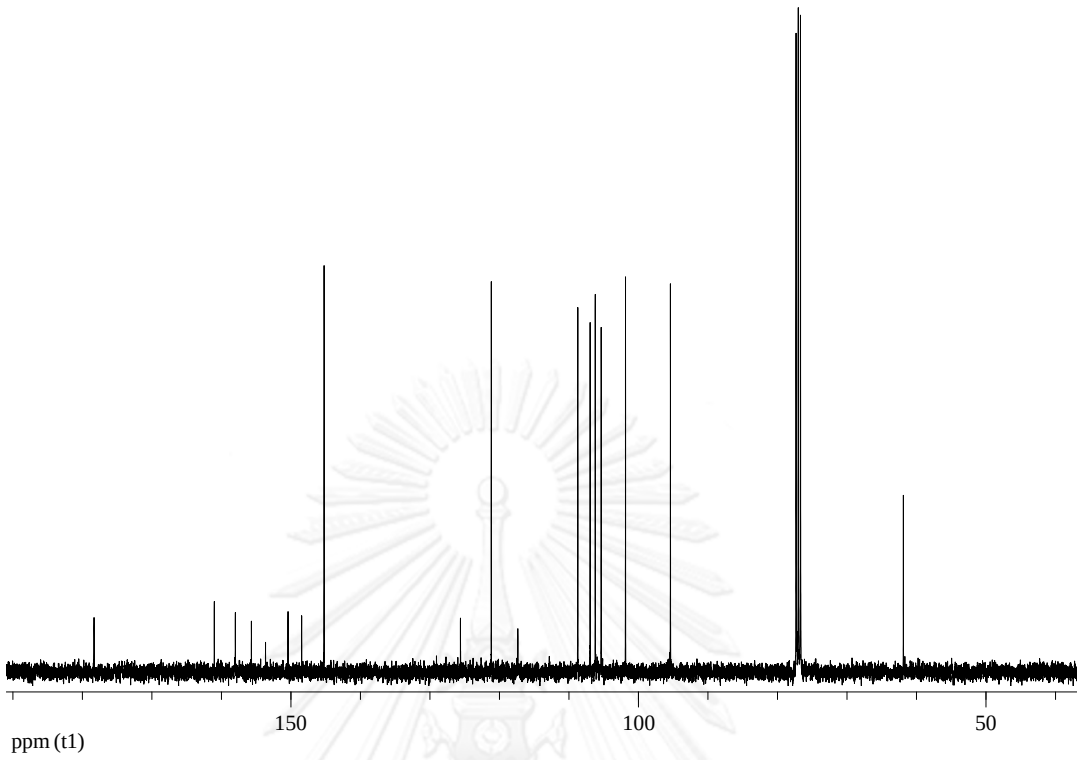

Figure A.65 ^{13}C NMR (100 MHz) spectrum of compound **13** ($CDCl_3$)

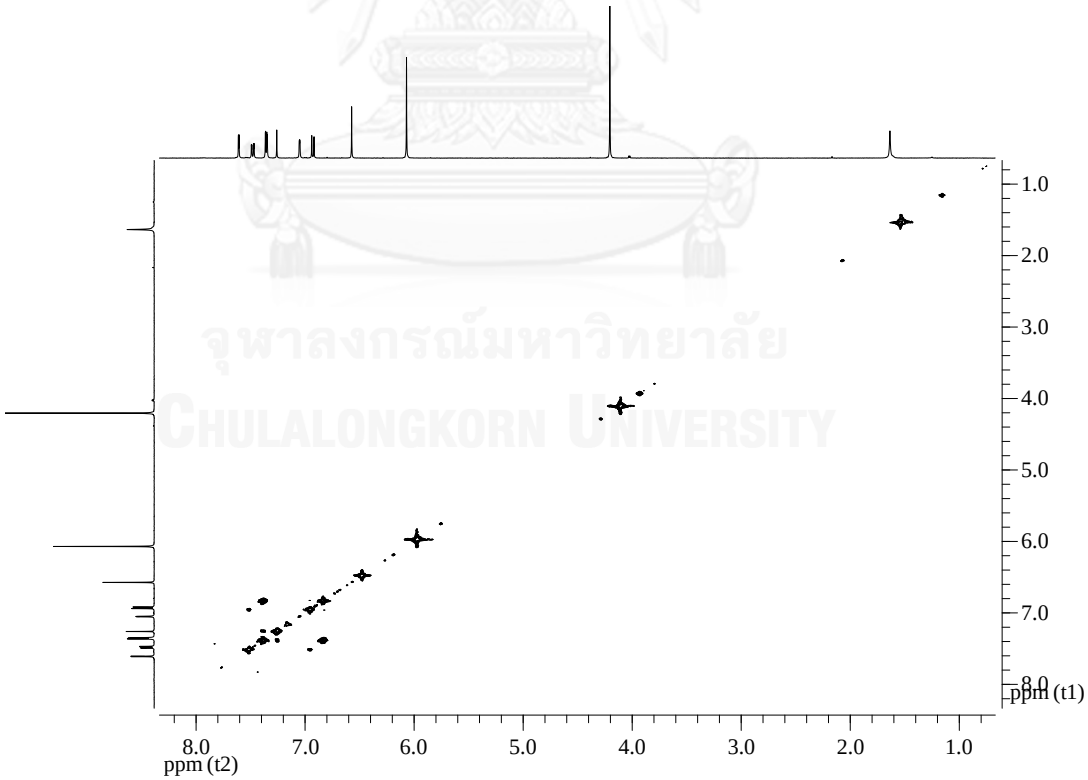

Figure A.66 ^{1}H-^{1}H COSY spectrum of compound **13** ($CDCl_3$)

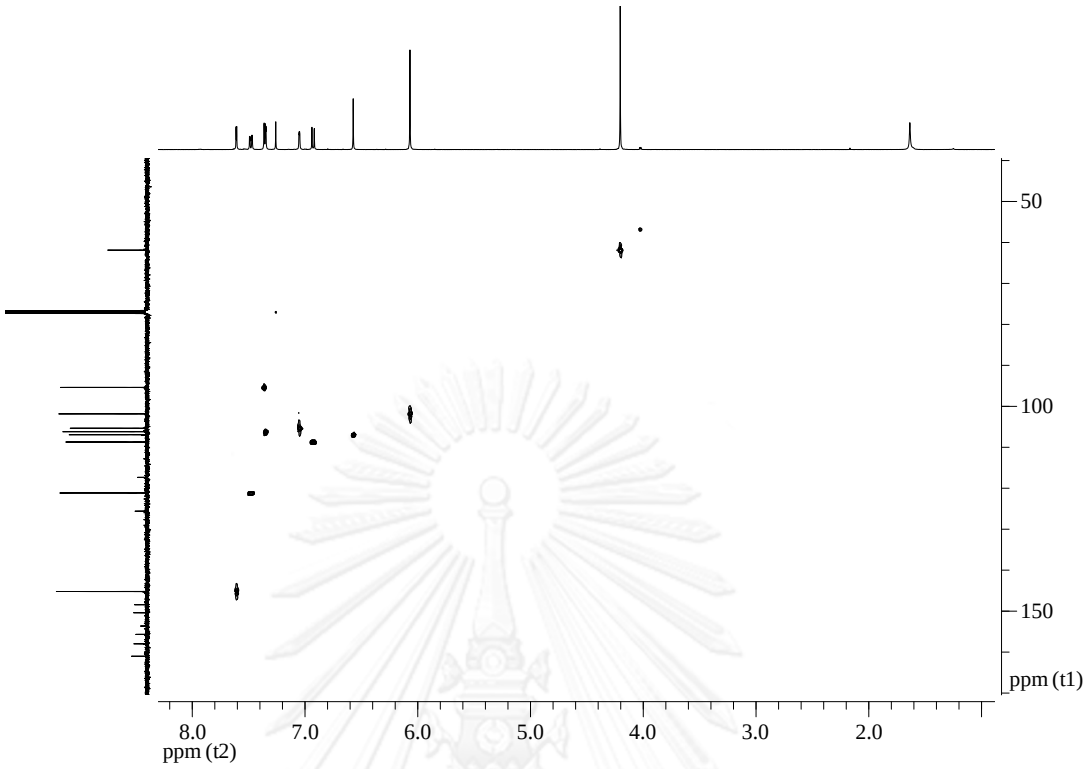

Figure A.67 HSQC spectrum of compound **13** ($CDCl_3$)

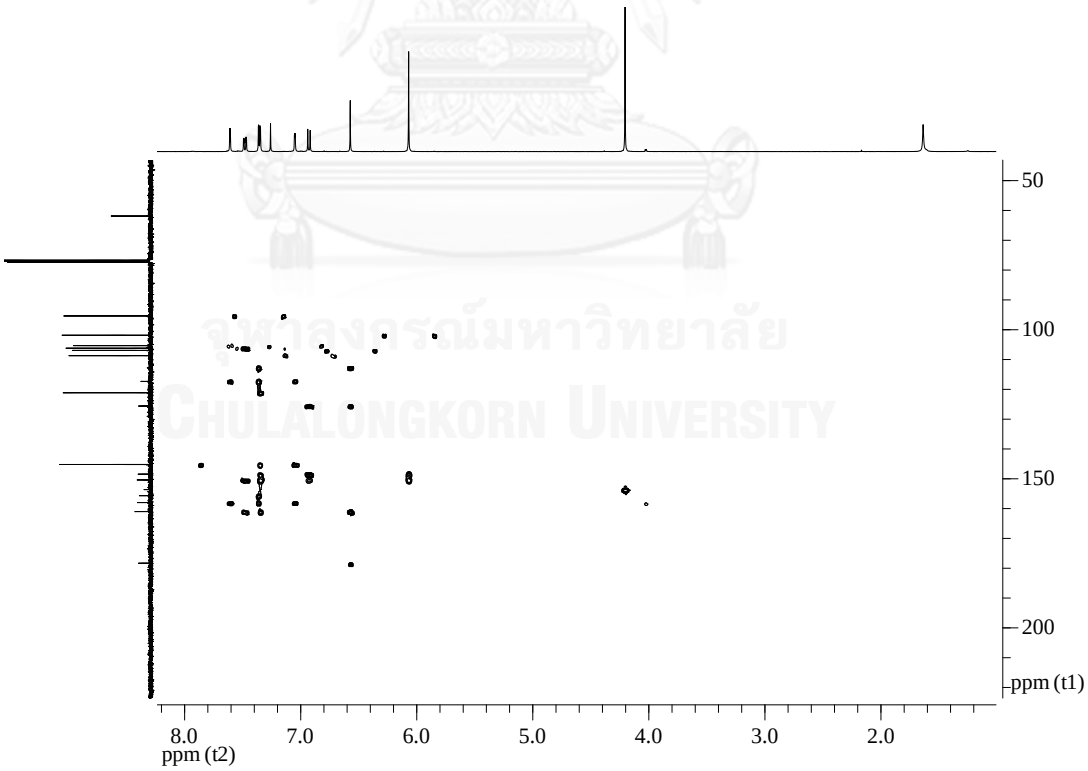

Figure A.68 HMBC spectrum of compound **13** ($CDCl_3$)

VITA

Miss Pornpat Anusiri was born on June 19, 1989 in Bangkok, Thailand. She graduated with Bachelor's Degree of Science in Biotechnology from Faculty of Science, King Mongkut's Institute of Technology Ladkrabang, in 2011.

Contact address is 3/105 Soi Vibhavadee 3 Yeak 15, Vibhavadee Road, Chompol, Chatuchak, Bangkok, Thailand, 10900.